Performance Evaluation and Optimizations of PV Powered DC Motor-Driven Home Appliance

"Site location of Kombolcha in south Wollo"

Kelemework Abate Workineh

A Thesis Submitted to the Program Chair of Electrical Power and Control Engineering

School of Electrical Engineering and Computing

Presented in Partial Fulfillment of the Requirement for the Degree of Master's in Electrical Power and Control Engineering (Specialization in Power Engineering)

Office of Graduate Studies

Adama Science and Technology University

Adama

October, 2019

Performance Evaluation and Optimizations of PV Powered DC Motor-Driven Home Appliance

"Site location of Kombolcha in south Wollo"

Kelemework Abate Workineh

Dr.-Ing. Getachew Biru Worku

A Thesis Submitted to the Program Chair of Electrical Power and Control Engineering

School of Electrical Engineering and Computing

Presented in Partial Fulfillment of the Requirement for the Degree of Master's in Electrical Power and Control Engineering (Specialization in Power Engineering)

Office of Graduate Studies

Adama Science and Technology University

Adama

October, 2019

APPROVAL of BOARD of EXAMINERS

We, the undersigned, members of the Board of Examiners of the final open defense by **Kelemework Abate** have read and evaluated his thesis entitled "PERFORMANCE EVALUATION AND OPTIMIZATIONS OF PV POWERED DC MOTOR-DRIVEN HOME APPLIANCE" and examine the candidate. This is, therefore, to certify that the thesis has been accepted in partial fulfillment of the requirement of the Degree of Masters of Science in Electrical Power and Control Engineering Program (Specialization in Electrical Power Engineering).

Dr.-Ing. Getachew Biru	________________	______________
Advisor	Signature	Date
__________________	_________________	_____________
Chair Person	Signature	Date
_______________	________________	_____________
Internal Examiner	Signature	Date
_______________	________________	_____________
External Examiner	Signature	Date

DECLARATION

I, the undersigned, declare that this MSc thesis is my original work, has not been presented for a degree in any other university, and all sources of materials used in this thesis have been fully acknowledged.

Kelemework Abate ______________

Student Name Signature

This MSc Thesis has been submitted for examination with my approval as thesis advisor.

Getachew Biru (Dr.-Ing) ______________

Advisor Signature

Date of submission: 01/10/2019 G.C

SUPERVISOR'S/ADVISOR'S APPROVAL SHEET

To: Electrical Power and Control Engineering Department

Subject: Thesis Submission

This is to certify that the thesis entitled "Performance Evaluation And Optimizations Of Pv Powered Dc Motor-Driven Home Appliance" submitted in partial fulfillment of the requirements for the degree of Master's in, the Graduate program of the department of Electrical Power and Control Engineering (in Power Engineering) and has been carried out by Kelemework Abate Id.No. GSR/0042/09 under my supervision. Therefore, I recommend that the student has fulfilled the requirements and hence hereby he can submit the thesis to the department.

Getachew Biru (D/r-Ing)	_____________	01/10/2019 G.C
Name of major Advisor/supervisor	Signature	Date

ACKNOWLEDGMENTS

First of all, I would take this opportunity to give glory to Almighty God without his support the completion of this work would have been impossible.

Next, to that, I would like to express my sincere gratitude to my advisor Dr.-Ing. Getachew Biru has been given of his generous guidance and constructive comments, encouragement, and suggestions.

And also, I would like to thank Mr. Endalamaw Wonde Director of East Amara Metrological service center Kombolcha South Wollo for their support by providing the required what I asked them all the solar power data of the site. Finally, I would like to give special thanks to my beloved family.

TABLE OF CONTENTS

APPROVAL of BOARD of EXAMINERS i
DECLARATION ii
SUPERVISOR'S/ADVISOR'S APPROVAL SHEET iii
ACKNOWLEDGMENTS iv
Table of contents v
LIST OF FIGURES ix
LIST OF TABLES xiii
ACRONYMS xiv
Abstract xv
CHAPTER ONE 1
INTRODUCTION 1
1.1 Background 1
1.2 Site Location 4
1.3 Statement of the Problem 6
1.4 Objectives of the Thesis 6
1.4.1 General objective 6
1.4.2 The specific objectives 7
1.5 Scope and Limitation of the Study 7
1.6 Significance of the Study 7
1.7 Delimitation 7
1.8 Organization of the Thesis 8
CHAPTER TWO 9
REVIEW OF LITERATURE 9
2.1 Theoretical Background 9
2.2 Theories of Renewable Energy 10
2.2.1 Solar Terminology 11
2.2.2 Solar Radiation Model 13
2.2.3 Direction of Beam Radiation 13

2.3. Converter Technologies 15
2.3.1 DC-DC Boosting Converter 15
2.3.2 Inverters 16
2.4 Energy Storage System / Battery/ 17
2.4.1. Introduction 17
2.4.2. Batteries 17
2.4.3 Types of batteries 17
2.4.4 Charge controller 19
2.5 DC MOTOR 19
2.5.1Brushed DC Motor 20
2.5.2 Brushless DC Motor 24
2.6 Converting an AC Refrigerator to DC Refrigerator 26
2.7 Performance Evaluation of DC Distribution System over the AC Existing System on home Appliance 27
2.8 Summary of Modes of PV Powering DC motor with Solar Energy 28
CHAPTER THREE 29
METHODOLOGY 29
3.1 Introduction 29
3.2 Design Procedure of solar-powered system 30
3.2.1 Solar Resource Assessment of Selected Site 30
3.2.2 Collected site data from NASA 33
3.3 Method of solar energy determination on the plane of the PV panel 34
3.3.1 Sizing of the PV system 35
3.3.2 Estimation of Solar Radiation 36
3.4 Peak Sun Hours 40
3.5 Sizing of PV Panel 40
3.6 MATLAB Model of Solar PV 46
3.7 Mathematical and Block diagram Modeling of Boosting DC-DC Converters 53

3.8 The mathematical modeling of Li-Ion battery......57
3.8.1 Discharge model:......57
3.8.2 Charge model:......58
3.8.3 Battery storage bank modeling......59
3.9 MATLAB Model of Charge Controller......61
3.10 Mat lab Modeling of Inverter......61
3.11 Maximum Power Point Tracking (MPPT)......63
3.12 Mathematical model of a typical BLDC motor......65
3.13 Home appliance equipment selection for the research......68
3.13.1 PV Module Boost Converter......68
3.13.2 PV Module Invertor......69
3.13.3 Refrigerator......70
3.13.4 Laptop......71
3.13.5 Lighting......71
3.13.6 Television, Radio, power stabilizer, and cellphones......72
3.13.7 DC fan, Washing machine, and Stove......75
3.14 Performance and efficiency evaluation......78
3.15 Economic Assessment of the Modeling DC Refrigerator and AC Refrigerator Running on Inverter all Powered by Solar PV......84
CHEPTER FOUR......86
RESULT AND DISCUSION......86
4.1 Simulating and modeling of PV powered DC Refrigerator using Matlab/SIMULINK......86
4.1.1 Simulation Result and Discussion of Boosting converter......87
4.1.2 Modeling and Simulating Result of MPPT......88
4.1.3 Modeling and Simulating Result of Lithium-ion Battery......89
4.1.4 Modeling and Simulating Result of Supercapacitor......90
4.1.5 Modeling of Lithium-ion Battery parallel with supercapacitor......92
4.1.6 Modeling and Simulation Result of Lithium-ion Battery Bank......93

4.1.7 Modeling and Simulation Result of the Charge controller 94
4.1.8 Modeling and Simulation Result of battery series with Charge controller 95
4.1.9 Modeling and Simulation Result of battery Bank series with Charge controller 96
4.1.10 Modeling and Simulation Result of Brushless DC motor 97
4.1.11 Modeling and Simulating Result of PV powered dc motor drive 99
4.1.12 Modeling and Simulating Result of PV with Battery Bank powered dc motor drive 101
4.2 Simulating and modeling of the solar-powered DC refrigerator using Matlab/ SIMULINK 103
4.2.1 Modeling and Simulation Result of DC/AC Inverter 103
4.2.2 Modeling and Simulating Result of PV powered AC motor drive 103
4.2.3 Modeling and Simulating Result of PV with Battery powered AC motor drive 106
4.3 Economic comparison analysis of DC distribution system and AC existing system 107
4.3.1 Modeling of DC system cost analysis using HOMER Software 107
4.3.2 Modeling of AC system cost analysis using HOMER Software 109
4.4 The solar-powered DC refrigerator compared to a conventional AC refrigerator 112
CHAPTER FIVE 113
CONCLUSIONS AND RECOMMENDATIONS 113
5.1 Conclusion 113
5.2 Recommendation 114
5.3 Future Work 114
References 115
APPENDIX 120
APPENDIX-A1 120
APPENDIX-A2 124
APPENDIX-A3 125

LIST OF FIGURES

Figure 1. 1: Schematic Diagram of Solar Battery- Based Refrigerator......................................2
Figure 1. 2: System Block Diagram of DC House Model Design 3
Figure 1. 3: Map of Site Location..5
Figure 2. 1: The angles and a set of consistent sign convention of beam radiation [44]…… …14
Figure 2. 2: Solar radiation angles [44] 15
Figure 2. 3: Simple inverter circuit [24] 16
Figure 2. 4: DC Series Motor [27]..21
Figure 2. 5: Common Source DC Shunt Motor [33] 22
Figure 2. 6: Compound Motor [27] 23
Figure 2. 7: Permanent Magnet Motor [32]..23
Figure 2. 8: Schematic of the Solar Powered DC Refrigeration System..................................26
Figure 3. 1: Schematic diagram of design procedure of solar power refrigerator…………. …30
Figure 3. 2: South wollo kombolcha PVGIS solar radiation data 31
Figure 3. 3: Flow Showing the Determination of Solar Energy on the Plane of PV Panel.......34
Figure 3. 4: variation of Rd and Rr with inclination 39
Figure 3. 5: current-voltage (I-V) and power – voltage (P-V) characteristics curves of a solar cell 48
Figure 3. 6: SIMULINK model of the PV equations 51
Figure 3. 7: V-I and V-P characteristics to the variation in temperature..................................52
Figure 3. 8: V-I and V-P characteristics to the variation in solar radiations 52
Figure 3. 9: Boost converter model in PSIM...53
Figure 3. 10: Boost converter in ON state during operation 54
Figure 3. 11: Boost converter in OFF state during operation...54
Figure 3. 12: Boost converter model in SimPowerSystems 56
Figure 3. 13: Nominal current discharge characteristic...57
Figure 3. 14: Typical charge characteristic 58
Figure 3. 15: - Series-parallel battery bank example configuration 60
Figure 3. 16: Internal circuit of the charge controller..61
Figure 3. 17: Pulse generation circuit..62

Figure 3. 18: Boost converter and single-phase inverter circuit 63
Figure 3. 19: PV panel characteristic curves 64
Figure 3. 20: Flowchart of the perturb and observe algorithm 64
Figure 3. 21: Brushless DC motor of the schematic diagram 65
Figure 3. 22: Brushless DC Motor Drive 68
Figure 3. 23: 24V-to-48V (Boost) DC-DC Converter 69
Figure 3. 24: Picture of the DC-AC inverter 70
Figure 3. 25: Single-phase AC motor 220V 300W for refrigerator 70
Figure 3. 26: Brushless DC motor 48V 300W for refrigerator bldc motor 70
Figure 3. 27: picture of AC adapter laptop charger [42] 71
Figure 3. 28: picture of DC-DC Buck converter for laptop charger in DC office [43] 71
Figure 3. 29: LED lamp with LED driver [58] 72
Figure 3. 30: picture of AC-DC adapter for Television [56] 72
Figure 3. 31: picture of DC-DC Buck Converter for Television 73
Figure 3. 32: AC-DC adapter picture for Radio 73
Figure 3. 33: DC-DC Buck converter picture for Radio 73
Figure 3. 34: single-phase 5000VA 220V Voltage Regulator 74
Figure 3. 35: picture of stabilizer DC-DC Buck converter 74
Figure 3. 36: picture of cellphone AC-DC adapter/charger 75
Figure 3. 37: picture of cellphone DC-DC Buck converter 75
Figure 3. 38: Single-phase AC motor 220V 300W for refrigerator 75
Figure 3. 39: Brushless DC motor 12V 36W for fan bldc motor 76
Figure 3. 40: Single-phase AC motor 220V 300W for refrigerator 76
Figure 3. 41: Brushless DC motor 24V 70W for washing machine bldc motor 76
Figure 3. 42: Picture of the ac-dc adapter of 24v-800w stove 77
Figure 3. 43: Picture of DC-DC Buck converter of 24v-800w stove 77
Figure 4. 1: Modeling of Boost DC/DC Converter 87
Figure 4. 2: Simulating Result of 24V to 48 V Boost Converters 87
Figure 4. 3:. Modeling of MPPT 88
Figure 4. 4: Simulation of MPPT 88
Figure 4. 5: Modeling of Lithium-Ion Battery 89

Figure 4. 6: Simulation Result of Lithium-Ion Battery 90
Figure 4. 7: Modeling of Supercapacitor 90
Figure 4. 8: Simulating Result of Supercapacitor 91
Figure 4. 9: Modeling of Lithium-Ion Battery Parallel With Supercapacitor 92
Figure 4. 10: Simulating Result of Lithium-Ion Battery Parallel With Supercapacitor 92
Figure 4. 11: Modeling of Lithium-Ion Battery Bank 93
Figure 4. 12: Simulating Result of Lithium-Ion Battery Bank 94
Figure 4. 13: Modeling of Charge Controller 94
Figure 4. 14: Simulation of Charge Controller 95
Figure 4. 15: Modeling of Battery Series With Charge Controller 95
Figure 4. 16: Simulating Result of Battery Series With Charge Controller 96
Figure 4. 17: Modeling of Battery Bank Series With Charge Controller 96
Figure 4. 18: Simulating Result of Battery Bank Series With Charge Controller 97
Figure 4. 19: Modeling of Brushless DC Motor 97
Figure 4. 20: Simulating Result of Brushless Motor 98
Figure 4. 21: Modeling of PV Powered DC Motor Drive 99
Figure 4. 22: Simulating Result of PV Powered DC Motor Drive 100
Figure 4. 23: Modeling of PV with Battery Bank Powered DC Motor Drive 101
Figure 4. 24: Modeling of PV with Battery Bank Powered DC Motor Drive 102
Figure 4. 25: Modeling of Single Phase PWM Inverter 103
Figure 4. 26: Modeling of Single Phase PWM Inverter 103
Figure 4. 27: Modeling of the Existing AC Distribution System 104
Figure 4. 28: Simulation Result of the Existing AC Distribution System 105
Figure 4. 29: Modeling of PV with Battery Bank Powered DC Motor Drive 106
Figure 4. 30: Simulating Result of PV with Battery Bank Powered Dc Motor Drive 107
Figure 4. 31: Modeling of PV Module DC Refrigerator Cost Analysis 107
Figure 4. 32: Simulating Result of solar PV of DC system cost analysis 108
Figure 4. 33: Simulating net present cost versus salvage in PV module of DC system 108
Figure 4. 34: Simulating Result of DC system from Battery to load cost analysis 109
Figure 4. 35: Simulating Result net present cost versus salvage from battery to load DC system 109

Figure 4. 36: modeling of PV module AC refrigerator cost analysis 109
Figure 4. 37: Simulating Result of solar PV of DC system cost analysis 110
Figure 4. 38: Simulating net present cost versus salvage in PV module of AC system.............110
Figure 4. 39: Simulating Result of AC system from Battery to load cost analysis 111
Figure 4. 40: Simulating Result net present cost versus salvage from battery to load AC system111

LIST OF TABLES

Table 2. 1: Recommended Average days for months and values of N by months (Duffie and Beckman, 1991)........15
Table 2. 2: Common rechargeable battery types........18
Table 3. 1: PVGIS estimates of solar electricity generation ……32
Table 3. 2: Annual irradiation shortage due to shadowing (horizontal)........33
Table 3. 3: monthly solar radiation data from NASA........34
Table 3. 4: Load Assessment........41
Table 3. 5: Summarized data collection of AC distribution of home equipment performance and efficiency evaluation of converter, inverter and AC drive motor.........78
Table 3. 6: Summarized data collection of DC distribution of home equipment performance and efficiency evaluation of converter, inverter and DC drive motor.........79
Table 3. 7: Comparison of AC and DC distribution by using Energy and Power evaluation of consumption, losses and saving of residential appliances.........80
Table 3. 8: Comparison of AC and DC distribution of home equipment Energy and Power consumption in terms of system efficiency........82
Table 4. 1: simulating Result existing AC system compared with new DC distribution system…… 112

ACRONYMS

A	Ampere
AC	Alternating Current
AC-DC	Alternating Current to Direct Current
BLDC	Brushless direct current motor
BOS	balance of system
D	Duty cycle
DC	Direct Current
DC-DC	Direct Current to Direct Current
EPBT	Energy payback time
FF	Fill factor
Fr.	Frequency
GCPV	Grid connected photovoltaic
KWh	Kilo Watt hour
KWh/yr.	Kilo Watt hour per year
LCD	Light Crystalline Diode
LCOE	Levelised cost of electricity
LED	Light Emitting Diode
MPPT	Maximum power point tracking
NASA	National Aeronautics and Space Administration
NOCT	nominal operating cell temperature
PV	Photovoltaic
RE	Renewable energy
SAPV	Stand-alone photovoltaic
PSIM	Pump Systems Improvement Modeling Tool
SISO	Single input single output
V	Volt
W	Watt
Wh	Watt-hour
Wh/yr.	Watt-hour per year

Abstract

In the current distribution system, almost all home appliances are designed to use AC supply for powering the home equipment like Refrigerator. But most of the equipment consumes the power first by converting the AC to DC internally or externally. Nowadays, due to the development of renewable energy or AC/DC converter, there is a possibility of getting DC power and supply to the equipment directly. So home appliances are can be designed using DC networks to use DC residential equipment. In the study, the DC supply system was modeled using MATLAB/SIMULINK with the DC loads that is use brushless DC motor instead of single-phase AC motor in the refrigerator, and a comparative analysis was done for AC and DC supply in terms of power loss, energy-saving, and efficiency in the steady-state operation of the system. The major engineering aspect of the DC devices was identified and the cost-benefit of manufacturing of the DC device was compared with the AC devices then analyzed using HOMER SOFTWARE and it was saved 10.32% of AC system of total Net Present Cost for refrigerator only. In this study, 80.11% of annual energy loss could be saved using DC system, 18.72% of drive equipment and 20.92% of non-drive home appliance efficiency saved. The overall system including the PV module efficiency was saved 3.65% and 4.08% of with drive and without drives respectively.

Keywords: *brushless DC motor, DC home appliance, HOMER Software, MATLAB/SIMULINK, Net Present Cost.*

CHAPTER ONE

INTRODUCTION

1.1 Background

During the beginning of the nineteenth century, the debate between alternating current (AC) and direct current (DC) had started. Tesla showed the practical advantages of alternating current. Transformers made it possible to step up an AC voltage easily; this allowed power to be transmitted over long distances with a low loss. This was not easy to achieve with Edison's dc voltage and there were huge transmission losses. Tesla's practical results were the deciding factor at least for the time being that an AC system was to prefer. This debate again came into light due to recent development in power electronics which gives better utilization of existing transmission corridors with high voltage DC connections. High voltage DC transmission allows more power to be transmitted over a long distance with less loss compared to an AC transmission. Power electronics make efficient and accurate control of electrical power possible. Efficient AC to DC, DC to AC and DC to DC conversion technology are now available on the market, where DC to DC conversion is more efficient than AC to DC conversion.

The number of devices that operate on DC continues to increase in both homes and offices. Most of the devices are using DC internally and this requires AC to DC conversion between the AC supply and the DC side of the device. Examples of these devices are PCs, radios, televisions, telephones and other electronic appliances. Energy storage devices such as batteries, mobile phones, and cordless tools, also require direct current as an energy source. They are equipped with adapters which convert 230V AC into low voltage DC. All of these AC to DC conversions have losses [4].

In case of small-scale electricity generation, almost all new sustainable energy sources are produce DC output such as solar cells, fuel cells, osmosis batteries, and others. On the other hand, AC system is connecting to the existing 230V AC [13] distribution network. Which further needs to be converted back to low voltage DC inside the DC power consuming apparatus. This results in low overall efficiency of the AC system.

The thesis deals, solar Energy is considered to be one of the most desired renewable energy resources. The Solar PV panels [5] are used to obtain solar energy from the Sun and which is converted into electrical energy for various applications. Among the renewable energy sources, the solar is considered to be the easy technique is obtaining the electric power because of the simple installation, and compact arrangement that can be considered to be more equivalent in the domestic and household requirements. The output of the solar PV panel is DC and which requires some DC-DC [6]. Converter is to provide a constant supply for many applications. A solar PV panel is connected to a DC-DC boost converter and to a load. The load here is a Stand-Alone application as DC Motor load. [7]

In the 1980s, solar refrigerators were introduced in areas without electricity as a solution to the problems cited for gas and kerosene refrigerators. However, one of the major draw backs of solar refrigerator technology has been the large battery systems that were required to store the sun's energy for use during the night and cloudy periods. These batteries have a relatively short life time of 3 to 5 years, and replacements are expensive and sometimes unavailable for purchase in low-income countries [8]. For these reasons solar refrigerators have often been abandoned when the battery dies well short of the useful life of the refrigerator itself.

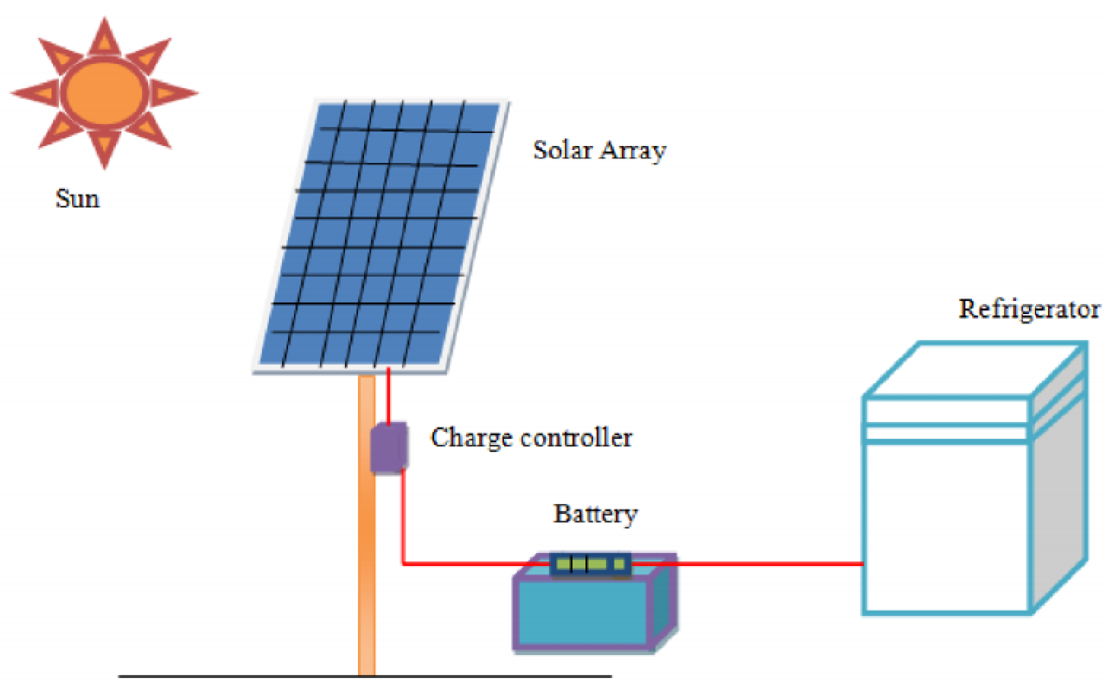

Figure 1. 1: Schematic diagram of solar battery- based refrigerator [19]

The use of the general type dc motor has its long history. It has been used in the industries for many years now. They provide simple means and precise way of control [9]. In addition, they have high efficiency and have a high starting torque versus falling speed characteristics which help high starting torque and helps to prevent sudden load rise [10].

The model design of the DC House must consider several variables. The purpose of the DC House is to develop a low-cost method of generating DC power and providing it to small village homes in developing countries where electricity is not available or affordable. The hardware needed for the DC system must be affordable and feasible. Therefore, the specific components of the DC House must be chosen to appropriately accommodate the energy demand of the family while considering their fiscal circumstances. Ultimately, the DC House has the potential to improve the lifestyles of many unfortunate villages around the world. The basic model design of the DC House is shown in Figure 1.2, which illustrates the DC power generation is photovoltaic.

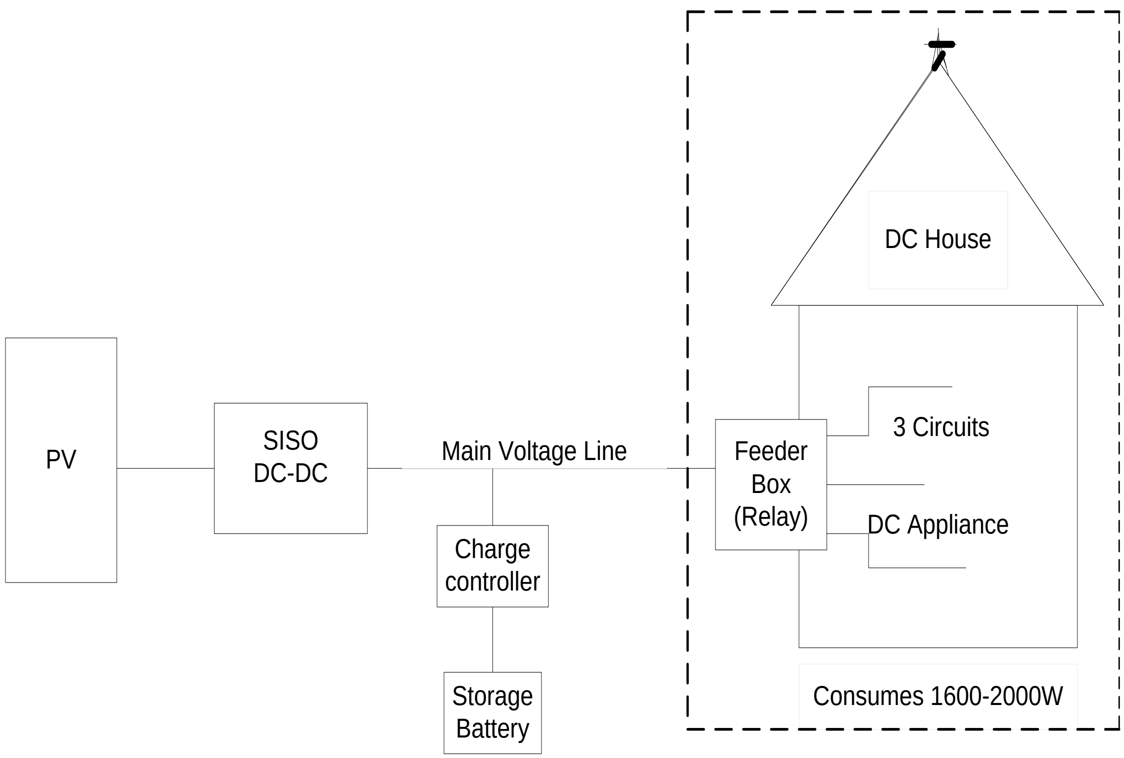

Figure 1. 2: System Block Diagram of DC House Model Design as a general

As seen in Figure 1.2, one renewable source of energy is connected to the boost DC-DC converters which step up the voltage from approximately 24V at the output of the renewable energy systems to the voltage of 48V. This voltage from the outputs then becomes an input to the single-Input Single-Output (SISO) DC-DC converter, which the power produced on the generation side and steps up the voltage again at the output while maintaining this power at certain efficiencies. In this system, the main system voltage is 48V, which has been found to be the most efficient voltage for a system of this size. The main voltage line is connected to a charge controller and a battery with a certain capacity to store excess renewable energy produced not being used by the house. Therefore, if the residents of the home are using little or no power for a certain period of time, excess energy that is produced can be stored in the batteries for later use when certain resources such as the sun are momentarily unavailable. The battery charge controller simply controls the charging and discharging of the battery according to energy production and current demand for consumption. The main voltage line is also connected to the house via a feeder box, which contains a few circuit breakers and fuses to control the distribution of power to home and protect the system from ground faults inside the home. It has been determined that three is the optimal number of circuits to be used for powering the appliances in the home. The DC appliances in the DC house must be chosen carefully to consume low power while sufficiently satisfying the basic needs of the residents.

1.2 Site Location

Ethiopia is located very close to the equator between 30 and 150N, receives abundant solar energy potential which can be harnessed and used in the form of both thermal and electrical energy. The average solar radiation of Ethiopia is around 5.2kWh/m^2/day which is more or less uniform. The value varies seasonally from a minimum of 4.55kWh/m^2/day in July to a maximum of 7.56kWh/m^2/day in February and March. With location the radiation varies more widely between 4.25kWh/m^2/day in extreme western low lands and 6.25kWh/m^2/day in northern part of the country. Ethiopian Rural Energy Development and Promotion Centre [2] has quantified the technical potentials of solar energy resource use for many applications.

Solar powered refrigerator is essential for different purpose especially in off-grid area. The some part of Ethiopia is desert like Afar, Gambela, Dire dawa, Borana, Kombolcha and etc. Temperature of this area is high, because of hot in that area; people living in this area want cooling water for drink.

In this work selected site is Berberie weniz which located around Kombolcha South Wollo. It is located at 11.08° latitude and 39.72° Longitude.

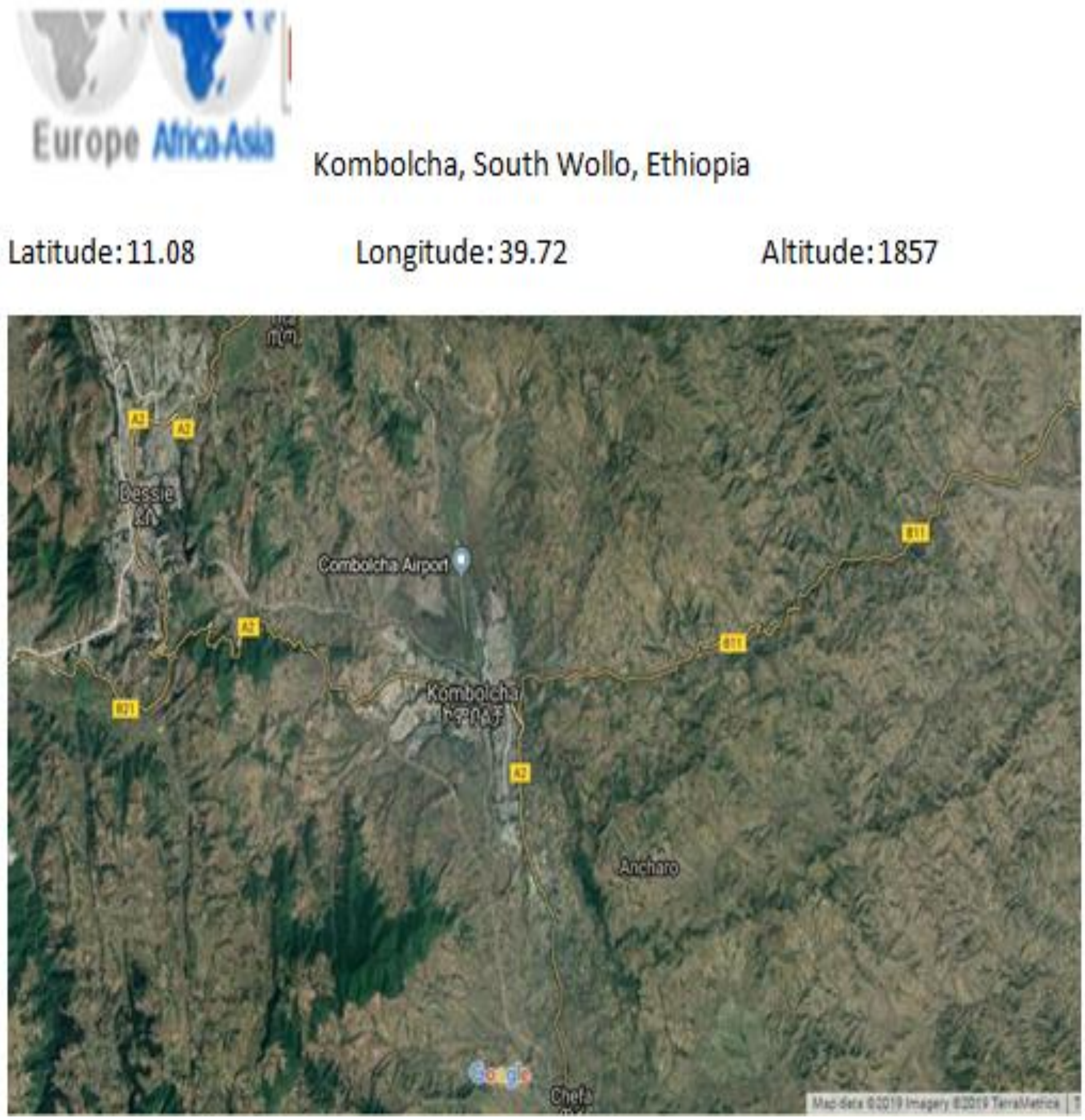

Figure 1. 3: Map of Site location

1.3 Statement of the Problem

Nowadays, getting power for home appliance in off grid area is not big problem. There is a possibility to get power from renewable energy sources like photovoltaic (PV). If we see the equipment used in the home, most of them are working in DC by converting the AC to DC internally or externally. Instead of supplying AC using the conventional AC network, it is possible to supply using the DC network to supply the DC power directly to the equipment using DC/DC converter.

The people living in grid connecting system use electric powered refrigerator for cooling water, but people exist desert and off-grid area can't get electric powered refrigerator. Therefore this problem would be solving when people exist in desert and off-grid areas use solar power refrigerators. The provision of energy storage is virtually non-existent in AC distribution systems but the storage of DC energy in batteries is very practical. The DC distribution system will also minimize conversion losses incurred in the existing systems along the way.

In Ethiopia, power reliability problem is a big concern. Hybrid AC/DC system for a home appliance with DC network is a solution of power interruption for homes that are used for businesses in grid area. In this thesis work, a comprehensive investigation of DC distribution system will be designing and evaluating by using DC motor derive instead of AC-motor load and directly plugging of DC end-user off-grid home appliances for the solution of the problem. This research will be provided a recommendation with a complete design of power distribution system by including detail evaluation of the power distribution efficiency and making an economic analysis of the design system.

1.4 Objectives of the Thesis

1.4.1 General objective

The general objective of this thesis is to study the technical and economic feasibility using DC motors for residential devices and make an analytic comparison with AC powered motors in terms of efficiency, energy-saving, and cost of the system.

1.4.2 The specific objectives

- To study the optimization of energy storage system (ESS) to handle the intermittency in PV output and high starting current.
- To design and model appropriate DC supply with DC motor load.
- To Simulate the DC supply system and evaluate the performance of the system in terms of energy saving, efficiency, consumption variations.
- To evaluate the cost benefits of using DC instead of AC.
- Make relevant conclusions and recommendations for the practical implementation of the model.

1.5 Scope and Limitation of the Study

To identify the various DC motors used for residential motor-driven equipment. The study encompasses optimizing, modeling and simulating the solar PV system, DC-DC converter, and battery storage system. It focuses on evaluation of the system in terms of efficiency and cost.

1.6 Significance of the Study

The proposed study will bring the following potential benefits.

- ✓ Significant energy saving and positive environmental impact.
- ✓ Increase power efficiency.
- ✓ Minimizing cost of production.

1.7 Delimitation

This research project was intended to evaluate the use of dc motor drive on home appliance. The study focuses only on the use of refrigerator and does not consider large size fridges.

1.8 Organization of the Thesis

This thesis consists of the following chapters:

Chapter 1: ***Introduction***

It is to provide the introduction, background, problem statement, objectives, significance, delimitations, location site, contributions and organization of the paper.

Chapter 2: ***Literature review***

It covers the theoretical background and literature review related to this thesis, basically on AC and DC power system, PV system, and conversion, types of battery and different types AC/DC motors.

Chapter 3: ***Design and Optimization of solar-powered refrigerator***

Solar radiation data collected and data analysis takes place to the site location. Analysis of refrigerator and home appliance load, *Modeling* of PV Module System, component of converter and DC motor load design. Assumptions made to carry out an economic analysis of a solar-powered refrigerator and payback cost.

Chapter 4: ***Results and discussions***

Summarize the main results achieved in the papers appended to this thesis and High light the main discussion points.

Chapter 5: ***Conclusion and Recommendation***

Conclusions Feature works and Recommendations are well to do.

CHAPTER TWO

REVIEW OF LITERATURE

2.1 Theoretical Background

For nearly 100 years, alternating current (AC) power has been the preferred means of transmitting and distributing electricity. Recently, however, diverse groups of product manufacturers, researchers, efficiency advocates, and even some electric utilities have questioned AC's primacy and have begun to explore direct current (DC) as an alternative generation and distribution choice, at least within buildings. [11]

Today, DC is becoming more and more prevalent in homes. A wide range of devices from lighting products to electronics fundamentally require DC power to drive semiconductors, charge batteries, and provide other useful services to end-users. [6]

Renewed interest in Direct-DC: Recent trends call for a renewal of the AC versus DC debate, at least in certain applications: Increased use of DC-based loads: An important factor that favours the use of DC is the growing number of electric appliances that operate internally on DC, and the fact that these new 'DC-internal' technologies tend to be more efficient than their AC counterparts. "DC-internal" appliances include communication technologies and all consumer electronics, such as computers, telephones, televisions, compact fluorescent lighting with electronic ballast, light-emitting diodes (LEDs), and efficient DC motors. The fluorescent and LED lighting uses one-fourth of the power or less than the traditional incandescent lighting it is replacing in the residential and commercial sectors [3]. Brushless DC permanent magnet motors can save 5-15% of the energy used by traditional AC induction motors, and up to 30-50% in variable speed applications for pumping, ventilation, refrigeration, space cooling. DC-driven heat pump technologies for water and space hearting can also displace conventional resistance heating with a savings of 50% or more. Thus, three factors together suggest that DC-internal loads will continue to grow, and will probably grow rapidly: the intensified focus on energy efficiency due to climate change, the fact that new DC internal technologies can be significantly more energy-efficient than their conventional AC counterparts, and the fact that those technologies are capable of servicing virtually all building loads. Indeed, the fact that global residential electricity consumption by electronic appliances grew by about 7% per annum between 1990 and 2008 and is expected to increase by 250% by 2030 (International Energy Agency [IEA], 2009) makes continued intensive investment in energy efficiency an imperative. [3]

2.2 Theories of Renewable Energy

Electricity plays an important role in the development of civilization. It is used to power up residential and office buildings, industries, information, and communication equipment as well as vehicles and transportation. Electricity in a conventional power system is generated using several types of energy resources such as fossil fuels, nuclear energy and renewable energy (RE). Renewable energy is introduced as its energy resource is inexhaustible and environmentally benign. RE can be defined as a continuous natural resource that can be replenished without failure and will not be depleted throughout time. RE technologies are developed using several types of energy resources such as solar, wind, hydro, biomass and geothermal. However, solar energy is one of the most popular REs as the sunshine is ample and available in wider region as compared to other RE resources. In electricity generation, solar energy is converted to electricity via photovoltaic (PV) effect. Therefore, a solar energy-based electricity generation system is known as PV system. It has the fastest market growth worldwide when compared with other RE technologies. The PV systems can be implemented using either Grid-Connected Photovoltaic (CPV) systems or Stand-Alone Photovoltaic (SAPV) systems. A GCPV system is a PV system that injects the solar electricity to a power utility grid network while a SAPV system is a PV system that is used to directly power up the electrical loads. Apart from that, a GCPV system typically consists of two major components i.e. the PV modules and inverter while a SAPV system consists of PV modules, charge controller, batteries and inverter. However, due to the ease of interconnection and small number of components involved, GCPV systems have become more widely used when compared to SAPV systems especially in locations with readily available utility grid network. In addition, GCPV system offers a distinctive advantage, i.e. the utility grid provides an energy backup to meet the load demand whenever the system fails. As a result, the design of GCPV system is often less critical when compared to SAPV system since the reliability of electricity supply for a particular location is often not an issue. In contrast, the issue of reliable electricity supply for a SAPV system continues to prevail in areas that are deprived of utility grid electricity since there is no back-up power to meet the load demand during the event of rainy or cloudy days as well as when there is a system failure. Therefore, the reliability of electricity supply for a SAPV system is frequently given the top priority in its system design. The dimensioning, selection and matching of SAPV system components are known as sizing, which is the issue that has been considered in this thesis.

2.2.1 Solar Terminology

The solar energy reached each year to the earth's surface is roughly 10k times the total energy consumed by humans. As sunlight passes through the earth's atmosphere some of it absorbed, some is scattered and some pass through the molecules in the atmosphere. The solar energy that reaches the earth's surface is solar radiation. Nuclear reactions occur in the sun as result hydrogen is converted into helium with a process called fusion.

This reaction caused the release of large amount of radiation, where its temperature reaches about 15 million degrees Celsius [12]. It is part of this energy that strikes the earth's surface.

The magnitude of solar irradiance which strikes on the surface of the earth depends on latitude, climatologically location parameters like air pressure, cloudiness, etc. Some of the direct applications of solar energy are to heat, to pump, and to desalinate water. Solar energy can be converted into electricity using different conversion technologies, among which photovoltaic and solar thermal are the basics. Photovoltaic technologies convert incoming solar insulation directly into electricity. Whereas, solar thermal technologies initially heats water then directs to mechanical systems such as steam turbines to generate electricity. This technology uses mirrors to concentrate the incoming solar energy, it captured in the form of heat. Taking an account for the PV systems and sunshine, it is necessary to take a note of the following important concepts.

Irradiance: It is the power density of the sun, measured in W/m^2. At night and on sunrise times, irradiance is often zero and increases respectively then reaches its highest value around noon. It again decreases from noon to sunset and dropping to zero at night.

Irradiation: it is the time integral of the power density of the sun (irradiance), measured in kWh/m^2.

Air mass: A parameter that influences the quantity of irradiance that is incident on the earth's atmosphere.

Solar constant: The amount of solar radiation incident on the earth's atmosphere at a vertical angle of air mass (AM=0), and its magnitude is about 1367 W/m^2.

Global solar radiation: The total summation of the sunbeam and diffuse radiations. In case of horizontal laid surfaces, global solar radiation is the summation of vertical radiation and diffuse radiation. This is part of the constant solar radiation that hits the ground.

Beam radiation: It is the sunbeam that reaches the earth right from the sun disk.

Diffuse radiation: It is the solar insulation that reaches the ground from the sky where its direction is changed by the atmosphere. The diffuse radiations magnitude depends on the solar height, and atmospheric transparency. The higher the cloud in the sky is the higher the dispersed radiation.

Albedo radiation: It is the reflected sunlight from the ground.

Extraterrestrial normal radiation: Is the quantity of solar insulation that arrives on a surface perpendicular to the atmosphere.

Extraterrestrial horizontal radiation: is the quantity of solar radiation reaching on a flat surface positioned on top of the atmosphere. If the entire direct solar radiation source is converted into usable form of energy in the earth, it would be more than enough to supply the energy requirement of the world. [25]

Solar energy is radiant light and heat from the Sun that is harnessed using a range of ever-evolving technologies such as solar heating, photovoltaic, solar thermal energy, solar architecture, molten salt power plants and artificial photosynthesis [14].

It is an important source of renewable energy and its technologies are broadly characterized as either passive solar or active solar depending on how they capture and distribute solar energy or convert it into solar power. Active solar techniques include the use of photovoltaic systems, concentrated solar power and solar water heating to harness the energy. Passive solar techniques include orienting a building to the Sun, selecting materials with favorable thermal mass or light-dispersing properties, and designing spaces that naturally circulate air. [15]

Generally, the sun is the largest energy source of life and at the same time it is the ultimate source of most renewable energy sources. That is why sun is considered as the mother or father of all renewable energy sources. Without sun; there is no wind, no water, and no biomass energy. Energy from the sun has been used to provide heat and electricity for many years. [16]

2.2.2 Solar Radiation Model

Solar radiation data provide information on how much of the sun's energy strikes a surface at a location on the Earth during a time period. These data are needed for effective research into solar energy utilization.

2.2.3 Direction of Beam Radiation

The geometric relationships between a plane of any particular orientation relative to the earth at any time (whether that plane is fixed or moving relative to the earth) and the incoming beam solar radiation, that is, the position of the sun relative to that plane, can be described in terms of several angles. Some of the angles are indicated in Figure 2-1. The angles and a set of consistent sign conventions are as follows

φ **Latitude**, the angular location north or south of the equator, north positive; $-90^\circ \leq \varphi \leq 90^\circ$.

δ **Declination**, the angular position of the sun at solar noon (i.e., when the sun is on the local meridian) with respect to the plane of the equator, north positive; $-23.45^\circ \leq \delta \leq 23.45^\circ$.

β **Slope**, the angle between the plane of the surface in question and the horizontal; $0^\circ \leq \beta \leq 180^\circ$. ($\beta > 90^\circ$ means that the surface has a downward-facing component.)

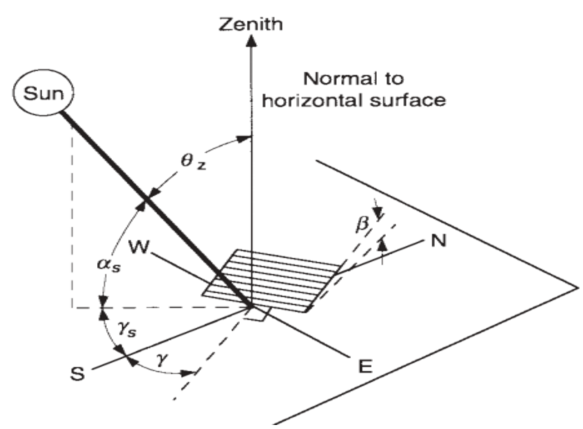

(a) Zenith angle, slope, surface azimuth angle, and solar azimuth angle for a tilted surface. [44]

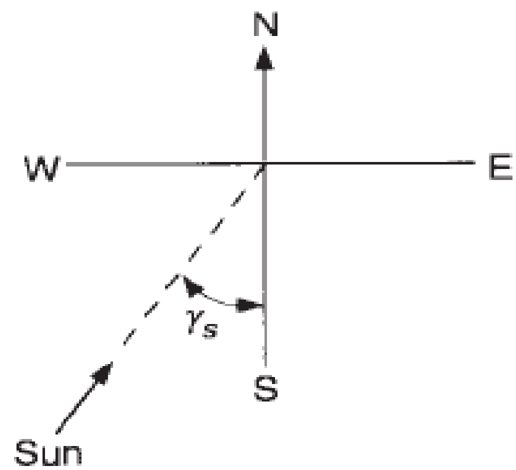

(b) Plan view showing solar azimuth angle. (Source: solar engineering of thermal processing)

Figure 2. 1: The angles and a set of consistent sign convention of beam radiation [44]

γ Surface azimuth angle, the deviation of the projection on a horizontal plane of the normal to the surface from the local meridian, with zero due south, east negative, and west positive; $-180^\circ \leq \gamma \leq 180^\circ$.

ω Hour angle, the angular displacement of the sun east or west of the local meridian due to the rotation of the earth on its axis at 15° per hour; morning negative, afternoon positive.

θ Angle of incidence, the angle between the beam radiation on a surface and the normal to that surface. Additional angles are defined that describe the position of the sun in the sky:

θz Zenith angle, the angle between the vertical and the line to the sun, that is, the angle of incidence of beam radiation on a horizontal surface.

αs Solar altitude angle, the angle between the horizontal and the line to the sun, that is, the complement of the zenith angle.

γs Solar azimuth angle, the angular displacement from south of the projection of beam radiation on the horizontal plane, shown in the above Figure. Displacements east of south are negative and west of south are positive. The sun's declination δ, needed to determine its position, is the angle between the sun's direction at the solar noon and its projection on the equatorial plane (Figure 2-2). It is described by Cooper's equation [8-10]:

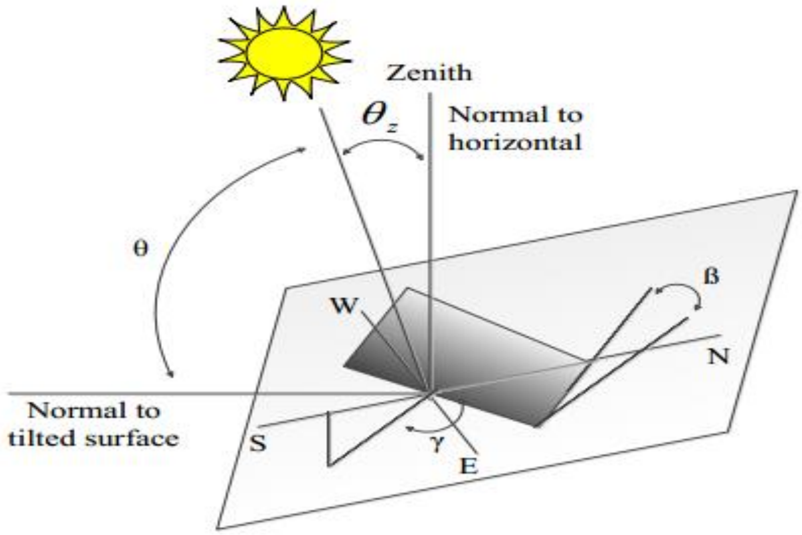

Figure 2. 2: Solar radiation angles [44]

Table 2. 1: Recommended Average days for months and values of N by months [44]

Month	N for ith Day of Month	For the average Day of Month		
		Date	Day of year N	Declination δ
January	I	17	17	-20.9
February	31+i	16	47	-13
March	59+i	16	75	-2.4
April	90+i	15	105	9.4
May	120+i	15	135	18.8
June	151+i	11	162	23.1
July	181+i	17	198	21.2
August	212+i	16	228	13.5
September	243+i	15	258	2.2
October	273+i	15	288	-9.6
November	304+i	10	318	-18.9
December	334+i	14	344	-23

2.3. Converter Technologies

2.3.1 DC-DC Boosting Converter

DC-DC converter steps up the input voltage magnitude to a required output voltage magnitude without the use of a transformer. The principal components of a DC-DC boost converter are an inductor, a high-frequency switch, and a diode. These in a coordinated manner supply power to the load at a voltage highest than the input voltage magnitude. The control strategy lies in the manipulation of the duty cycle (D) of the switch which causes the voltage change. A process that changes one DC voltage to another DC voltage is named boost converter. DC-DC power converter (boost) is a boost converter with an output voltage is higher than its input voltage. The boost converter is also renowned as step-up converter since it steps up the source voltage. The input voltage of the boost converter is controlled to adjust the maximum power point of the PV array. Boost converter plays an important role in solar PV system. MPPT process will raise the current and voltage. Finally, the power from DC-DC power converter is fed to the load.

2.3.2 Inverters

Inverters are used to convert DC current into AC currents in PV systems. Different types of inverters produce a different "quality" of electricity. So, the user must match the power quality required by your loads with the power quality produced by the inverter. Major discrepancies exist between power generation with PV modules and the requirements of the public grid. The job of the inverter is to connect the systems with each other and to feed the solar power into the grid with the highest possible efficiency. The simplest inverter can be accomplished with a circuit similar to that shown in Fig. 2.11. The ideal switches in the circuit can be selected depending on the power and voltage requirements.

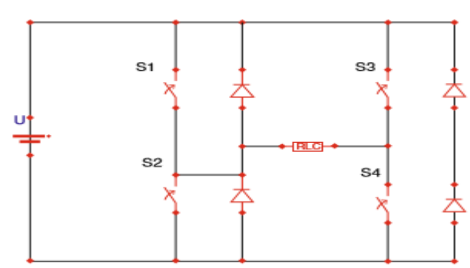

Figure 2. 3: Simple inverter circuit [24]

A simple control strategy to get the inverter output is to turn on and off the switches at the required AC frequency to obtain a square wave voltage but it consists of high harmonic currents and voltages. It can be reduced by using high-frequency pulse width modulation techniques to diminish harmonic distortion and provide load voltage control. Because harmonic content can cause overheating in the case of motor loads due to higher copper losses as well as uneven magnetic fields affecting overall operation. Sensitive electronic loads may also display erratic operation. Today, advanced control schemes and creative topologies allow the creation of AC with very low harmonic distortion; three-phase designs are also possible by incorporating additional switches. The efficiency indicates the percentage of the available solar power that is actually converted and fed into the utility grid. Modern inverters currently consume between 4 % and 8 % of the converted energy in the conversion process, which corresponds to an overall efficiency of 92–94 %. Further reducing this already low energy consumption is a major technical challenge and one which can only be achieved with new and innovative designs.

2.4 Energy Storage System / Battery/

2.4.1. Introduction

At present, the overviews of battery energy storage in the application of the electric power system mainly focus on introducing the characteristics of each type of energy storage battery, the control of the energy storage system and configuration modes and various application fields in power system, etc. However, the battery degradation cost plays a significant role in the cost optimization and dispatch control because extending the battery service life can effectively reduce the battery switching and operation maintenance cost. [22]

2.4.2. Batteries

A battery is a device that converts chemical energy directly to electrical energy. It contains one or more cells. Each cell consists of three main parts: a positive electrode (terminal), a negative electrode, and a liquid or solid separating them called the electrolyte. When a battery is connected to an electric circuit, a chemical reaction takes place in the electrolyte causing ions (in this case, an atom with a positive electrical charge) to flow through it one way. With electrons (particles with a negative charge) flowing through the outer circuit in the other direction. This movement of electric charge makes an electric current flow through the cell and through the circuit it is connected to [18].

2.4.3 Types of batteries

There are two types of batteries:

- Primary batteries (disposable batteries): which are designed to be used once and discarded.
- Secondary batteries (rechargeable batteries): which are designed to be recharged and used multiple times.

Most of the batteries used today with a hybrid power system are from the rechargeable type (Rivera 2008). There are several kinds of rechargeable batteries. Among them, as shown in Table 2.2: NiCd (Nickel Cadmium), NiMH (Nickel Metal Hydride), Lead-Acid, and Lithium-Ion (Li-Ion).

Table 2. 2: Common rechargeable battery types

Parameters	NiCD	NiMH	Lead-Acid	Lithium-ion
Nominal cell voltage (V)	1.2	1.2	2.1	3.6
Energy density (Wh/kg)	40-60	30-80	30-40	150-250
Specific power (W/kg)	150	250-1000	180	1800
Charge/discharge efficiency %	70%-90%	66%	70%-90%	99%+
Self-discharge rate in (% month)	20%	30%	3%-4%	5%-10%
Cycle durability3 (#)	1500	500-1000	500-800	1200-10000

As shown in Table 2.2, Lithium-Ion battery has many advantages than other rechargeable batteries, such as :

- High energy density: it is typically twice that of the standard Nickel Cadmium.
- High cell voltage with 3.6 volts.
- Low battery maintenance: an advantage that most other chemistries cannot claim.

- Relatively low self-discharge: self-discharge is less than half that of Nickel based batteries.
- High charge/discharge efficiency: more than 99%.
- High cycle durability: it can last for many hundreds or even thousands of charge/discharge cycles.

These characteristics have made the Li-Ion battery the fastest growing and most promising battery system for renewable energy applications [18]. Used it, the Li-Ion battery is the rechargeable battery that will be investigated in this work.

2.4.4 Charge controller

Charge controller is an essential component in PV systems where a storage system is required. In other words, the battery charge controller works as a voltage regulator. It protects the battery against both excessive overcharges by a generating unit system and deep discharge by a load. The charge controller shall switch off the load when a certain state of discharge is reached, also shall switch off the battery from the DC bus when it is fully charged. The charge controller can be adjusted to deal with different charging and discharging conditions. The controller's average efficiencies range from 95% to 98%. [6]

There are two types of charge controllers. These are pulse width modulation (PWM) which is used in this thesis and Maximum power point tracker (MPPT). The first one or PWM controller is most simple, less expensive, the source voltage and also battery voltage are the same. The MPPT controller is the most expensive and more efficient. The cost difference is maybe 30-60% and also the source voltage is bigger than the storage batteries voltage. [11]

2.5 DC MOTOR

The DC motors are comprehensively used in various industrial applications such as electrical equipment, computer peripherals, robotic manipulators, actuators, steel rolling mills, electrical vehicles, and home appliances. Its applications spread from low horsepower to the multi-megawatt due to its wide power, torque, speed ranges, high efficiency, fast response, and simple and continuous control characteristics. The speed of DC motor can be changed by controlling the armature and field voltages. The dynamic regimes of DC motor, such as starting and stopping, occur very often during normal work [14].

Conventional DC motors have many properties such as high efficiency and linear torque-speed characteristics. The control of DC motor is also simple and does not require much complex hardware. However, the main drawback of the dc motor is the need of periodic maintenance. The Brushes of the mechanical commutator eventually wear out and need to be replaced. The mechanical commutator has other undesirable effects such as sparks, acoustic noise and carbon particles coming from the brushes with rapid developments in power electronics, power semiconductor technologies, modern control theory for motors and manufacturing technology for high-performance magnetic materials.

DC motors were the first type of motor widely used and the systems (motors and drive) initial costs tend to be typically less than AC systems for low power units, but with a higher power, the overall maintenance costs increase and would need to be taken into consideration. The DC Motors speed can be controlled by varying the supply voltage and are available in a wide range of voltages, however, the most popular type are 12 & 24V, with some of the advantages being:

- Easy installation
- Speed control over a wide range
- Quick Starting, Stopping, Reversing and Acceleration
- High Starting Torque
- Linear speed-torque curve

DC motors are widely used and can be used from small tools and appliances, through to electric vehicles, lifts & hoists. The two common types are:

2.5.1 Brushed DC Motor

These are the more traditional type of motor and are typically used in cost-sensitive applications, where the control system is relatively simple, such as in consumer applications and more basic industrial equipment, these type of motors can be broken down as:

Series Wound – This is where the field winding is connected in series with rotor winding and speed control is by varying the supply voltage, however, this type offers poor speed control and as the torque to the motor increase, then the speed falls. Applications include automotive, hoists, lifts and cranes as it has a high starting torque.

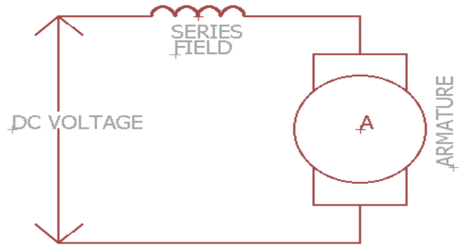

Figure 2. 4: DC Series Motor [27]

The series motor is widely known as series wound motor. In a DC series motor the field winding is connected in series to the armature winding. The field strength varies with the variation in armature current. The series motor provides high starting torque and is commonly used for starting high inertia loads, such as trains, elevators, etc. The speed of a series motor varies widely between the no-load and the full load conditions. Series motor cannot be used where a constant speed is required under varying loads; this is because the velocity of this motor varies greatly with the varying load [30]. A series motor should never be started with no load, because with no mechanical load the current is low, so the back emf is weak and the armature starts rotating faster to produce sufficient back emf to balance the supply voltage, and the motor can get damaged due to over speed, the speed of a series motor with no load increases to a point where the motor could get damaged therefore some load should always be connected to a DC series motor. The series motor is also known as universal motors as they can also be operated on alternating current as well as direct current. Since armature voltage and the field direction reverses at the same time, torque is continuously produced in the same direction; however it runs at lower speed with low torque on AC supply as compared to the DC supply [31]. Series motors have many advantages such as it has high starting torque, motor is cost-efficient, easy to design and maintain simple construction, etc.

Shunt Wound – This type has one voltage supply and the field winding is connected in parallel with the rotor winding and can deliver increased torque, without a reduction in speed by increasing the motor current. It has a medium level of starting torque with constant speed, so suitable for applications include lathes, vacuum cleaners, conveyors & grinders. In a DC shunt motor the field winding is connected in parallel (shunt) to an armature with the common DC power supply. The field winding can be either separately excited or be connected to same source as that of the armature. DC shunt motors have different working characteristics than that of DC series motor. The shunt Connected motors offer good speed regulation but does not have as much starting torque as that in DC series motor [10]. Due to its ability of self-regulation the switching of motor from no load to full load conditions there is no considerable change in its running speed. As the shunt field coil is made up of thin wire it cannot produce large current for starting like in DC series motor, this implies that DC shunt motors have extremely low starting torque [30]. The DC shunt motors have best speed regulation.

In a shunt motor as the input voltage is supplied it first passes through the field winding and the armature current slowly increases as the current in the field winding decreases.

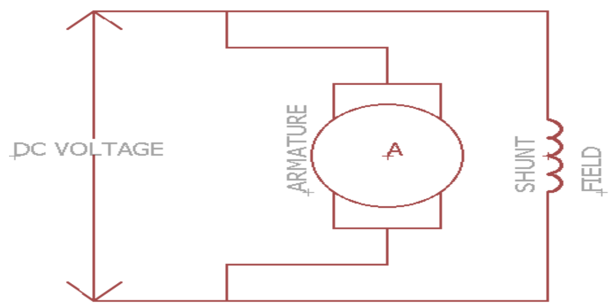

Figure 2. 5: Common Source DC Shunt Motor [33]

This is given by an equation i.e. $I_a = I_t - I_f$.

Where

I_t = Total Current

I_a = Armature current

I_f = Field current

Simple control performance results in high flexibility for solving complex drive problems. Very smooth running, therefore low mechanical stress and high dynamic control process. The motor has low speed and wide control range this characteristic makes it preferable to be used in industries on a large scale.

Compound Wound – This is a cumulative of Series and Shunt, where the polarity of the shunt winding is such that it adds to the series fields. This type has a high starting torque and runs smoothly if the load varies slightly and is used for driving compressors, variable-head centrifugal pumps, rotary presses, circular saws, shearing machines, elevators and continuous conveyors. Compound motors have a field connected in series with armature and a separately excited shunt field; hence it provides the characteristics of both series as well as shunt DC motors. The series field provides better starting torque and a shunt field provides better speed regulation.

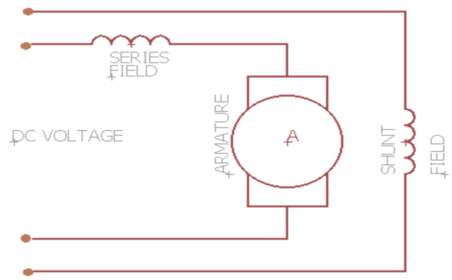

Figure 2. 6: Compound Motor [27]

Permanent Magnet – As the name suggests rather than electromagnet a permanent magnet is used and is used in applications where precise control and low torque, such as in robotics, servo systems. A permanent magnet motor does not have a field winding; instead, it uses permanent magnet to supply the field flux. A permanent magnet motor has a good starting torque along with a better speed. As the field supply is fixed due to permanent magnet and cannot be varied, this motor does not have an adjustable speed control function. So the permanent magnet field is well-preferred in small motors. However, large permanent magnets are costly, as well as dangerous and difficult to be assembled, this favors wound fields for large machines.

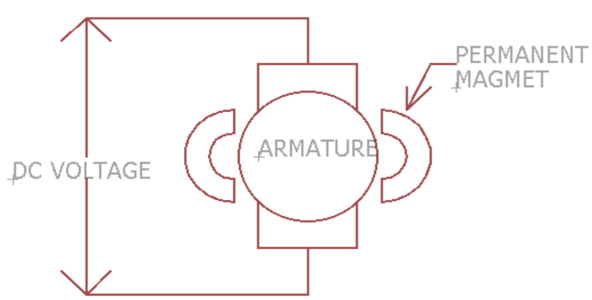

Figure 2. 7: Permanent Magnet Motor [32]

Permanent magnets are best suited for small motors to eliminate the power consumption of the field windings. To minimize the overall weight and size permanent magnet motors may use high energy magnets. The major disadvantage of permanent magnet DC motor is that they are limited to the amount of load, due to its preferred smaller size. These motors are also found to have low horsepower applications. Another disadvantage is that its torque is limited to 150% of the rated torque to prevent demagnetization of the permanent magnets used in the motor.

2.5.2 Brushless DC Motor

Brushless motors alleviate some of the issues associated with the more common brushed motors (short life span for high use applications) and are mechanically much simpler in design (not shaving brushes). The motor controller uses Hall Effect sensors to detect the position of the rotor and using this controller can accurately control the motor via current in the rotor coils to regulate the speed. The advantages of this technology are long life, little maintenance and high efficiency (85-90%), whereas the disadvantages are higher initial costs and more complicated controllers. These types of motors are generally used in speed and positional control with applications such as fans, pumps and compressors, where reliability and ruggedness are required.

The Brushless DC (BLDC) motors have been widely used in many applications. BLDC Motor has many advantages over conventional DC motors [42]. Brushless motor technology makes it possible to achieve high reliability with high efficiency, and for a lower cost in comparison with brush motors. Although the Brushless characteristic can be applied to several kinds of motors – AC synchronous motors, stepper motors, switched reluctance motors, AC induction motors - the BLDC motor is conventionally defined as a permanent magnet synchronous motor with a trapezoidal Back EMF waveform shape. Permanent magnet synchronous machines with trapezoidal Back-EMF and (120 electrical degrees wide) rectangular stator currents are widely used as they offer the following advantages. first, assuming the motor has pure trapezoidal Back EMF and that the stator phases commutation process is accurate, the mechanical torque developed by the motor is constant; secondly, the Brushless DC drives show a very high mechanical power density. Brushless Direct Current (BLDC) motors are one of the motor types rapidly gaining popularity. BLDC motors are used in industries such as Appliances, Automotive, Aerospace, Consumer, Medical, Industrial Automation Equipment, and instrumentation. [39] as the name implies, BLDC motors do not use brushes for commutation; instead, they are electronically commutated. BLDC motors have many advantages over brushed DC motors and induction motors. Better speed versus torque characteristics, High dynamic response, High efficiency, long operating life, Noiseless operation, and higher speed ranges. In addition, the ratio of torque delivered to the size of the motor is higher, making it useful in applications where space and weight are critical factors. BLDC Motors are available in many different power ratings, from very small motors as used in hard disk drives to larger motors used in electric vehicles. [27]

The Brushless direct current (BLDC) motor is gaining grounds in the industries, especially in the areas of appliances production, aeronautics, medicine, consumer and industrial automation and so on. The BLDC are typically permanent synchronous motor; they are well driven by dc voltage. They have a commutation that is done mainly by electronics applications. Some of the many advantages of a Brushless dc motor over the conventional brushed dc motors are highlighted. [3]

1) Better speed versus torque characteristics 2. High dynamic response
3) High efficiency 5. Long operating life 6. High speed ranges
4) Low maintenance (in terms of brushes cleaning; which is peculiar to the brushed dc motor).

One of the major differences between the DC motor and the BLDC is implied from the name. The conventional dc motor has brushes that are attached to its stator while the "brushes" DC motor does not. Also, unlike the normal DC motor, the commutation of the BLDC could be done by electronic control [10 on page 23]. Under the BLDC motor, the stator windings are energized in sequence for the motor to rotate. More also, there is no physical contact whatsoever between the stator and the rotor. Another vital part of the BLDC is the hall sensor(s); these hall sensors are systematically attached to the rotor and they are used as major sensing devices by the Hall Effect sensor embedded into the stator [30 on page 39]. This works based on the principle of the Hall Effect. The BLDC motor operates in many modes (phases), but the most common is the 3-phase. The 3-phase has better efficiency and gives quite low torque. Though it has some cost implications, the 3-phase has a very good precision in control [31]. And this is needful in terms of the stator current.

2.6 Converting an AC Refrigerator to DC Refrigerator

This section presents the design considerations and procedures for converting a conventional AC refrigerator to serve as a stand-alone solar-powered DC refrigerator. Theoretically, the domestic refrigerator comprises of a thermally insulated cabinet and a vapour-compression refrigeration loop. In conventional refrigerators, the refrigerant is circulated by an AC compressor relying on AC power source. To convert such a system to a stand-alone DC power dependent, the AC compressor of the cooling unit is replaced with an equivalent DC compressor. This makes it possible to power the system with direct current from a stand-alone solar PV system without an inverter. Therefore the major work of the conversion process is based on the selection of an appropriate DC compressor to replace the existing AC compressor. Apart from the bulb inside the refrigerator cabinet, all other components such as the evaporator, condenser, capillary tube, and thermostat do not require replacement. The next section looks at the procedure used to assess the AC refrigerator to be converted.

Solar energy is geographically distributed and highly dependent on location, changing weather and climate conditions. This makes their direct control extremely challenging and requires proper sizing and system optimization to ensure maximum power generation. This section discusses the approach used in sizing the various components of the system (solar PV Panel, Charge controller and battery Bank). The schematic of the solar PV refrigeration system is shown in Figure 3.25. It is composed of four major parts; i) the refrigeration unit (refrigerator), ii) the energy production unit (PV panels), iii) the energy control unit, and iv) the energy storage unit (the battery bank).

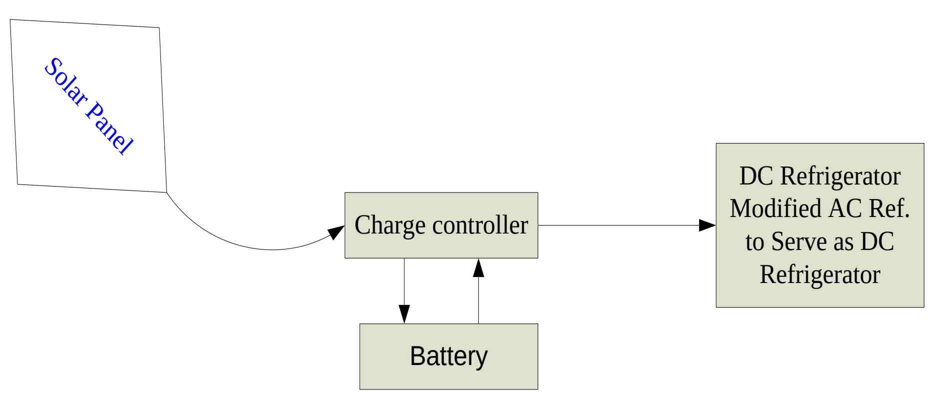

Figure 2. 8: Schematic of the Solar Powered DC Refrigeration System [29]

2.7 Performance Evaluation of DC Distribution System over the AC Existing System on home Appliance

To do the comparative analysis of AC and DC power distribution which is evaluating the performance of home appliances or equipment that is supplied power from solar PV System. It generates DC output and then distributes the power either AC system or DC system. Most of the residential home appliances are DC end users. But in long time the power distribution has been used predominantly by alternative current system. The DC distribution system is more advantages in dc end-user home appliances with highly efficient than that of AC system.

$$\eta = \frac{P_{out}}{P_{in}} * 100\% \tag{2.1}$$

Where:

η: $Efficiency$

Pout: Converter Output Power

Pin: Converter Input Power

$$P_{in} = P_{out} + P_{loss} \tag{2.2}$$

The efficiency becomes

$$\eta = \frac{P_{out}}{P_{out} + P_{loss}} * 100\% \tag{2.3}$$

Where, loss: Converter power loss

The converter power loss becomes:

$$P_{loss} = P_{out} \frac{(1-\eta)}{\eta} \tag{2.4}$$

The total power loss of the AC system becomes:

$$P_{Total\ loss} = (I_{ac}^{2} * R) + P_{out} \frac{(1-\eta)}{\eta} \tag{2.5}$$

For known value of efficiency of AC-DC converter and load power, the energy loss during the operation of the equipment can be obtained as:

$$E_{loss} = P_{Total\ loss} * T \tag{2.6}$$

Where:

$ELoss$: Energy loss

T: Time period

The power loss on the connecting wire:

$$P_{loss} = I_{dc}^{2} * R \tag{2.7}$$

The total power loss of the DC system becomes:

$$P_{Total\ loss} = (I_{dc}^{2} * R) + P_{out} \frac{(1-\eta)}{\eta} \tag{2.8}$$

The energy loss of the DC-DC converter is determined from the power loss and duration of the operation of the equipment as seen in Equation (3.53). Smaller total power loss in the system means smaller Energy loss.

2.8 Summary of Modes of PV Powering DC motor with Solar Energy

The power delivered by a photovoltaic cell is not enough to supply a DC load like motor-mill group. It is necessary to associate multiple solar cells in series and in parallel to have a solar panel and attain the desired power. Similarly, the interconnection of several solar panels in series and in parallel enables us to obtain a power higher than that of the solar panel; that is why the notion of PV generator is created [44].

Providing solar energy for off-grid refrigeration normally requires four major components namely, solar PV generator (module), battery backup, inverter, charge controller if not included in the inverter. In the current study, the use of inverter was eliminated because the load (refrigerator) requires the supply of direct current from the PV generator. Therefore, in this thesis, the selected type of components are from the above reviews the Lithium-ion battery, Brushless DC motor, 300-watt refrigerator for the manner of modeling and simulating.

CHAPTER THREE

METHODOLOGY

3.1 Introduction

In chapter two, the Literature and background of different parameters of PV-powered dc derive appliance in the dc distribution system have been discussed. The major causes of problems and options to reduce them are highlighted with reference to different Authors. Under this chapter, data have been collected and analyzed. After analysis of the data, mitigation solutions have been proposed.

The collected data have been analyzed and the levels of the disturbances have been compared to the existing AC distribution system. The schematic diagram of PV-powered dc derive appliance in the dc distribution system shown in [APPENDIX-A3].

- DC distribution system with an electrical load power capacity of 300W for the refrigerator.
- For other DC home appliances load power is 1300 W, totally 1600 W and 48Vdc rating system voltage is forecasted or designed.

Several criteria are considered in the model design of the DC House. Since the MATLAB along with its tool boxes in Solar PV Systems to promote Modeling, and Simulation with emphasis on Analysis, and Design. In renewable energy systems applications, MATLAB helps for selecting the matrix manipulations in the converters to grid inverter, plotting of functions and data, implementation of MPPT algorithms, creation of user interfaces for monitoring the Solar PV modules and for interfacing with inverters and converters, wherein which control algorithms would be written in other languages. In addition, such models discussed in this chapter would provide a tool to predict the behavior of solar PV cell, module and array, charge controller, SOC battery, inverter, and MPPT, under climate and physical parameters changes.

3.2 Design Procedure of solar-powered system

In this section design the Performance Evaluation and Optimizations of PV Powered DC Motor-Driven Appliance at selected site and home equipment of refrigerator. This design is depends on Collect data of site and desired parameter of the system that the design follows the procedure of system to get complete new model and simulation is shown in the below diagram.

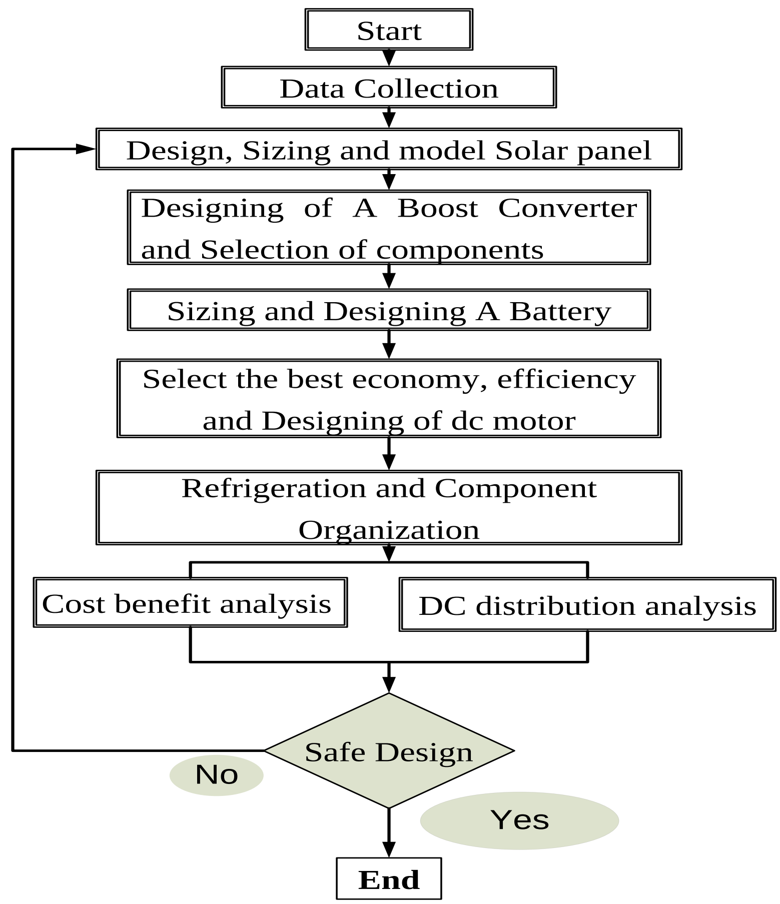

Figure 3. 1: Schematic diagram of design procedure of solar power refrigerator

3.2.1 Solar Resource Assessment of Selected Site

Data of selected site solar radiation is collected from Photovoltaic Geographical Information System (PVGIS). In this section solar radiation data is obtain from PVGIS by inserting required parameter as shown in below figure.

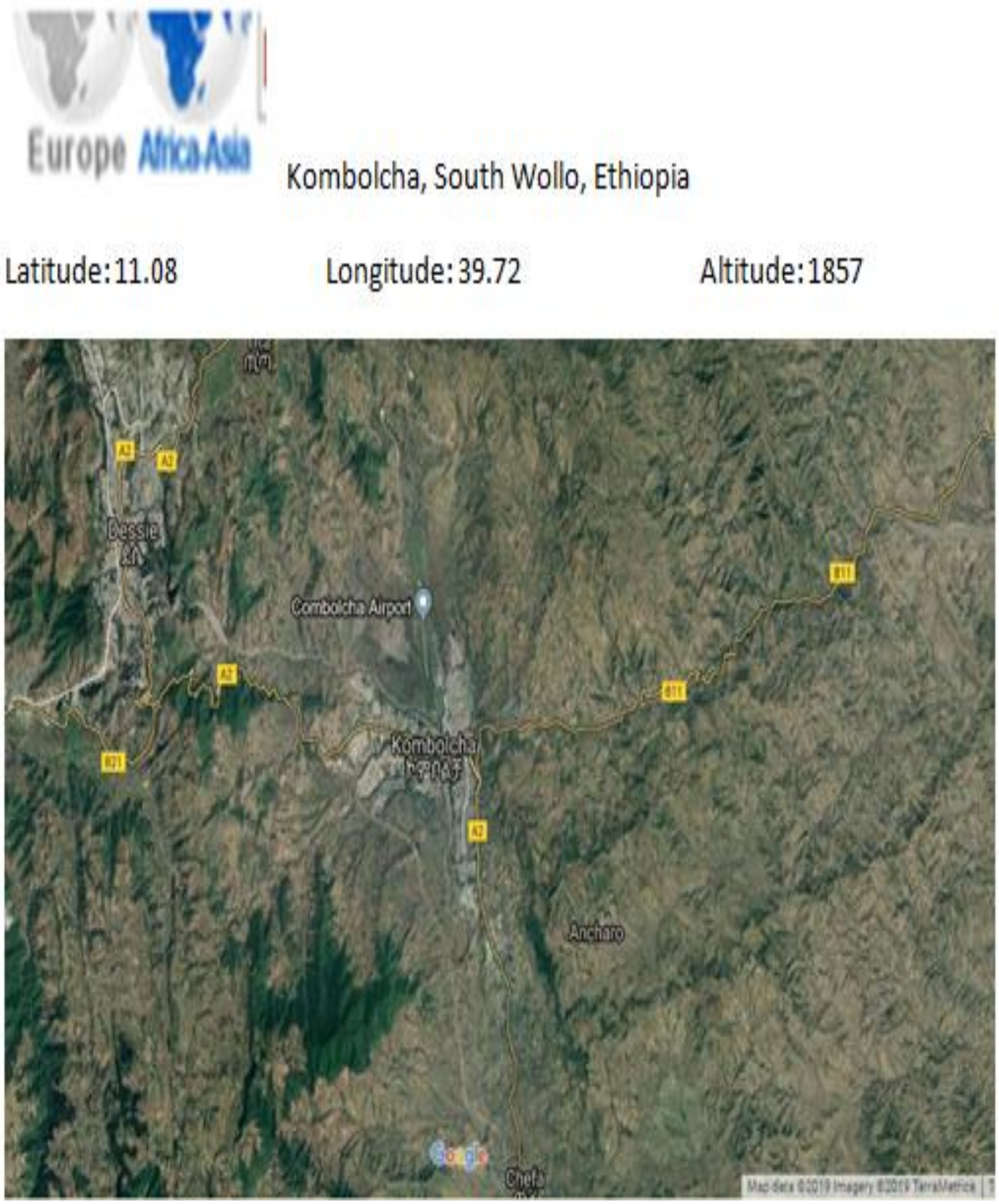

Figure 3. 2: South wollo kombolcha PVGIS solar radiation data

PVGIS estimates of solar electricity generation

Location: 11.08° North, 39.72° East, Elevation: 1857 m a.s.l.

Solar radiation database used: PVGIS.

Table 3. 1: PVGIS estimates of solar electricity generation

Fixed system: inclination= 9.6°, Orientation= 0°					Earth Temperature ℃
Month	E_d	E_m	H_d	H_m	
Jan	5.17	160	7.12	221	9.5
Fed	5.44	152	7.56	212	11.4
Mar	5.28	164	7.37	228	13.2
Apr	4.59	138	6.36	191	14.3
May	4.48	139	6.17	191	14.9
Jun	4.52	136	6.16	185	15.2
Jul	4.64	139	6.38	198	15.3
Aug	4.43	137	6.02	187	15.1
Sep	4.74	142	6.58	197	14.1
Oct	4.85	150	6.76	209	11.6
Nov	5.1	153	7.04	211	9.5
Dec	5.13	159	7	217	8.5
Yearly average	4.86	148	6.7	204	12.72
Total for year	1770		2450		

E_d: Average daily electricity production from the given system (kWh)/day

E_m: Average monthly electricity production from the given system (kWh)

H_d: Average daily sum of global irradiation per square meter received by the modules of the given system (kWh/m2)/day

H_m: Average monthly sum of global irradiation per square meter received by the modules of the given system (kWh/m2).

Table 3. 2: Annual irradiation shortage due to shadowing (horizontal)

Month	Hh	Hopt	H(90)	Iopt
January	6330	7070	5200	39
February	6720	7220	4150	29
March	6620	6750	2530	13
April	6520	6350	939	-4
May	6910	6460	889	-18
June	6800	6230	872	-25
July	6570	6090	898	-22
August	6620	6330	911	-10
September	6770	6780	1940	7
October	6710	7060	3510	23
November	6650	7350	5030	36
December	6270	7090	5550	41
Year	6620	6730	2690	12

Where, H_h: Irradiation on horizontal plane (Wh/m2/day), H_{opt}: Irradiation on optimally inclined plane (Wh/m2/day), $H_{(90):}$ Irradiation on plane at angle: 90deg. (Wh/m^2/day)

I_{opt}: Optimal inclination (deg.)

3.2.2 Collected site data from NASA

Latitude 11.08 / Longitude 39.72 were chosen.

Elevation: 1857 meters

Geometry information is taken from the NASA GEOS-4 Model elevation

Northern boundary

12

Western boundary **39**

Center

Latitude **11.08**

Longitude **39.72**

Eastern boundary **40**

Southern boundary **11**

Table 3. 3: monthly solar radiation data from NASA

Table Monthly Averaged Clear Sky Insolation Incident On A Horizontal Surface (KWh/m^2/day)												
Lat. 11.08 Lon. 39.72	Jan	Feb	Mar	Apr	May	Jun	Jul	Aug	Sep	Oct	Nov	Dec
22-year average	6.43	6.97	7.24	7.2	6.88	6.4	6.35	6.57	6.65	6.68	6.4	6.2

3.3 Method of solar energy determination on the plane of the PV panel

The solar radiation is very important in calculating the amount of electricity generated by PV modules. The long term statistical data of solar sunshine hour is also very significant in deriving an equation to calculate the solar radiation, and to know the amount of energy generated by solar array. However, solar radiation could be generated by the mathematical model which is developed based on the meteorological sunshine hour data. The analysis follows from extra-terrestrial solar radiation calculation, monthly average terrestrial solar radiation determination up to daily solar radiation on the plane of solar module for the site. The algorithm used to calculate the radiation on the plane of the solar array would be shown as follows:

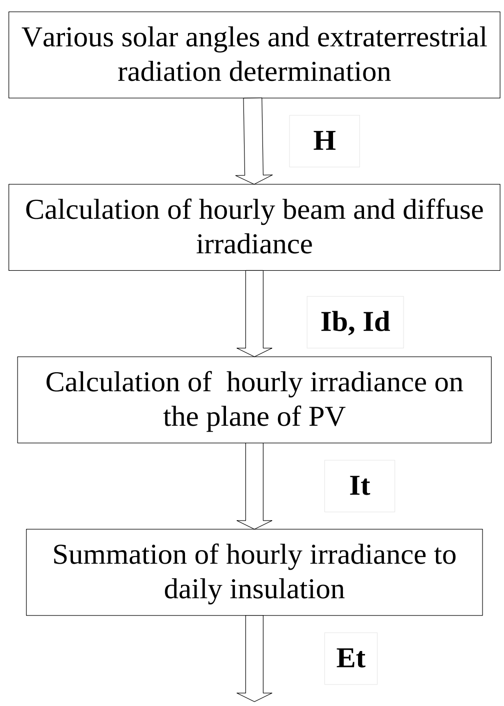

Figure 3. 3: Flow Showing the Determination of Solar Energy on the Plane of PV Panel

3.3.1 Sizing of the PV system

Sizing of the photovoltaic system is based on the worst operating condition. For the purpose of the solar PV system design, solar data is available but check by numerically analysis in this method uses the minimum monthly solar irradiation. Since, August month is minimum solar irradiation as shown in table 3-1 assume August 16 i.e. N=228 is chosen for PV sizing, and the declination angle can be calculated using the declination δ can be found from the approximate equation. [51] In equation (3-1).

$$\delta = 23.45 \sin(360 \frac{284+n}{365}) \tag{3.1}$$

$\delta = 23.45 \sin(360 \frac{284+228}{365}) = 13.5°$, as shown in Table 2.1.

Solar time is the time used in all of the sun-angle relationships; it does not coincide with local clock time. It is necessary to convert standard time to solar time by applying the sun takes 4min to transverse 1◦ of longitude and the equation of time, which takes into account the perturbations in the earth's rate of rotation which affect the time the sun crosses the observer's meridian. The difference in minutes between solar time and standard time is

Hour angle ω and solar time ST in an hour are related as equation (3.2).

Assuming 1:15 PM for the selected site:

$$\text{Solar time - standard time} = 4(\text{Lst- Lloc}) \tag{3.2}$$

ω = (Lst -12hr.) *15°

ω = (Lst -12hr.) *15° = 18.75°

where Lst is the standard meridian for the local time zone, L_{loc} is the longitude of the location in question, and longitudes are in degrees west, that is, $0◦ < L < 360◦$. Here, 1:15PM = 7:15hr at night in local time and the solar time is by minus 12 O, clock. Then it yields 7:15hr at day time.

For the horizontal surface, zenith (θz) can be calculated using equation (3.3).

$$\cos \theta z = \cos\phi \times \cos\delta \times \cos \omega + \sin \delta \times \sin \phi \tag{3.3}$$

$\cos \theta z = \cos 11.08° \times \cos 13.5° \times \cos 18.75° + \sin 13.5° \times \sin 11.08° = 0.948$

Where, the latitude ϕ of the site is 11.08°.

$\theta z = 18.56°$

The relationship for the angle of incidence of surfaces sloped due north or due south can be derived. From the fact, that is surfaces with slope β to the north or south have the same angular relationship to beam radiation as a horizontal surface at an artificial latitude of (ϕ − β). Slope β for all year $\beta = \phi$, for summer $\beta = \phi$- (10° - 15°) and for winter $\beta = \phi +$ (10° - 15°) (3.4)

$$\text{Cos } \theta = \cos \delta \times \cos \omega \times \cos (\phi\text{-}\beta) + \sin \delta \times \sin (\phi\text{-}\beta) \quad (3.5)$$

$$\text{Cos } \theta = \cos 13.5° \times \cos 18.75° \times \cos (11.08 - 11.08)° + \sin 13.5° \times \sin (11.08 - 11.08)° = 0.920766$$

$\theta = \cos^{-1}$ (0.920766) = 22.96° $\quad \therefore \theta = 22.96°$

The above calculation depends on the worst operating month and its design serve as for all month in the year. Even if the month august is categorize under summer, it is used for all year then $\beta = \phi$ that means the altitude and slope angle is equal to calculate the incident angle.

Where: δ is the declination (°) calculated from (3-1) and ϕ is the site's latitude (°)

3.3.2 Estimation of Solar Radiation

The solar radiation passing through the atmosphere and reaching the earth's surface is classified into two components:

- **Beam radiation I_b**: is radiation scattered by aerosols, dust, and molecules. It does not have a unique direction. The solar radiation propagating along the line joining the receiving surface and the sun. It is also referred to as direct radiation.
- **Diffuse radiation Id**: is the solar radiation scattered by aerosols, dust, and molecules. It does not have a unique direction.

The total radiation I: is the sum of the beam and diffuse radiation and is sometimes referred to as the global radiation.

Estimation of Clear Sky Radiation on Horizontal Surface

A simple model for the estimation is the transmittance of beam radiation in clear sky conditions. The inputs needed are the altitude of the location A in km above mean sea level, day number of the year N and the zenith angle (θz). Combined with Liu and Jordan's model for the transmittance of diffuse radiation through clear sky, the clear sky beam, and diffuse radiation can be easily computed [51].

The clear sky beam radiation on a horizontal surface is:

$$I_b = I_n \tau_b \cos \theta z \quad (3.6a)$$

Where: I_b is beam radiation on a horizontal surface, τ_b is the transmittance of the standard atmosphere for beam radiation through clear sky.

$$In = Isc[1.0 + 0.033\cos(\frac{360n}{365})]$$

Where *Isc* is the solar constant in watts per square meter, and *n* is the day of the year. I_n for a horizontal surface at any time between sunrises and sunset is Isc=1367w/m^2 that the solar constant, the mean radiation flux density outside of the earth's atmosphere, is 1367 W/m2 (within $\pm$1%), with most of the radiation in a wavelength range of 0.3 to 3 μm.

$$In = 1367 w/m^2 \ [1.0 + 0.033 \cos(\frac{360*228}{365})] = 1335 \ w/m^2$$

$$\tau_b = a_0 + a_1 e^{(-k/\cos\theta z)} \quad (3.6b)$$

$a_o = a_o^* r_o$, $a_1 = a_1^* r_1$, $k = k* r_k$

The constants a_0, a_1, and k for the standard atmosphere with 3km visibility are found from a_0*, a_1*, and $k*$ respectively and those constants are unit less, which are given for altitudes less than 2.5km by;

Where,

$a_o* = 0.4237 - 0.00821(6 - A)^2$

$a_1 * = 0.5055 + 0.00595(6.5 - A)^2$

$k* = 0.2711 + 0.01858(2.5 - A)^2$

$r_o = 0.95$, $r_1 = 0.91$, $r_k = 1.02$ are given in the 2km visibility, A= altitude or elevation of the site in (1.857km) =1857m

Where A is an altitude of the observer in kilometers, (Hottel also gives equations for a_0*, a_1*, and $k*$ for a standard atmosphere with 2km visibility.) Correction factors are applied to a_0*, a_1*, and $k*$ to allow for changes in climate types. The correction factors $r_0 = a_0/a_0*$, $r_1 = a_1/a_1*$, and $r_k = k/k*$ are calculated. Thus, the transmittance of this standard atmosphere for beam radiation can be determined for any zenith angle and any altitude up to 2.5km.

$a_o* = 0.4237 - 0.00821(6 - 1.857)^2 = 0.283$

$a_1 * = 0.5055 + 0.00595(6.5 - 1.857)^2 = 0.634$

$k* = 0.2711 + 0.01858(2.5 - 1.857)^2 = 0.279$

Therefore,

$a_o = a_o* ro = 0.283 \times 0.95 = 0.2688$

$a_1 = a_1 * r_1 = 0.634 \times 0.91 = 0.5769$

$k = k * r_k = 0.279 \times 1.02 = 0.2846$

Substitute the values into equation 3-6(b) gives:

$\tau_b = 0.2688 + 0.5769\, e^{-0.2846/\cos 18.56} = 0.741$

Then using equation 3-6(a) to calculate beam radiation

$I_b = 1335 w/m^2 \times 0.741 \times \cos 18.56° = \mathbf{937.7857 w/m^2}$

The transmittance of diffuse radiation through clear sky can be estimated from the beam radiation transmittance based on the study of Liu and Jordan:

$\tau_d = 0.271 - 0.2939\,\tau_b = 0.271 - 0.2939 \times 0.741 = 0.053$

where the transmittance beam and diffuse is have no unit or it is unit less.

The clear sky diffuse radiation is:

$$I_d = I_n \tau_d \cos \theta z \qquad (3.7)$$

$I_d = 1335\ w/m^2 \times 0.053 \times \cos 18.56° = \mathbf{67 w/m^2}$

Therefore, the total clear sky radiation on a horizontal surface could then be estimated as:

$$I_n = I_b + I_d \qquad (3.8)$$

$I_n = 937.7857 w/m^2 + 67 w/m^2 = \mathbf{1005 w/m^2}$

Estimation of Solar Radiation on Inclined Surface

The following formula was given by Liu and Jordan (1962), for evaluating the total radiation on a surface of arbitrary orientation from knowledge of beam and diffuses radiation on horizontal surface.

$$I_T = I_b R_b + I_d R_d + r R_r\,(I_b + I_d) \qquad (3.9)$$

Where: I_T = Total reflected radiation

r = reflectivity of the ground = 0.2.

R_b, $R_{d,}$ and R_r are known as conversion factors for beam, diffuse and reflected components respectively.

The expressions for these are as follows:

R_b: is defined as the ratio of flux of beam radiation incident on an inclined surface to that on a horizontal surface. The flux of beam radiation incident on a horizontal surface (Rb) is given by:

$$R_b = \frac{\cos\theta}{\cos\theta_z} = \frac{\cos 22.96°}{\cos 18.56°} = 0.97129$$

R_d: is the ratio of the flux of diffuse radiation falling on the tilted surface to that on the horizontal surface. This conversion factor depends on the distribution of diffuse radiation over the sky and on the portion of sky seen by the surface.

$$R_d = \frac{1+\cos\beta}{2} = \frac{1+\cos 11.08°}{2} = 0.991$$

R_r: The reflected component comes mainly from the ground and other surrounding objects.

$$R_d = \frac{1-\cos\beta}{2} = \frac{1-\cos 11.08°}{2} = 0.0093$$

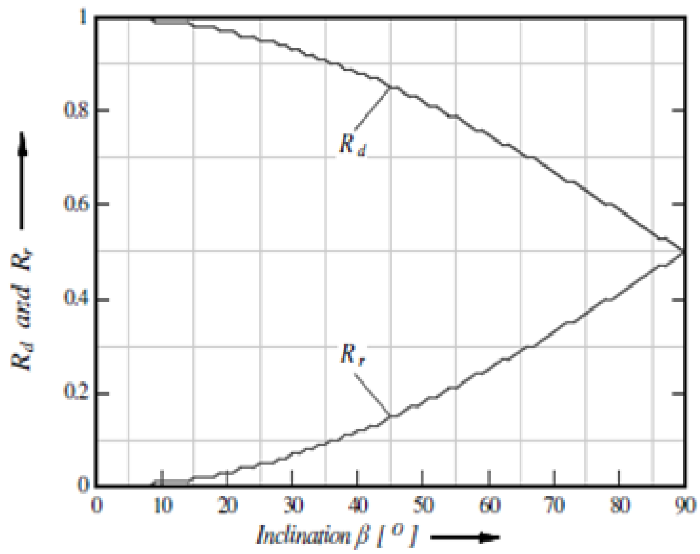

Figure 3. 4: variation of Rd and Rr with inclination

In this case (**β** = 11.08), Rd=0.991 and Rr = 0.0093

This indicates that small slop planes receive little reflected radiation and more deflection radiation. Using equation 3-9 to determine solar radiation on inclined surface:

I_T = 937.7857w/m^2 × 0.97129 + 67w/m^2 × 0.991 + 0.2 × 0.0093(937 + 67)w/m^2

I_T =911w/m^2 +66.397w/m^2+1.8689 w/m^2 = 979.24 ≈ 979w/m^2

I_T = **979 w/m^2.**

August month is minimum solar radiation in a selected site, but the calculated total solar radiation above that taken from data collection. Therefore solar radiation of selected sites is enough for this system.

3.4 Peak Sun Hours

For the purpose of the solar PV system design, the minimum monthly solar irradiation is used in determining the peak sun shine hours. This approach is usually required for the design of solar PV systems (designing for worst conditions).

The performance of solar PV system depends largely on the peak sun hours of the location of application. The peak sun hour(s) of an area is determined from the available solar irradiance of the location. The peak sun hours and total irradiation are related by Equation 3-10

$$PSH = \frac{\text{Irradiation}[\text{Wh/m}^2\ /\text{day}]}{\text{Peak sun}[\text{W/m}^2]} \tag{3.10}$$

After comparing the collected data of PVGIS and NASA, take the minimum solar radiation. Now by definition Peak Sun hour is equivalent to calculated irradiance 979[w/m2], the number of peak sun hours can be obtained by equation 3-10 using minimum monthly solar irradiation data in August is 6.02kwh/m^2 from Table 3-2.

$$PSH = \frac{\text{Irradiation}[\text{Wh/m}^2/\text{day}]}{\text{Peak sun}[\text{W/m}^2]} = \frac{6020\ \text{Wh/m}^2}{979\text{W/m}^2} = 6.149 hr/day \text{(this PSH is in August).}$$

3.5 Sizing of PV Panel

This study outlines the design process that must be completed before the purchase and installation of any PV system components. The process includes the following steps:

- Estimating electric loads
- Sizing and specifying PV modules
- Sizing and specifying batteries
- Specifying a charge controller
- Sizing and specifying an inverter
- Sizing system wiring

This method is not biased toward any product but will result in generic product specifications for the system. Each step is described in the following sections based on the following design situation. Design Situation:

*******Design a Stand-Alone PV System for the following household electrical appliances:

Step 1: Load Assessment

The PV System is designed to operate the loads as given in the table below.

Table 3. 4: Load Assessment

Devices/ Appliances	Quantity	Output Wattage	Hours per day	Watt-Hours per day
Laptop	1	19V x 5A= 95W	x 6	x 1 unit =570 Whr/d
Phones	2	5V x 1A= 5W	x 2.5	x 2 unit = 25 Whr/d
Stove	1	24V x 33A= 800W	x 6	x 1 unit = 2400 Whr/d
Stabilizer	1	13V x1.2A = 15.6W	x 10	x 1 unit =156 Whr/d
LED Bulb	5	48V x 0.15A = 7.2 W	x 8	x 5 unit =288 Whr/d
DC Bath Fan	1	12V x 3A = 36W	x 1	x 1 unit =36 Whr/d
water purifier	1	12V x0.92A = 11W	x 2	x 1 unit = 22 Whr/d
DC Oven vent	1	12V x1.3A = 15.6W	x 0.5	x 1 unit = 7.8 Whr/d
DC Fans	2	12V x 3A = 36W	x 4	x 2 unit = 288 Whr/ d
Refrigerator	1	48V x 6.25A = 300W	x 10	x 1 unit =3000 Whr/d
32 inch TV	1	24V x5A=120W	x 4	x 1 unit = 480 Whr/ d
Radio	1	12V x 1.7A = 20W	x 9	x 1 unit = 180 Whr/d
Washing machine	1	24v x 3.0 = 70W	x 2	x 1 unit = 140 Whr/d
Total	**1591.2W≈ 1600W**			**7592.8 ≈7600 Whr/d**

*** The refrigerator has power rating of 300 W, daily energy of 3000 Whr/d (3kwhr/d) and 48V system voltage. Therefore, the annual energy can be calculated:

3000Whr/d*365day= 1095000Whr/year = **1095kwhr/y**

Step 2: PV Module Sizing

The module sizing is based on the month of August with the lowest figure for daily solar insolation.

$$\text{PV Module Size} = \frac{\text{Total Daily Watt Hours}}{\text{Average daily solar insulation}} \qquad (3.11)$$

$$\text{PV Module Size} = \frac{7600}{4.43} = 1715.575 = 1716 \text{ Watts}$$

where, 4.43 is from Table 3.1.

Taking into consideration of the temperature losses, battery efficiency and wiring losses, the 1716W should be increased according to typical loss percentages in a PV System as follows:

Typical percentages of the losses in a PV System are:

- 90% for temperature loss
- 99% for battery losses
- 97% for wiring losses

Total Losses = 0.90 × 0.99 × 0.97 = 0.86

PV Module Size = $\frac{1716}{0.86}$ = 1994.8554 Watts =**1995 Watts**

****** 10 each of 200W PV Modules are parallel connected together to deliver 2000 watt load of home appliances.

Step 3: Battery Sizing

In standalone PV Systems, the electrical energy produced by the PV array cannot always be used when it is produced, because the demand for energy does not always coincide with production. As such, electrical storage batteries are commonly used in PV Systems. When sizing the battery, the following factors have been taken into consideration:

- Battery Efficiency Most batteries have an efficiency of about 85%, but Li-ion= 99%+
- Allowable DOD The maximum percentage of full rated capacity that can be withdrawn from a battery is known as its Allowable Depth of Discharge. The allowable depth of discharge for Lithium-ion Batteries (Li-ion) Battery is 80%
- Days with no sunshine/number of days of autonomy generally expressed as the days of storage in a PV System, autonomy refers to the time a fully charged battery can supply energy to the systems loads when there is no energy supplied by the PV modules. The number of days of autonomy typically ranges from 2 to 6.

******* 3 days has been used as a good approximation for the number of no sun days in sizing the battery for this PV System.

$$\text{Battery Capacity} = \frac{\text{Daily energy load}}{\text{Battery Efficiency}} \tag{3.12}$$

$$\text{Battery Capacity} = \frac{7600\text{whr}}{0.99} = 7676.76 \text{ Watts hrs}$$

Multiplying by 3 (number of sun days)

Battery Capacity = 7676.7676 x 3 = **23030.3030 Watt Hrs**

Multiplying by 80% depth of discharge

Battery Capacity = 23030.303 × 0.8 = **18424 Watt Hrs**

However, batteries are usually rated in amp-hours:

$$\text{Amp Hours} = \frac{\text{Watt-Hours}}{\text{Volt}}, \text{ Battery Capacity} = \frac{18424\text{whr}}{48\text{V}} = 383.8383 \text{ Ah}$$

This is the rough calculation for the size of a home appliance you would need to keep up with a specific load, as an inverters efficiency is only rated around 85%, the current requirement will need to be 15% higher; for example, to keep up with a continuous draw of 18424W, you would need: Amp. Hours = (18424Whr/48V) *115% = (383.8383Ah)*1.15= 441.4141Ah = 445Ah. Amp. Hours = 445Ah

$$\text{Therefore, Hour} = \frac{\text{Ah}}{\text{A}} = \frac{445\text{Ah}}{2000\text{w}/48\text{V}} = \frac{445\text{Ah}}{41.6667\text{A}} = 10.68\text{Hours}$$

The maximum of one PV Module current is 6.67A. Then, the Battery capacity (Ah) of one PV Module is: 6.67A*10.68Hrs. = **71.24Ah.**

How many batteries are connected parallel and series strings?

The system/bus voltage is 48V and the battery voltage is also 48V. Then, a number of series PV module Battery = 1. But, number of parallel Batteries **= (445Ah÷ 71.24Ah) = 6.2465≈ 7**

*****Therefore, seven Lithium-ion Batteries are parallel connected for a capacity of 445Ah and 48V battery Voltage.

Step 4: Charge Controller Sizing

The primary function of a battery charge controller in a standalone PV system is to maintain the battery at highest possible state of charge while protecting it from overcharge by the array and from over-discharge by the loads.

A charge controller with a higher current rating than the maximum PV System and load current should be selected.

*__Module Current = 6.67 A__

The assumed load current drawn by table 5: Load Assessment current is the summation of individual devices, so it exceeds more than 6.67A or total load power divided by system voltage.

$$I_{ch.con} = \frac{\text{Total load power}}{\text{system voltage}} = \frac{2000w}{48V} = 41.66647A \cong 45A$$

*******Therefore, a 45A charge controller is selected for the stand-alone PV System.

Step 5: Inverter Sizing

An inverter is a piece of equipment that converts DC electricity into AC electricity, allowing the PV system to be used for appliances that require AC.

Most inverters have a DC to AC conversion efficiency of 85%.

A DC to AC inverter should be selected to match the PV system with the following characteristics (as calculated above):

- Peak Power = 1600W
- System Voltage = 48V
- Inverter Power Rating = 1600W

*****Dividing by 0.85 for Inverter Efficiency= $\frac{1600W}{0.85}$ = **1882.3529 W**

To calculate the approximate start-up load:

Power (Watts) × 2 = Start-up Load

This formula yields a close approximation of the starting load required by the appliance, although some appliances may require an even greater starting load.

Note: Induction motors such as air conditioners, refrigerators, freezers, and pumps may have a startup surge of up to seven times their continuous power rating. [10]

Most often the start-up load of the appliance or power tool determines whether an inverter has the capability to power it.

*Inverter continuous power rating = (1882.3529W) *2 = 3764.706W = **3765W**

Final Total = 3765 W

*******A 3765 W of 48V DC and 220V AC sine wave inverter is desirable for the PV System.

Step 6: Wire Sizing

The wiring is what carries the electricity from the panels through the charge controller to the batteries and from the batteries through the charge controller out to the loads. Two main considerations are the wire size and the terminations to avoid too much resistance to the flow of electricity.

A properly designed wiring system should have a voltage drop of not more than 5%, and, therefore, on a 48V system, voltage loss should not be more than 2.4V.

The wire-sizing chart below should be used to select the correct wire cross-section for a given current and length of wire. The voltage loss values given in the table are for 100m length of wire at a given current. The table can be used for lengths of wire that are less than 100m by first dividing the selected length by 100 and multiplying by the corresponding voltage drop given in the table to get the correct voltage drop. The wire cross-section that gives a voltage drop of less than 2.4V will be the most appropriate.

Wire Sizing

Whenever current passes through a wire, voltage is drop as a result of the resistance in the copper wire(s). In low voltage systems like the 48 Volt system, voltage loss is of significant importance. For example, losing 1volt on a 220V system only represents less than 1% of the voltage lost to resistance, but losing 1volt on a 48V system represents almost 2.083% which is quite significant. The amount of voltage that is lost for given wire size and current flow is based on how much wire there is, or the length of the wire.

A wire sizing chart is used to determine the wire size for a solar system.

It must be noted that voltage losses in the table are theoretical, calculated using Ohm's Law. As such the state of wires must be considered. In this thesis, $4mm^2$ is selected for 6.67A current. [APPENDIX A-2]

Area of solar panel would be calculated as flow:

Power requirement to operate other home appliance is 1300Wp and power requirement for refrigerator 300Wp. In this case total power requirement for solar powered is 1600Wp and the minimum solar radiation of site is $6.02kwh/m^2$. The efficiency of maximum power point of module is 19.5% as shown in [Index A-1] and efficiency of maximum power point of electronic is 80% -90% [19].

$$\text{Requirement power for home appliance (WP) x PSH} = \text{Area of PV panel x irradiation (kwh/m2) x } \eta_{pv} \text{ x } \eta_e$$

$$\text{Area of PV panel } (m^2) = \frac{\text{Requirement power for home appliance(WP) * PSH)}}{\text{Irradiation}(\frac{KWh}{m^2})* \eta_{PV} * \eta_e)} \tag{3.13}$$

$$\text{Area of PV panel } (m^2) = \frac{(1.6kw * 6.149hr)}{(6.02kwhr/m^2 * 0.195 * 0.85)} = 9.86m^2$$

Depending on the calculated area, select a standard PV panel of $9.86m^2$ it can produce 200W [Index A-1]. The selected PV panel can produce above required power. Therefore the design is safe.

Where: PSH is the peak sun hours of the location where the system would be installed.

3.6 MATLAB Model of Solar PV

The solar system configuration consists of a required number of solar photovoltaic cells, commonly referred to as PV modules, connected in series or in parallel to attain the required voltage output.

The basic equation from the theory of semiconductors that mathematically describes the I–V characteristic of the ideal PV cell is:

$$I = I_{pv,\,cell} - I_{o,\,cell}\left[\exp\left(\frac{qv}{\alpha KT}\right) - 1\right] \tag{3.14}$$

The basic (3.14) of the elementary PV cell does not represent the I–V characteristic of a practical PV array. Cells connected in parallel increase the current and cells connected in series provide greater output voltages. Practical arrays are composed of several connected PV cells and the observation of the characteristics at the terminals of the PV array requires the inclusion of additional parameters to the basic equation

$$I = I_{pv} - I_o\left[\exp\left(\frac{V + \mathrm{RsI}}{\alpha + V}\right) - 1\right] - \frac{V + \mathrm{RsI}}{\mathrm{Rp}} \tag{3.15}$$

All PV array datasheets bring basically the nominal open-circuit voltage ($V_{oc,n}$), the nominal short-circuit current ($I_{sc,n}$), the voltage at the MPP (V_{mp}), the current at the MPP (I_{mp}), the open-circuit voltage/temperature coefficient (K_V), the short circuit current/temperature coefficient (K_I), and the maximum peak output power (P_{max}). This information is always provided with reference to the nominal condition or standard test conditions (STC's) of temperature and solar irradiation.

The practical PV device has a series resistance R_s whose influence is stronger when the device operates in the voltage source region and a parallel resistance R_p with stronger influence in the current source region of operation. The assumption $I_{sc} \approx I_{pv}$ is generally used in the modeling of PV devices because in practical devices the series resistance is low and the parallel resistance is high. The diode saturation current is given by

$$I_o = \left[\frac{Isc,n + KI\Delta T}{\left(\frac{Voc,n + KV\Delta T}{\alpha Vt}\right) - 1} \right] \quad (3.16)$$

The saturation current Io is strongly dependent on the temperature so that the net effect of the temperature is the linear variation of the open-circuit voltage according to the practical voltage/temperature coefficient. This equation simplifies the model and cancels the model error at the vicinities of the open-circuit voltages, and consequently, at other regions of the I–V curve.

$$Ipv = (Ipv, n + KI\Delta T) \frac{G}{Gn} \quad (3.17)$$

The relation between R_s and R_p, the only unknowns of (3.18) may be found by making $P_{max,m}$ and solving the resulting equation for R_s, as shown

$$P_{max,m} = V_{mp} \{I_{pv} - I_0[\exp((\frac{q}{KT}) \frac{Vmp + RsImp}{\alpha Ns})\text{-}1] - \frac{Vmp + RsImp}{RP} \quad (3.18)$$

$$R_p = \frac{Vmp + RsImp}{\{VmpIp - VmpI0 \exp\left[\frac{q}{KT}\left(\frac{Vmp + RsImp}{\alpha Ns}\right)\right] + VmpI0 - Pmax,m\}} \quad (3.19)$$

Equation (3.19) means that for any value of Rs there will be a value of Rp that makes the mathematical I–V curve crosses the experimental (Vmp, Imp) point. The goal is to find the value of Rs (and hence, Rp) that makes the peak of the mathematical P–V curve coincides with the experimental peak power at the (Vmp, Imp) point. This requires several iterations until $P_{max,m}$. Each iteration updates R_s and R_p toward the best model solution.

$$Ipv, n = \frac{RP + RS}{RP} Isc, n \quad (3.20)$$

The initial value of R_s may be zero. The initial value of R_p may be given by

$$Rp, min = \frac{Vmp}{Isc,n - Imp} - \frac{Voc,n - Vmp}{Imp} \quad (3.21)$$

Equation (3.21) determines the minimum value of R_p, which is the slope of the line segment between the short-circuit value and the maximum-power remarkable points. Although R_p is still unknown, it surely is greater than $R_{p,min}$ and this is a good initial guess.

According to [APPENDEX-A1], along with Figs. 3.6, the developed model and the input data are exactly matched at the nominal remarkable points of the I–V curve, the modeling and

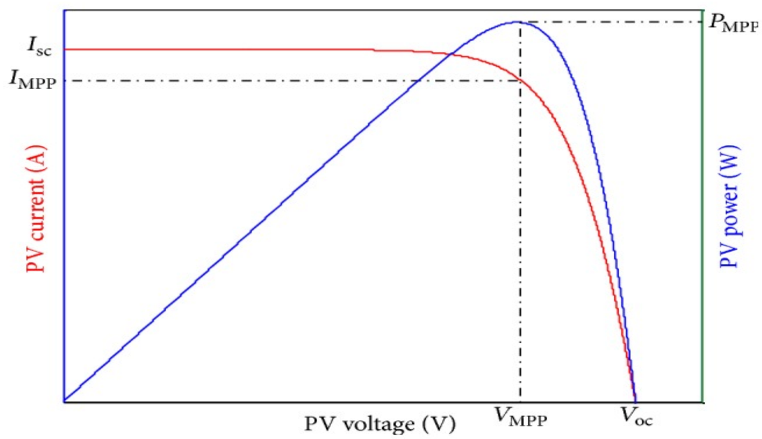

Figure 3. 5: current-voltage (I-V) and power – voltage (P-V) characteristics curves of a solar cell

Mathematical maximum peak powers coincide. The objective of adjusting the mathematical I–V curve at the three remarkable points was successfully achieved. The PV array can be simulated with an equivalent circuit model based on the PV model of Fig. 3.6. The circuit model composed of only one current source. The value of the current is obtained by numerically solving the I–V equation. For every value of V, a corresponding I that satisfy the I–V (3.6) is obtained.

$$I_{sh} = (V + I * R_s)/R_{sh}$$

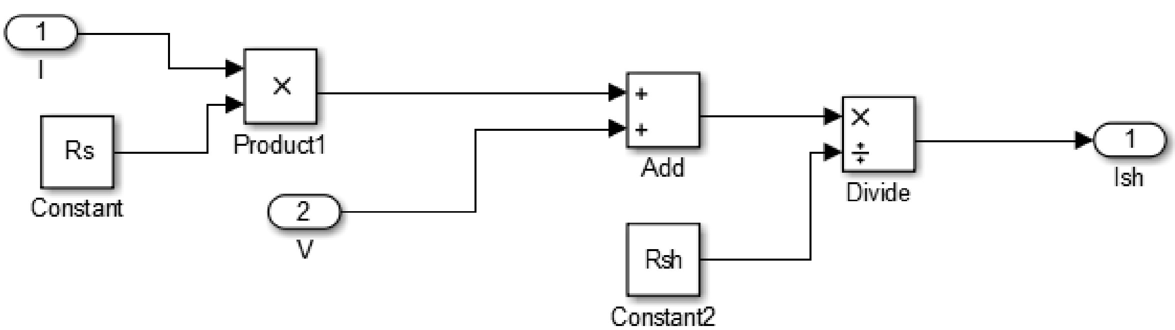

Figure 6a. model of shunt current

Where, I_{sh}= shunt current

R_{sh}= shunt resistance

V = nominal voltage

R_s= series resistance

I = nominal current

$$I_{ph} = [(T - 298) * k_i + I_{sc}] * G/100$$

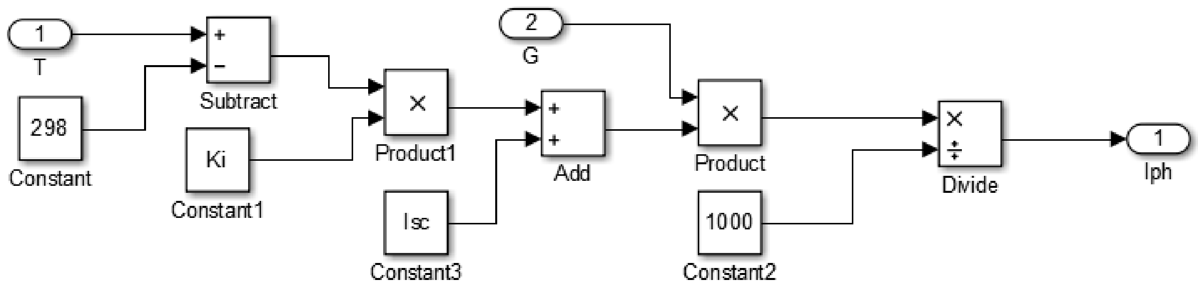

Figure 6b model of photovoltaic

Where, I_{ph} = photo-current

I_{sc}= nominal short circuit current

G= irradiance

T = operating temperature

Ki = current/temperature coefficient

$$I_{rs} = I_{sc} / [\exp({}^{q*v_a/(n*N*K*T)}) - 1]$$

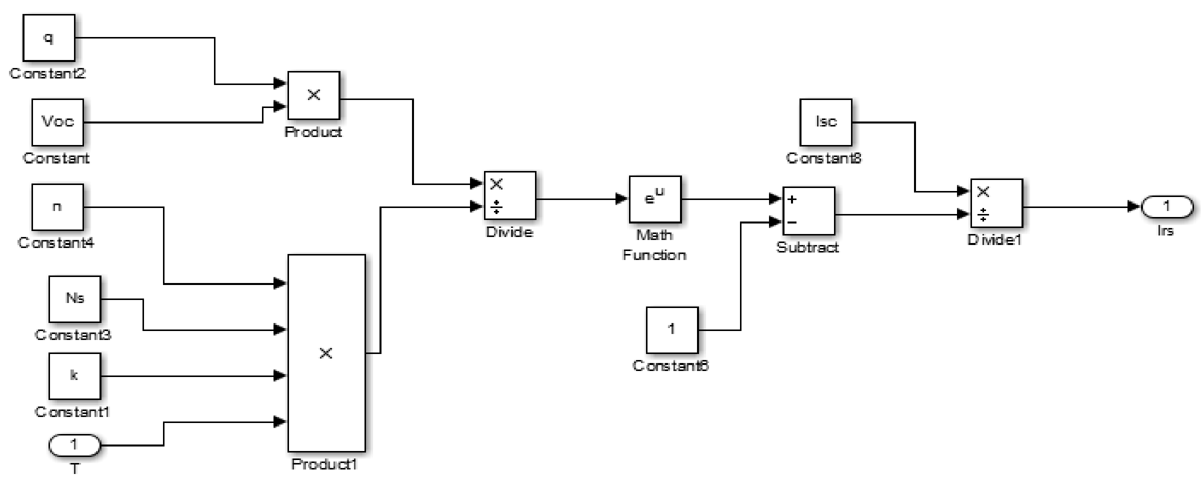

Figure 6c. model of Reverse current

Where, I_{rs}= diode reverse current

q= electronic charge

V_{oc}= nominal open circuit voltage

n = diode constant

N_s = number of series cells

K = Boltzmann constant

$$I_o = I_{rs} * (T / T_n)^3 * \exp[^{q*E_{g0}*(\frac{1}{T_n}-\frac{1}{T})} \big/ (n*K)]$$

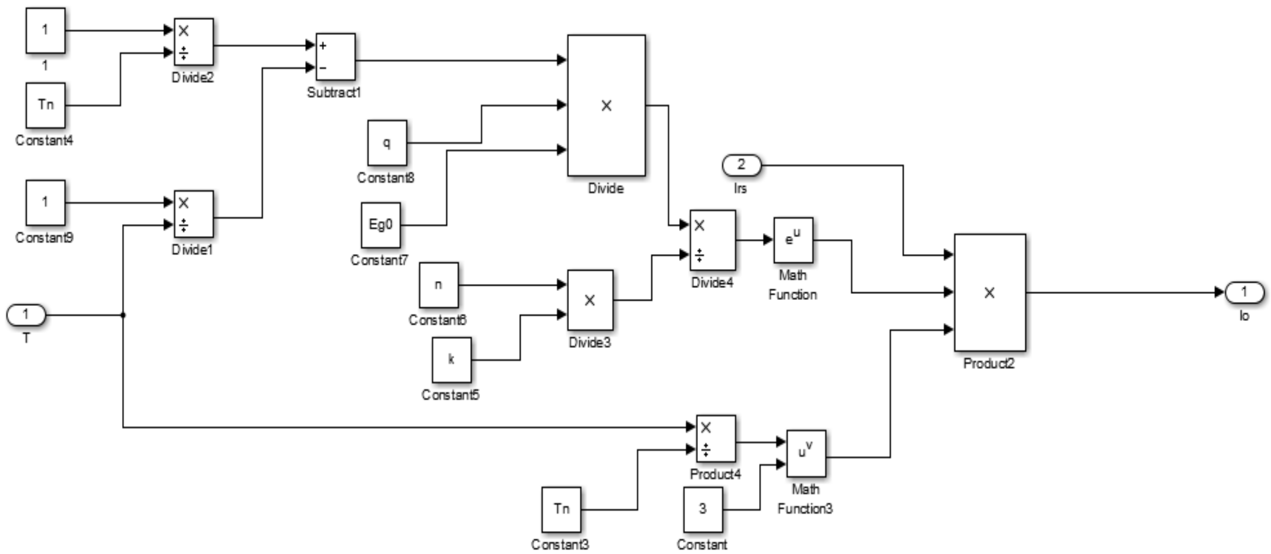

Figure 6d.model of saturation current

Where, Io = nominal diode saturation current

Tn = nominal operating temperature

$$I = I_{ph} - I_o * [\exp(q*(V + I*R_s)/n*N_s*k*T) - 1] - I_{sh}$$

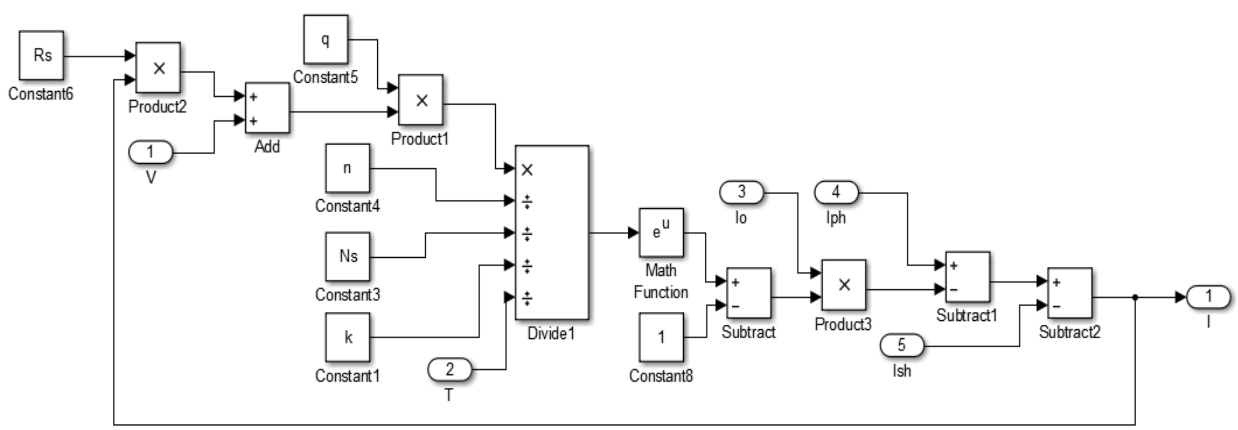

Figure 6e. Model of terminal PV output current

Where, I = nominal pv system output current

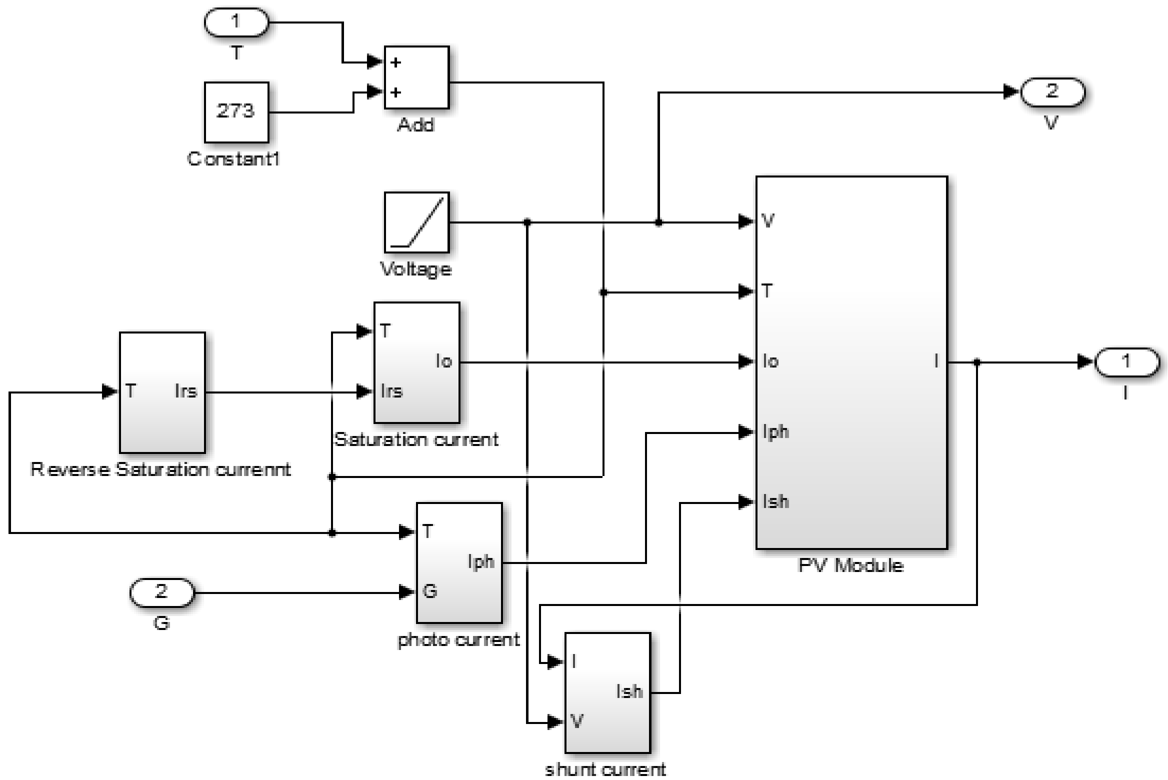

Figure 6f. model of interconnected a, b, c, d, e block diagram

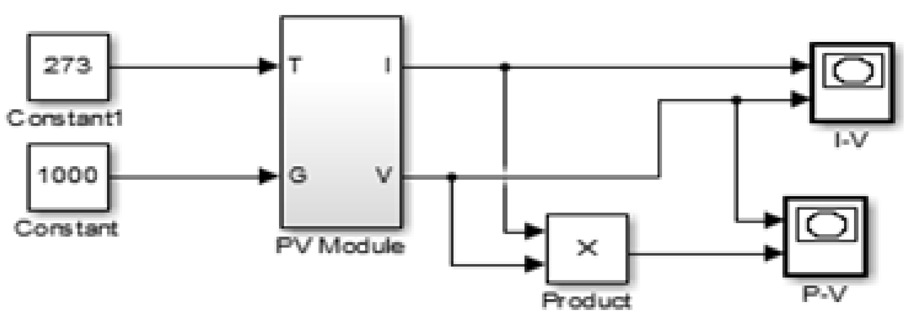

Figure 3. 6: SIMULINK model of the PV equations

The model of the PV array was designed and the calculation of Im, Ipv, and Io are presented as separate sub-systems in Fig. 3.6 [APPENIX A-1]

The characteristics of PV cell are a combination of current source and diode. The current source V-I characteristics are considered separately and the diode V-I characteristics are determined separately. Here these two elements are in parallel connection so by adding currents the PV array characteristics are achieved. The simulation results for the single PV cell are shown W/m^2 in Figs. 3.7. And 3.8. The V-I characteristics and V-P characteristics for different temperatures such as 15_, 25_ and 45_℃ are presented. It is observed that as the temperature increases the open-circuit voltage decreases without any considerable change in the short circuit current. As a result, the maximum power from the cell is decreasing. Similarly, the

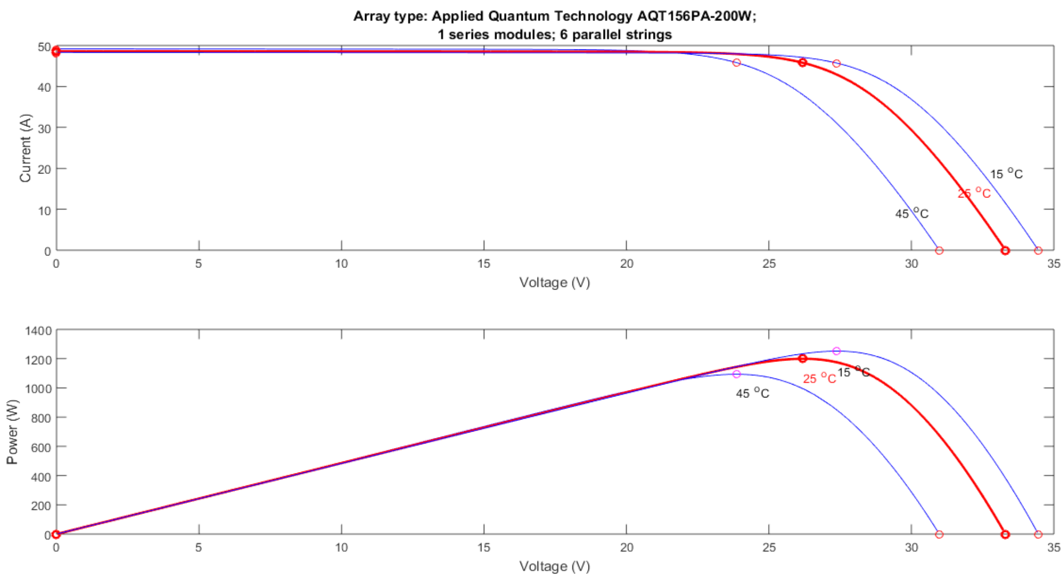

Figure 3. 7: V-I and V-P characteristics to the variation in temperature

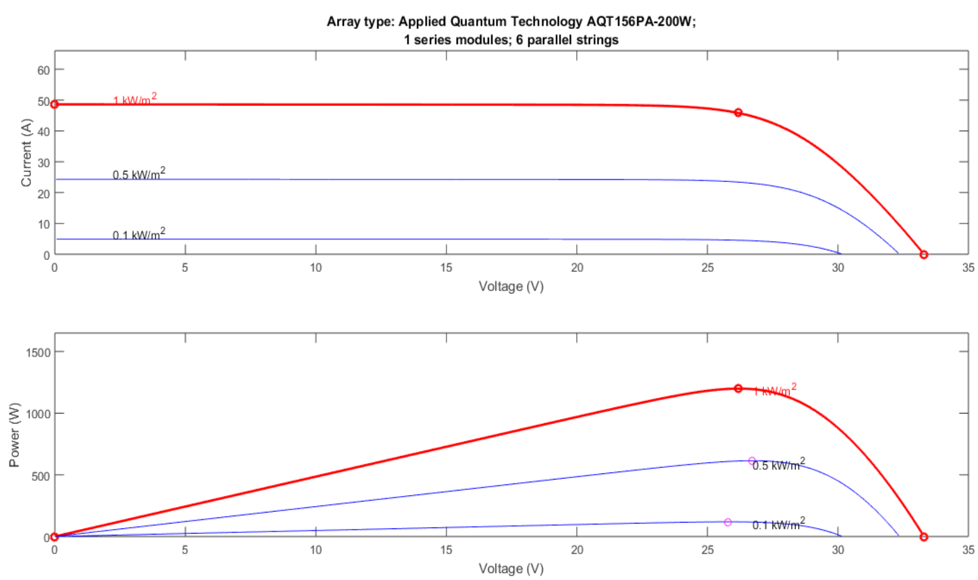

Figure 3. 8: V-I and V-P characteristics to the variation in solar radiations

V-I and V-P characteristics for radiations 100, 500 and 1000 W/m2 are given. For low values of solar radiations, the short circuit current is reducing considerably but the change in open circuit voltage is very less, thus proving that the maximum power from the module is dropping.

3.7 Mathematical and Block diagram Modeling of Boosting DC-DC Converters

Since the DC-DC converter is still in the design stage, an alternate configuration will be used as a temporary substitute until the design is perfected. The requirement for the boost converters is to step up the voltage from 24VDC on the generation side to a regulated 48VDC on the main system line.

The mathematical modeling begins with storage elements capacitor and inductor in the boost converter as shown in Fig.3.9. Inductor voltage and capacitor current are given in eqn (3.22) and (3.23) respectively.

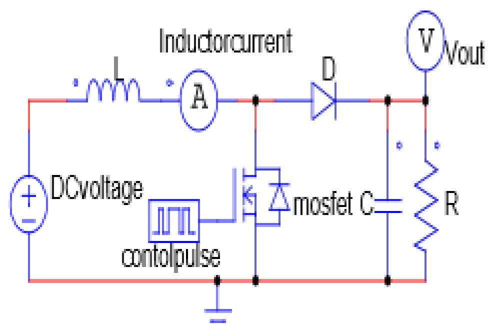

Figure 3. 9: Boost converter model in PSIM

$$v_L = L \frac{d\,iL}{dt} \quad (3.22)$$

$$i_C = C \frac{dvC}{dt} \quad (3.23)$$

The boost conversion begins when the switching process starts, which results in two forms of circuits as shown in Fig 3.12a.and Fig. 3.10 While inductor VL for switching condition of ON and OFF are shown in (3.24) and (3.25) respectively.

$$V_L = V_{in} * PWM \quad (3.24)$$

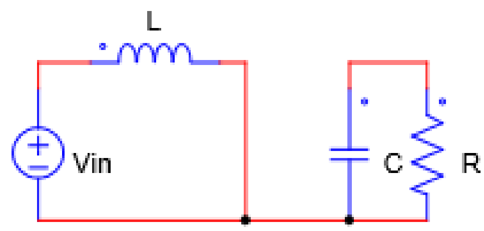

IGBT "ON" condition

Figure 3. 10: Boost converter in ON state during operation

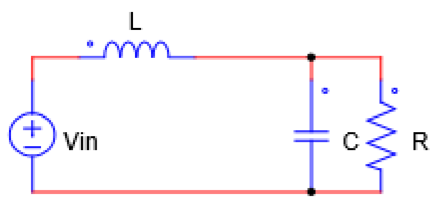

IGBT "OFF" condition

Figure 3. 11: Boost converter in OFF state during operation

$$V_L = (V_{in} - V_{out}) * PWM \quad (3.25)$$

The switching time between (3.23) and (3.24) is determined by the PWM switching frequency and its duty cycle shows in (3.25), here duty cycle is the ratio of V0 - Vin to V0.

$$PMW = \frac{(Vin - Vout)}{Vo} f^{-1} \quad (3.26)$$

The current flowing through can be determined by integrating into (3.27).

$$i_C = C\frac{1}{L}\int VLdt \quad (3.27)$$

After obtaining, the current through the capacitor can be determined in (3.28), where is the current through the load resistor.

$$i_c = i_L - i_R \quad (3.28)$$

After obtaining i_C, the capacitor voltage can be calculated in (3.29), which indicates the load voltage of the boost converter in case of the ideal model.

$$V_C = C\frac{1}{L}\int iLdt \quad (3.29)$$

The boost converter [14] with inverter interfaces PV panel and the load. The designed equations for the Boost converter are given from equations (3.30) to (3.31) the voltage ratio of the Boost converter is given as,

$$\frac{Vo}{Vin} = \frac{1}{1-D} \quad (3.30)$$

The duty ratio of the Boost converter is given as

$$D = 1- \frac{Vin}{Vo} \quad (3.31)$$

Where;

Vin: Input voltage

Vo: Output voltage

D: Duty cycle

In figure 3.11. The simulation model of the boost converter is given. The inductor and capacitor is designed based on the following given equations for the continuous operations of converter,

$$L = \frac{Vin*D}{f*\Delta IL} \quad (3.32)$$

$$C = \frac{D}{f} *Ro*(\frac{Vo}{V}) \quad (3.33)$$

The designed parameters used in simulation are:

Selection of component parameters

$V_{in\ min}$= 29v → minimum input Voltage

f_s =20000Hz → switching frequency

V_{out} = 48V → initial output Voltage

Power = 2000W → converter power

n= 0.9 → efficiency

dv percent = 1% → percent of output Voltage

D: Duty cycle

$$D = 1- \frac{Vin\ min*n}{Vout}$$

$$\%D = 1- \frac{29*0.9}{48} = 45.625\%$$

di: input current ripple $\quad di = I_{ripple} * I_{out} * \frac{Vout}{Vin}$

C_{ripple}: A good estimation for the inductor ripple current is 20% to 40% of the output current.

I_{out}= power/Vout = 2000W/48V= 41.667A

di = 0.4*41.667*48/29 = 27.586A

di= 27.586A

L: inductance (hennery) $\quad L= \frac{Vin*(Vout-Vin)}{(di*fs*Vout)} = \frac{29*(48-29)}{27.586*20000*48}$ = **2.08*10^-5H = 20.8µH**

Dv: output voltage ripple

Dv = Vout * dv percent/100 = 48* 1/100 = **0.48V**

C: capacitor (Farad) $C = \frac{I*D}{fs*dv} = \frac{41.667*0.45625}{20000*0.48}$ = **1.98 x 10^-3F = 1.98mF**

R: load Resistance

R= Vout/I = 48/41.667 = **1.152Ω**

Circuitry Modeling

It is a graphical method of representing the system in terms of circuit diagram which consists of apparatus which are interconnected with each other to form the system. Circuit modeling is carried out in SimPowerSystems of Simulink and PSIM which are two different simulation environments. Fig. 3.10 and Fig. 3.11, shows the circuit modeling of boost converter using SimPowerSystems and PSIM respectively.

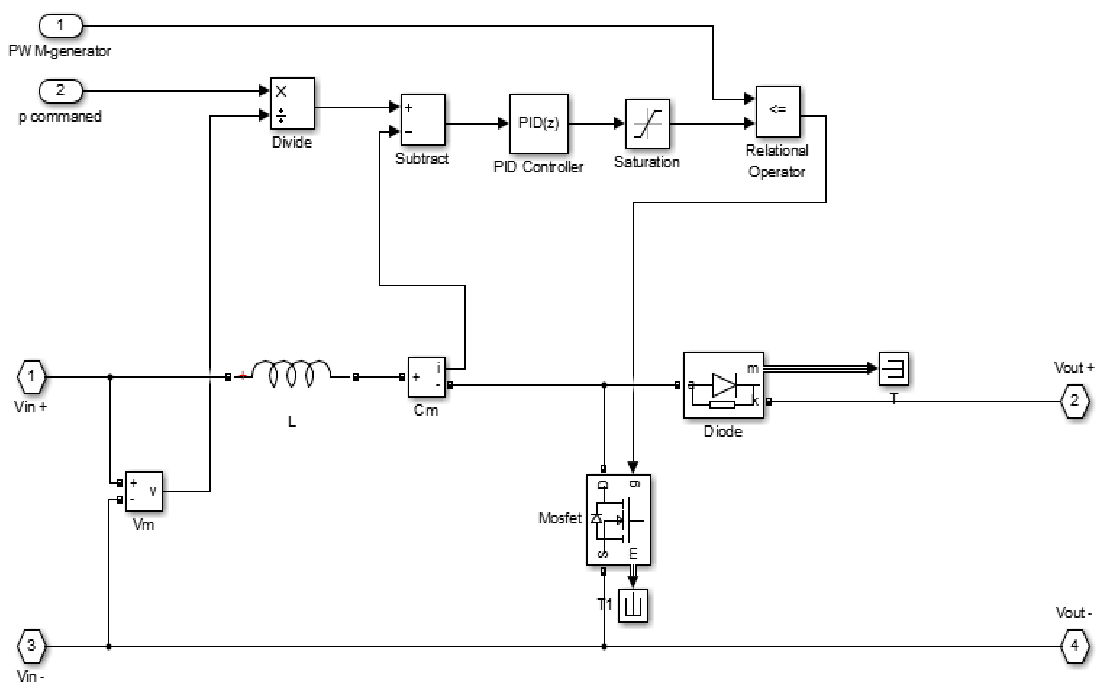

Figure 3. 12: Boost converter model in SimPowerSystems

3.8 The mathematical modeling of Li-Ion battery

In the literature, several studies have been reported regarding to Li-Ion battery (Zhang & Lee 2011). In this work, the Li-Ion battery is modeled using a controlled voltage source in series with a constant resistance.

3.8.1 Discharge model:

The discharge battery model used is based on the Shepherd model. But, it can represent accurately the voltage dynamics when the current varies and takes into account the open circuit voltage (OCV) as a function of state-of-charge (SOC).
The OCV varies non-linearly with the SOC. Therefore, a term concerning the polarisation voltage has been added ($k\frac{Q}{Q-it}it$) to better represent the OCV behavior.
The battery voltage (Vbatt) obtained can be described as:

$$V_{batt} = E_o - k\frac{Q}{Q-it}it - Ri - k\frac{Q}{Q-it}i + A\exp(-Bit) \quad (3.34)$$

Where Eo is the battery constant voltage (V), K is the polarization constant (Ah^{-1}), Q is the maximum battery capacity (Ah), it (∫ i dt) is the actual battery charge (Ah), R is the internal resistance (Ω), i is the battery current (A), i* is the low frequency current dynamics (A), A is the exponential zone amplitude (voltage drop during the exponential zone) (V), and B is the exponential zone time constant inverse $(Ah)^{-1}$.

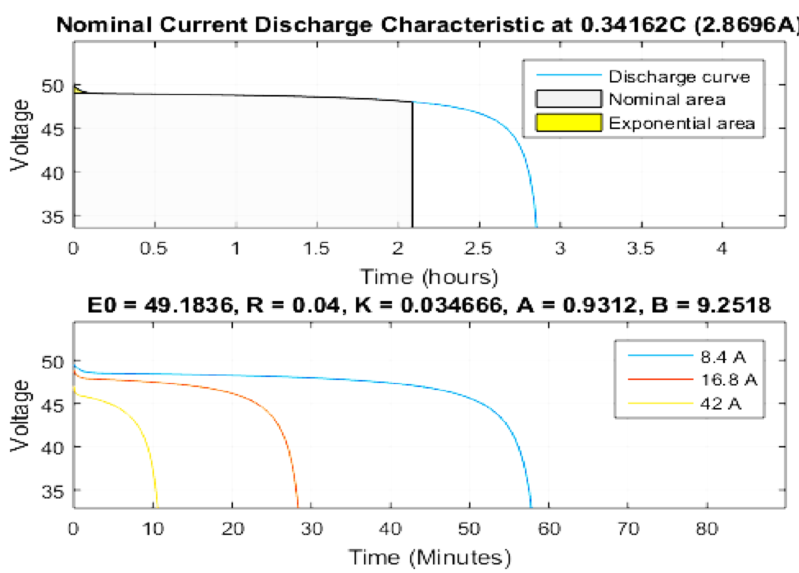

Figure 3. 13: Nominal current discharge characteristic

3.8.2 Charge model:

The battery charge behavior, especially the end of the charge characteristic, is different and depends on the battery type. In the Li-Ion battery, the voltage will increase rapidly when the battery reaches the full charge, as shown in Figure 3.15. This phenomenon can be modeled by the polarisation resistance term ($k\frac{Q}{it}$). The polarisation resistance increases until the battery is almost fully charged (it = 0).

Above this point, the polarisation resistance increases suddenly.

Theoretically, when it = 0 (fully charged), the polarisation resistance is infinite. This is not exactly the case in practice. Actually, experimental results have shown that the contribution of the polarisation resistance is shifted by about 10% of the capacity of the battery (Tremblay & Dessaint 2009). Hence the polarization resistance of the charge model can be described as:

$$\text{Pol. Resistance} = k\frac{Q}{it+0.1Q} \quad (3.35)$$

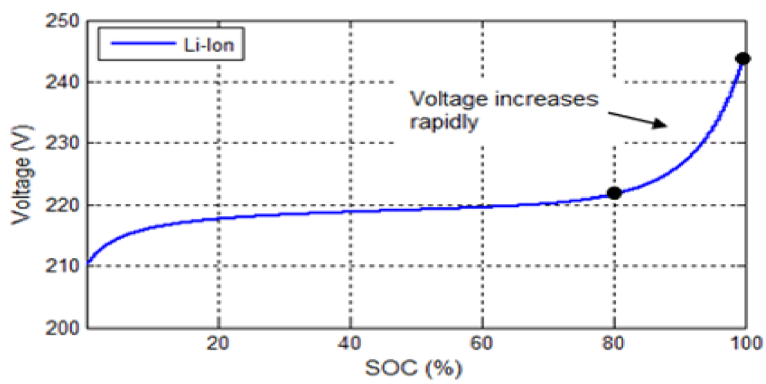

Figure 3. 14: Typical charge characteristic

Similar to the discharge model, the exponential voltage for the Li-Ion battery is the Aexp (-Bit) term. Hence, the battery voltage obtained can be described as (Tremblay & Dessaint 2009):

$$V_{batt} = E_o - k\frac{Q}{Q-it}it - Ri - k\frac{Q}{it+0.1Q}i + A\exp(-Bit) \quad (3.36)$$

The main feature of this battery model is that the parameters can easily be deduced from a manufacturer's discharge curve. Figure 3.16 shows a typical discharge characteristic for Li-Ion battery. As shown, the first section represents the exponential voltage drop when the battery is charged. Depending on the battery type, this area is more or less wide. The second section represents the charge that can be extracted from the battery until the voltage drops below the battery nominal voltage. Finally, the third section represents the total discharge of the battery when the voltage drops rapidly.

The three necessary points used to extract the model parameters are: the fully charged voltage, the end of the nominal zone and the end of the exponential zone. With these three points, it is possible to solve, using Equation (5.1), the following set of Equations (5.4), (5.5) and (5.6). For the fully charged voltage (V_{full}), the extracted charge is 0 (it = 0) and the filtered current (i*) is 0 because the current step has just started:

$$V_{full} = E_o - R*i + A \quad (3.37)$$

For the end of the exponential zone, factor B can be approximated to ($\frac{3}{Qexp}$) since the energy of the exponential term is almost 0 after 3-time constants (Tremblay & Dessaint 2009).

In steady-state, the filtered current is equal to (i). Hence, the exponential zone voltage (Vexp) can be described as:

$$V_{exp} = E_o - k\frac{Q}{Q-Qexp}(Qexp + i) - Ri + A\exp\left(\frac{3}{Q\ exp}Qexp\right) \quad (3.38)$$

And the nominal zone voltage (V_{nom}) can be given by:

$$V_{nom} = E_o - k\frac{Q}{Q-Qnom}(Qnom + i) - Ri + A\exp\left(\frac{3}{Q\ nom}Qnom\right) \quad (3.39)$$

3.8.3 Battery storage bank modeling

Calculating the number of batteries needed for a solar power system mainly depends on the days of autonomy desired. Days of autonomy are the number of days a battery bank will supply a given load without being recharged by a PV array or another source. For critical loads, 5 days of autonomy are recommended. If the load being supplied is not critical then 2 to 3 autonomy days are commonly used. A critical load is a load that must be used all the time.

Another important factor is the maximum depth of discharge of the battery. The depth of discharge solar renewable energy system can be calculated as follow:

$$B_{R\text{-}C} = \frac{IC*ND}{MDOD} \quad (3.40)$$

Where I_C is the Amp-hour consumed by the load in a day (Ah/day), N_D is the number of autonomy days, and M_{DOD} is the maximum depth of discharge.

The number of batteries to be connected in parallel ($N_{B\text{-}P}$) to reach the Amp-hours required by the system can be calculated as follow (Rivera 2008):

$$B_{R\text{-}P} = \frac{BR-C}{BC} \quad (3.41)$$

Where B_C is the capacity of the selected battery (Ah). While the number of batteries to be connected in series (NB-S) to reach the voltage required by the system can be calculated as follow:

$$N_{B\text{-}S} = \frac{Sv}{Bv} \quad (3.42)$$

Where, S_V is the DC system voltage (V), and B_V is the battery voltage (V).

Now let's size a battery bank needed to supply 4800Wh per day to a DC electric load.

Assume that:

- The DC voltage of the battery bank is 48V.
- The number of autonomy days is 3 days.
- The maximum depth of discharge is 80%.
- The selected rechargeable battery is (48V-70.43Ah) Li-Ion

Then, by using the Equations from (3.25) to (3.27) we can calculate the batteries required by this system as follow:

$B_{R\text{-}C} = \frac{ICND}{MDOD} = \frac{117.333Ah*3}{0.80} = 440Ah.$

Number of batteries in parallel = $B_{R\text{-}P} = \frac{BR-C}{BC} = \frac{440}{70.43} = 7.$

Number of batteries in series = $N_{B\text{-}S} = \frac{Sv}{Bv} \frac{48}{48} = 1$

Total number = $B_{R\text{-}P} * N_{B\text{-}S} = 7*1 = 7$

Figure 3.17 shows the example battery bank wired connection.

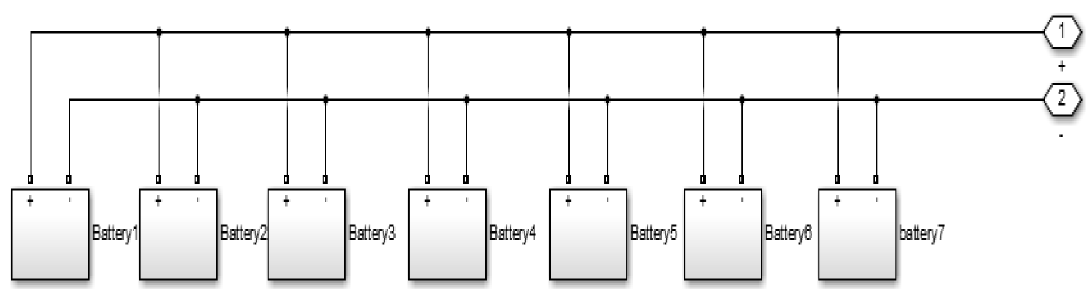

Figure 3. 15: - Series-parallel battery bank example configuration

3.9 MATLAB Model of Charge Controller

The minimum function of a PV charge controller is to disconnect the array when the battery is

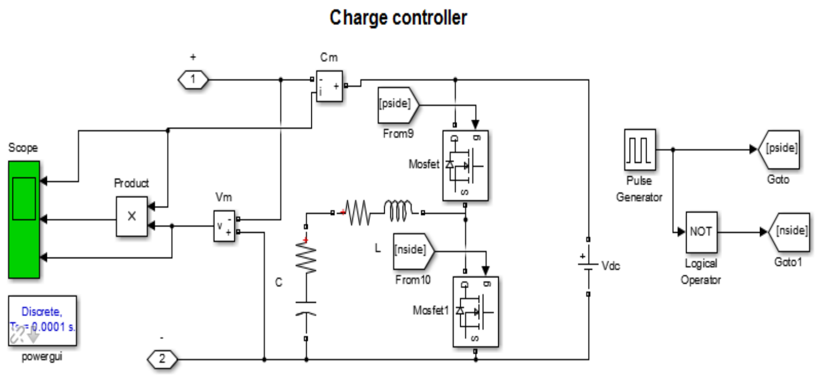

Figure 3. 16: Internal circuit of the charge controller

Fully charged and keep the battery fully charged without damage. A charge controller is important to prevent battery overcharging, excessive discharging, reverse current flow at night and to protect the life of the batteries in a PV system. The power electronics circuit is used in a PV charge-controller to get highest efficiency, availability, and reliability. The use of power electronics circuits such as various DC to DC converters topologies like buck converter, boost converter, buck-boost converter and other converter topology as power conditioning circuitry enable the effective flow of desired current to charge the battery. A PV array with 7 subsystems was developed to implement the charge controller model. The charge controller unit is designed according to Fig.3.18 based on the battery voltage level, which was considered to be 48 V and with a current level of 45 Amp-hr. The function of charge controller is as follows: if the battery voltage reaches the more than 49 V, battery disconnected from the PV-array, and if the voltage drops lesser than 43 V then it has to be connected to PV array, so if voltage of battery in between 43 and 49 V then only connection between PV-array and battery exist. This logic is implemented by taking considering the hysteresis relay. If the voltage of battery is between 43 and 49 V, normal load is connected else dummy load is connected to battery.

3.10 Mat lab Modeling of Inverter

For a solar PV output of 29 V DC, we design a boost converter with output voltage = 48 V, supply current= 6.67 A. Switching Frequency=20 KHz such that the variation in inductor current is not more than 40 % of average inductor current for all operating conditions. The output ripple should be not more than 20 %.

DC-DC Converter (Boost):

In a boost converter, the output voltage is related to input voltage by the formula

$$V_o = \frac{\text{Vin}}{(1-D)}$$

Switching frequency=20 kHz

Vin = 29 V To obtain an output of 48 V and load current of 6.67 A,

$48 = \frac{29}{(1-D)}$ = 48D =48-29, D =19/48 = 0.45625

$$\Delta Vc = \frac{\text{IoD}}{Cfs}, \qquad \Delta I = \frac{\text{Vs}*\text{D}}{Lfs}$$

The tolerable limits of voltage and current ripple are 20 % and 40 % respectively.

I_0 = 41.667 A ΔV_C = (0.45625 * 41.67)/(1.98mF*20kHz) = 0.48V, ΔI = 27.586A

SIMULINK Model

For inverter development, the power system block set provides the required components such as a full-bridge, batteries, resistors, inductors, capacitors etc. The pulse generation circuit is modeled as shown in Fig. 3.19. The single phase inverter designed using IGBT, diode and ideal switch is presented. The input voltage was set to 220V based on the design specifications in the DC voltage source block. The internal resistance of the ideal switch was set to 1.152Ω with the initial state 'open'. The diode's internal resistance was also maintained at 1.152Ω with a forward voltage of 220 V.

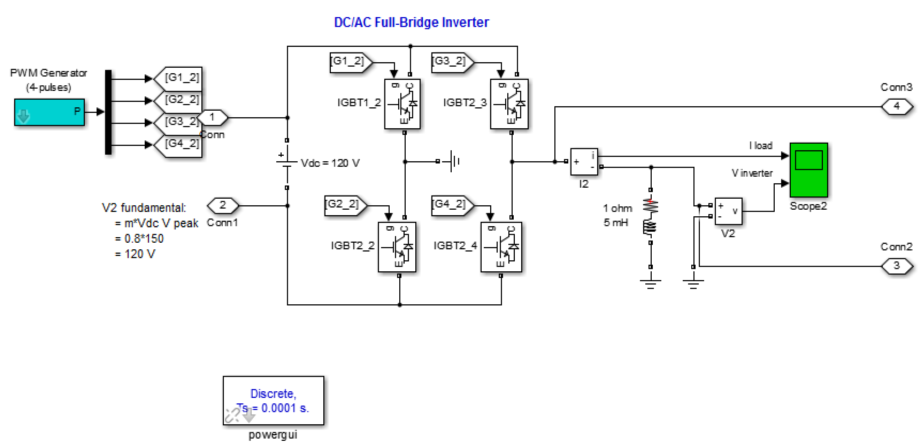

Figure 3. 17: Pulse generation circuit

The boost converter was designed for a 220 V input from solar PV panel with L=**20.8μH** and C=1.98 mF. A single-phase full-bridge inverter (PWM) circuit was used to convert the boosted DC voltage to alternating voltage. The above model can be conveniently used for integrating the Solar PV system to grid system. The inverter system modeled with MATLAB/SIMULINK was achieved using the power system and standard SIMULINK block sets. The system was analyzed by sending the required signal to scopes and the workspace, which allowed for analysis and design of the inverter model.

3.11 Maximum Power Point Tracking (MPPT)

Maximum Power Point Tracking, frequently referred to as MPPT, operates Solar PV modules in a manner that allows the modules to produce all the power they are capable of generating. MPPT is not a mechanical tracking system but it works on a particular tracking algorithm and is based on a control system. MPPT can be used in conjunction with a mechanical tracking system, but the two systems are completely different. MPPT algorithms are used to obtain the maximum power from the solar array based on the variation in the irradiation and temperature. The voltage at which PV module can produce maximum power is called 'maximum power point' (or peak power voltage). Maximum power varies with solar radiation, ambient temperature, and solar cell temperature.

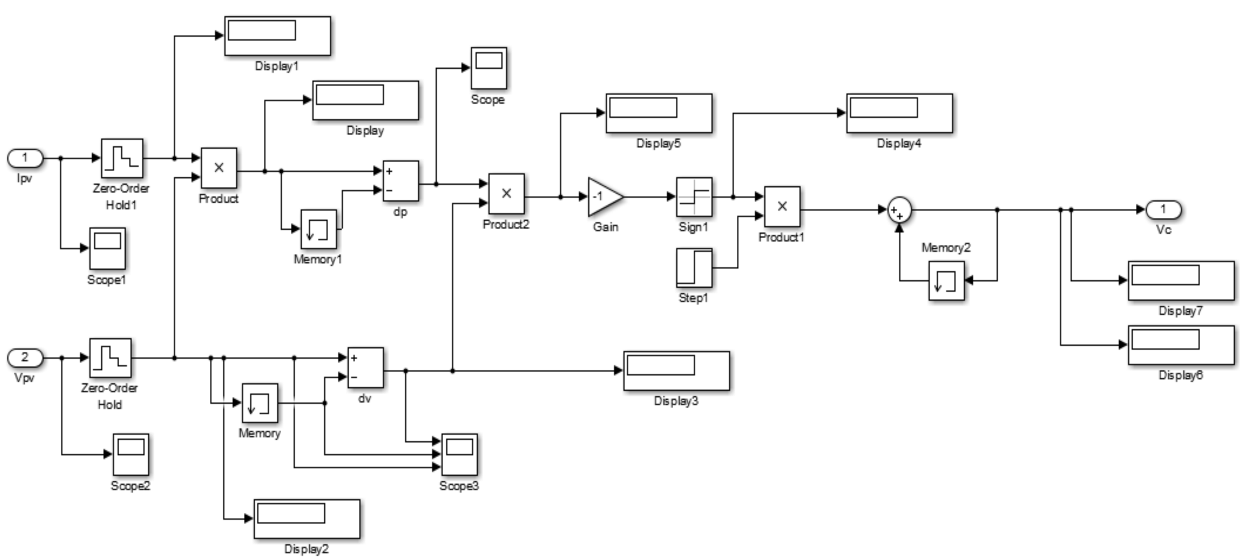

Figure 3. 18: Boost converter and single-phase inverter circuit

Perturb and Observe

In the P&O method, only one voltage sensor is used to sense the PV array voltage and hence the cost of implementation is less. The algorithm involves a perturbation on the duty cycle of the power converter and a perturbation in the operating voltage of the DC-link between the PV array and the power converter. Perturbing the duty cycle of the power converter implies modifying the voltage of the DC-link between the PV array and the power converter. In this method, the sign of the last perturbation and the sign of the last increment in the power are used to decide the next perturbation. As can be seen in Fig. 3.19, on the left of the MPP incrementing the voltage increases the power whereas on the right decrementing the voltage decreases the power. If there is an increment in the power, the perturbation should be kept in the same direction and if the power decreases, then the next perturbation should be in the opposite direction. Based on these facts, the algorithm is implemented as show in the flowchart in Fig. 3.20 and the process is repeated until the MPP is reached. The operating point oscillates around the MPP.

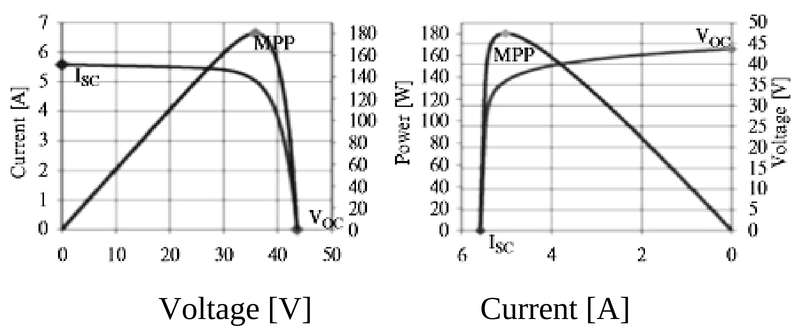

Figure 3. 19: PV panel characteristic curves

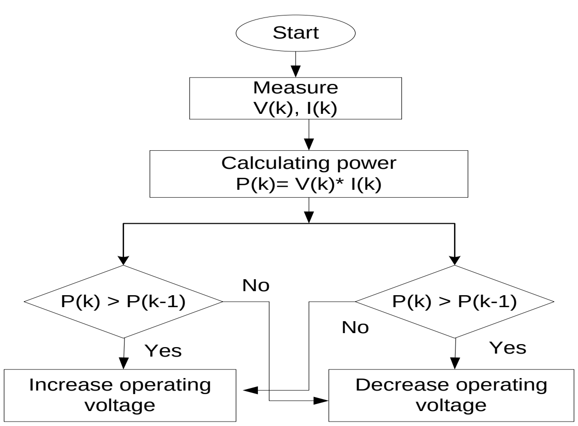

Figure 3. 20: Flowchart of the perturb and observe algorithm

The time complexity of this algorithm is very less but on reaching very close to the MPP it doesn't stop at the MPP and keeps on perturbing on both the directions. To avoid such a condition, an appropriate error limit can be set or a wait function can be used to stop the increase in time complexity of the algorithm. However the method does not take account of the rapid change of irradiation level (due to which MPPT changes) and considers it as a change in MPP due to perturbation and ends up calculating the wrong MPP. To avoid this problem we can use incremental conductance method.

3.12 Mathematical model of a typical BLDC motor

Typically, the mathematical model of a Brushless DC motor is not totally different from the conventional DC motor. The major thing addition is the phase involved which affects the overall result of the BLDC model. The phase peculiarly affects the resistive and the inductive of the BLDC arrangement.

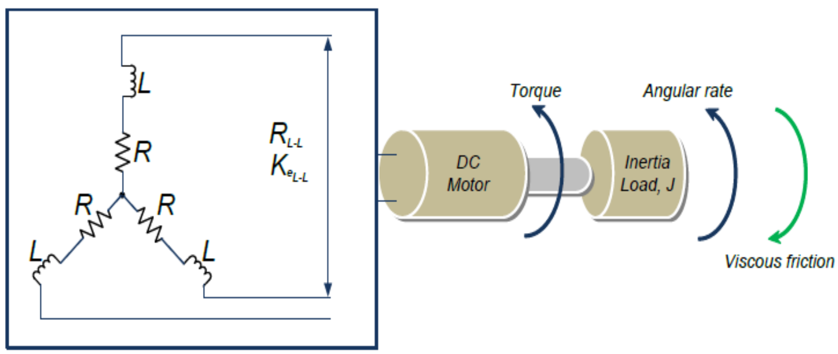

Figure 3. 21: Brushless DC motor of the schematic diagram

For the mechanical time constant (with symmetrical arrangement), the equation becomes:

$$\tau m = \sum \frac{RJ}{Ke.Kt} = \frac{J\sum R}{Ke.Kt} \quad (3.43)$$

The electrical (time constant), where, $k_e = [\frac{V.secs}{rad}]$: the electrical torque

$k_t = [\frac{N.m}{A}]$: the torque constant

$$\tau e = \sum \frac{L}{R} = \frac{L}{\sum R} \quad (3.44)$$

Therefore, since there is a symmetrical arrangement and a there phase, the mechanical (known) and electrical become:

Mechanical constant,

$$Ʈm = \frac{J \sum R}{Ke.Kt} \qquad (3.45)$$

Electrical constant,

$$Ʈe = \frac{L}{\sum R} \qquad (3.46)$$

Therefore, the equation for the BLDC is:

$$G(s) = \frac{\frac{1}{Ke}}{Ʈm.Ʈe.S2 + ƮmS+1} \qquad (3.47)$$

Speed controller

The speed regulator shown below uses a PI controller. The controller outputs the armature current reference (in pu) used by the current controller in order to obtain the electromagnetic torque needed to reach the desired speed. During torque regulation, the speed controller is disabled. The controller takes the speed reference (in rpm) and the rotor speed of the DC machine as inputs. The speed reference change rate will follow the user-defined acceleration and deceleration ramps in order to avoid sudden reference changes that could cause armature over-current and destabilize the system. The speed measurement is filtered by a first-order low-pass filter. The current reference output is limited between symmetrical lower and upper limits defined by the user.

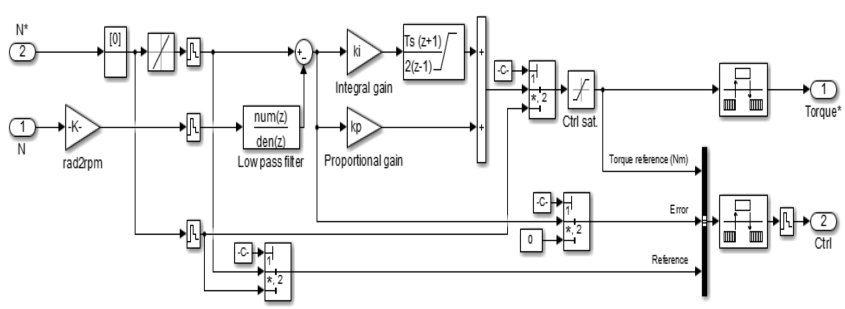

Fig.3.24a. Speed controller of BLDC motor

Current controller

The armature current regulator shown below is based on a second PI controller. The regulator controls the armature current by computing the appropriate duty ratios of the fixed frequency pulses of the four IGBT devices (Pulse Width Modulation). This generates the average armature voltage needed to obtain the desired armature current and thus the desired electromagnetic torque. For proper system behavior, the instantaneous pulse values of IGBT devices 1 and 4 are the opposite of those of IGBT devices 2 and 3. The controller takes the current reference (in pu) and the armature current flowing through the motor as inputs. The current reference is either provided by the speed controller during speed regulation or computed from the torque reference provided by the user during torque regulation. This is managed by the "regulation switch" block. The armature current input is filtered by a first-order low-pass filter. The pulse width modulation is obtained by comparison of the PI output and a fixed frequency sawtooth carrier signal (as shown in the figure called Pulse Width Modulation (PWM))

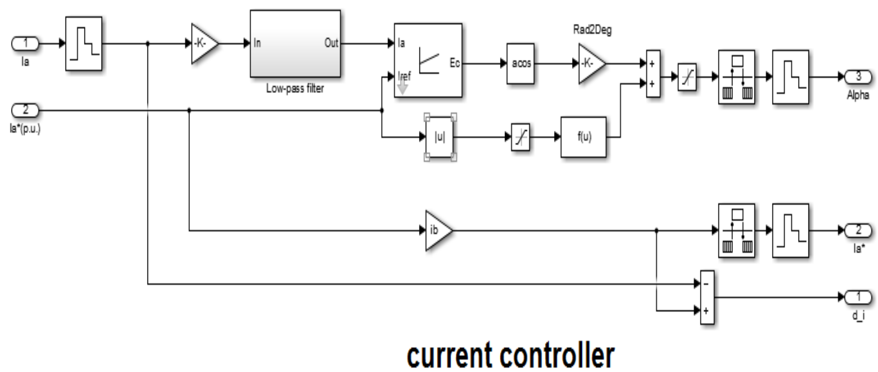

Fig.3.24b. The current controller of BLDC motor

Braking chopper

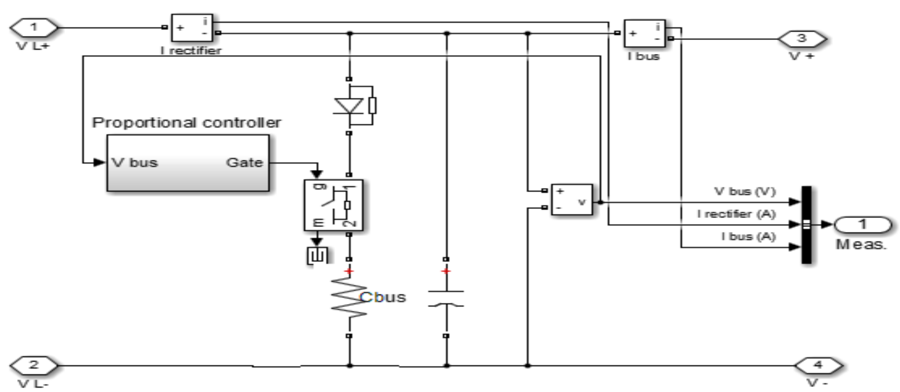

Fig.3.24c. Braking chopper

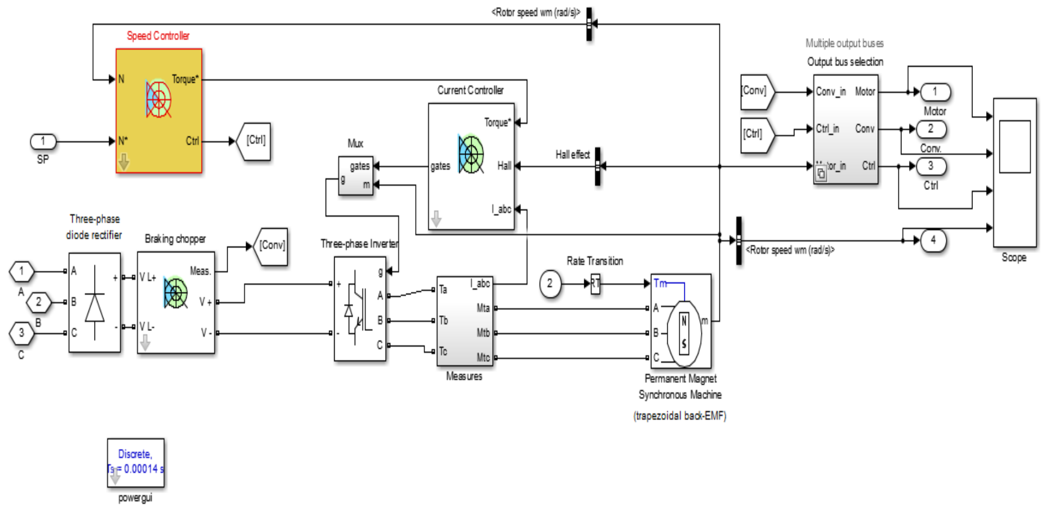

Figure 3. 22: Brushless DC Motor Drive

3.13 Home appliance equipment selection for the research

3.13.1 PV Module Boost Converter

A boost converter (step-up converter) is a DC-to-DC power converter that steps up voltage (while stepping down current) from its input (supply) to its output (load). The requirement for the boost converters is to step up the voltage from 24VDC on the generation side to a regulated 48VDC on the main system line. Figure 3.25 shows the 24V-to-48V DC-DC converter being used for this task. To operate this boosting converter from PV module output DC source to DC home appliance the same load power should be provided. In order to use this boosting DC/DC converter in a PV system having 29V DC voltage source boost DC-DC converter which has an output of 48V, 41.667A with an efficiency of 90% and aggregate load power consumes 2000W power with model number IPS-DTD48S195 is chosen [47].

Figure 3. 23: 24V-to-48V (Boost) DC-DC Converter

This converter has an input voltage range of 29V to 48V and a rated current of 41.667A, thus a power rating of 2000W. This converter must have a higher power rating than the max power output of the solar energy source. The maximum energy source is designed to produce a maximum of 800W; therefore, this converter is adequate. To verify this power rating, consider the output voltage, which calculates the power rating based on regulated output voltage and output current rating.

3.13.2 PV Module Invertor

Inverters are used to convert DC current into AC currents in PV systems. Solar PV systems produce DC output voltage which can be supplied for AC distribution or AC end-user loads by using inverter (DC-AC) converter. In this thesis a typical DC-AC inverter product model is SKU: PICOGLF40W48V240VSCategories is chosen to convert the input DC voltage of 48V to 220V, 17.1A AC with an efficiency of 85% and consumes 3762W power. 48 Volt DC Pure Sine Power Inverter Chargers, 48 Volt DC Pure Sine Power Inverters, 220/230 VAC International Inverters, African European Power Inverters, Inverter Chargers, Power Inverters, Pure Sine Power Inverters The AIMS 4000 Watt 220 Volt pure sine wave inverter charger with built-in transfer switch and battery charger is the solution for backup or off-grid power solutions. This inverter is split-phase and will output 110/120 or 220/230/240Vac, and it can output 50 or 60Hz via the SW4 dipswitch on the DC side of the product. This means that this inverter works internationally and is operable with nearly any electrical system on the planet. 4000 Watt, 12,000 Watt surge, 48 Vdc, 120 & 240 Vac, Inverter, Charger & Transfer Switch. 33.3 amps at 220 Vac. Input chargers are 240 Vac.[48]

Figure 3. 24: Picture of the DC-AC inverter

3.13.3 Refrigerator

The equipment is portable and can be used in the home refrigerator. This day's fridge is a common device for cooling foods and beverages in any homes and at many offices. The refrigerator can be supplied power from solar PV output DC source by using DC-AC converter and single phase AC motor. In this thesis a typical single phase AC motor model of ISO9001 is chosen to the input AC voltage of 220V, 50/60Hz AC with efficiency of 87% and consumes 300W power [46].

Figure 3. 25: Single-phase AC motor 220V 300W for refrigerator

To operate this fridge from DC source in DC home appliance the same voltage and wattage should be provided. In order to use this fridge in a household having a 48V DC voltage source brushless DC motor which has an output of 48V, 6.25A with an efficiency of 97.3% and consumes 300W power with model number ISO4001-BL66 is chosen [44].

Figure 3. 26: Brushless DC motor 48V 300W for refrigerator bldc motor

3.13.4 Laptop

The equipment is portable and can be used in the office and at home. These days laptop is a common device for work at many offices.

Internally laptop circuit has active and passive components and designed to operate in DC. This DC voltage can be supplied from AC-DC or DC-DC converter. Usually Laptop adapter is used to supply DC voltage from traditional AC source. In this thesis a typical AC-DC adapter model number ZF120A-1804000 is chosen to convert the input AC voltage of 100-240V to 19V, 5A DC with an efficiency of 88% and consumes 95W power [42].

Figure 3. 27: picture of AC adapter laptop charger [42]

To operate this laptop from DC source in DC home appliance the same voltage should be provided. In order to use this laptop in a household having 48V DC voltage source buck DC-DC converter which has an output of 19V, 5A with an efficiency of 95% and consumes 95W power with model number DR100N is chosen DC/DC wide-range input, Regulated output, Input filtered against interference from thyristor vehicle drives, Solid construction, Parallel connectable without control lead and Non-isolated output [53].

Figure 3. 28: picture of DC-DC Buck converter for laptop charger in DC office [43]

3.13.5 Lighting

The LED lamp is the most recently used lamp in the world. The lamp replaced incandescent and CFL lamps due to luminous intensity, power-saving and lifetime. The chosen LED product item number is TD-TYA22-12W-120d. The power system has an input voltage of 85-

265V AC output power of 7.2W [22]. The LED lamp has driver circuit for its operation. The driver circuit is to convert the input AC voltage to the LED 12V DC [39].

Figure 3. 29: LED lamp with LED driver [58]

For the available power of the 48V DC source, the LED lamp used in AC system is chosen for DC home. The lamp is already designed to operate in DC but needs AC-DC converter to operate in AC system. As far as the voltage obtained from the AC-DC converter is obtained from DC source, the lamp can be operated from the DC source of 48V without any DC-DC converter. The LED driver used in AC system is eliminated.

3.13.6 Television, Radio, power stabilizer, and cellphones

*** Television:** This is the display parts of technology that designed to operate with AC supply. The model chosen is 4 pin type adapters Suitable for 24V version of JVC TV with the model numbers: LT-20A60SJ and Suitable for TOSHIBA TVs with model number: 20WL56B which operated with AC/DC adapter. A Barrel-To-4Pin type plug converter is included so the adapter can be used for those 24V version JVC and Toshiba TVs that request a 4-Pin type power input plug has an input AC voltage of 100-240v and DC output of 24V, 5A, 120W having an efficiency of 88% is chosen [46].

Figure 3. 30: picture of AC-DC adapter for Television [56]

To supply DC power from the DC source in the DC home television the same model is chosen. For the chosen TVS, the AC-DC used in the AC system is replaced by the DC-DC converter to use it in DC home. To supply 24v DC to the load from the source of 48v DC-

DC converter is necessary. Model DR125N having an input of nominal DC input of 48V and DC output 24V, 5A, 125W which has an efficiency of 95% is used DC/DC wide-range input, Regulated output and Non-isolated output. [47]

Figure 3. 31: picture of DC-DC Buck Converter for Television

*** Radio:** This is the audio parts of technology that designed to operate with AC supply. The model chosen is Item model number: 12v 2a Power Supply Adapter ASIN: B0711FB8WH which operated with AC/DC adapter. 12v 2a Power Supply Adapter by Keple power input plug has an input AC voltage of 100-240v and DC output of 12V, 1.7A, 20W having an efficiency of 85.3% is chosen [46].

Figure 3. 32: AC-DC adapter picture for Radio

To supply DC power from the DC source in the DC home radio the same model is chosen. For the chosen AC-DC used in AC system is replaced by the DC-DC converter to use it in DC home. To supply 12V DC to the load from the source of 48v DC-DC converter is necessary. Model E20UW Isolated DC-DC converter having an input of nominal DC input of 48V and DC output 12V, 1.7A, 20W which has an efficiency of 90% is used [48]

Figure 3. 33: DC-DC Buck converter picture for Radio

*** Stabilizer:** is fluctuations cause temporary or permanent failure of the load. The voltage fluctuations occur due to sudden load changes or due to faults in the power system. So, it is required to supply stable voltage to the load, considering home appliances' importance and the need for their protection. Voltage stabilizers are used for maintaining a stable voltage supply to the load such that the home appliances can be protected from over and under voltages.

This equipment is portable and can be used in the TV-SET, HI-FI, DVD, FAX, Copy machine, Scanner, Air Conditioner, Computer, Test equipment, Fridge& Freezer, Lighting, Etc. The DC voltage can be supplied from AC-DC or DC-DC converter. In this thesis, a typical AC-DC stabilizer model number SLE-5000VA is chosen to convert the input AC voltage of 220V to 13V, 1.2A DC with an efficiency of 80% and consumes 15.6 W powers.

Figure 3. 34: single-phase 5000VA 220V Voltage Regulator

To supply DC power from the DC source in the DC home stabilizer the same model is chosen. For the chosen AC-DC used in AC system is replaced by the DC-DC converter to use it in DC home. To supply 12V DC to the load from the source of 48v DC-DC converter is necessary. Model E15ZW Isolated DC-DC converter having an input of nominal DC input of 48V and DC output 13V, 1.2A, 20W which has an efficiency of 89% is used [47].

Figure 3. 35: picture of stabilizer DC-DC Buck converter

*** Cellphones:** is any portable telephone which uses cellular network technology to make and receive calls. The equipment is portable and can be used in the office, at home and totally at any place. Internally cellphone circuit has active and passive components and designed to operate in DC. This DC voltage can be supplied from AC-DC or DC-DC converter. Usually, cellphone adapter is used to supply DC voltage from a traditional AC source. In this thesis a typical AC-DC adapter model number MLF-A420501000UE is chosen to convert the input AC voltage of 100-240V 50/60Hz 0.4A to 5V, 1A DC with working efficiency of 75% and consumes 5W power.

Figure 3. 36: picture of cellphone AC-DC adapter/charger

To operate this cellphone from DC source in DC home appliance the same voltage and wattage should be provided. In order to use this cellphone in a household having 48V DC voltage source which has an output of 5V, 1A with an efficiency of 92% and consumes 5W power with model number E6DW is chosen [45].

Figure 3. 37: picture of cellphone DC-DC Buck converter

3.13.7 DC fan, Washing machine, and Stove

*** DC fan:** The equipment is portable and can be used in the home fan. The fan can be supplied power from solar PV output DC source by using a DC-AC converter and single-phase AC motor. In this thesis a typical single-phase AC motor model of YP96 is chosen to the input AC voltage of 220V, 0.164A AC with an efficiency of 85.5% and consumes 36W power [44].

Figure 3. 38: Single-phase AC motor 220V 300W for refrigerator

To operate this fan from DC source in DC home appliance the same wattage should be provided. In order to use this fan in a household having a 48V DC voltage source brushless DC motor which has an output of 12V, 3A with an efficiency of 93.5% and consumes 36W power with model number BL43-1 is chosen [45].

Figure 3. 39: Brushless DC motor 12V 36W for fan bldc motor

***Washing machine:** The equipment is portable and can be used in the home washing machine. This is a device that uses washing and cleaning the clothes in-home and laundries. The washing machine can be supplied power from solar PV output DC source by using DC-AC converter and single-phase AC motor. In this thesis a typical single-phase AC motor model of 2704#70W is chosen to the input AC voltage of 220V, 0.318A 50/60 Hz AC with an efficiency of 87% and consumes 70W power [47].

Figure 3. 40: Single-phase AC motor 220V 300W for refrigerator

To operate this washing machine from DC source in DC home appliance the same wattage should be provided. In order to use this washing machine in a household having a 48V DC voltage source brushless DC motor which has an output of 24V, 2.92A with an efficiency of 92% and consumes 70W power with model number BL80-1 is chosen [46].

Figure 3. 41: Brushless DC motor 24V 70W for washing machine bldc motor

*** Stove:** A **stove** is an enclosed space in which uses electricity to heat either the space in which the stove is situated or items placed on the heated stove. There are many types of stoves, such as the kitchen stove, which is used to cook food. The equipment is portable and can be used in the home. Internally stove circuit has passive components and designed to operate in DC. This DC voltage can be supplied from AC-DC or DC-DC converter. Usually stove adapter is used to supply DC voltage from traditional AC source. In this thesis a typical AC-DC adapter model number S-800-24 and Brand-SMUN are chosen to convert the input

AC voltage of 220V 50/60Hz 3.64A to 24V, 33A DC with the efficiency of 85.5% and consumes 800W power.

Figure 3. 42: Picture of the ac-dc adapter of 24v-800w stove

To operate this stove from DC source in DC home appliance the same voltage and wattage should be provided. In order to use this stove in a household having 48V DC voltage source DC-DC converter which has an output of 24V, 33A with an efficiency of 97.5% and consumes 800W power with model number DVC800 is chosen and it characteristics are Protection against unfavorable environmental conditions, DC/DC wide-range input, Regulated output, very high efficiency, Short-circuit / No-load protection, Parallel connectable (Option: Smart output characteristic), Protection against unfavorable environmental conditions, Rugged construction / potted device and Designed for the use in rough environment [48].

Figure 3. 43: Picture of DC-DC Buck converter of 24v-800w stove

3.14 Performance and efficiency evaluation

Table 3. 5: Summarized data collection of AC distribution of home equipment performance and efficiency evaluation of converter, inverter and AC drive motor.

Equipment type	Refrigerator	Laptop	LED Light	Television	Radio	Stabilizer	Cellphone	DC Fan	Washing Machine	Stove
Input AC Voltage	220V, 50Hz	220V, 50Hz	220V, 50Hz	220V, 50Hz	220V, 50Hz	220V, 50Hz	220V, 50Hz	220V, 50Hz	220V, 50Hz	220V, 50Hz
Input AC Current	1.568A	0.4907A	0.3991 A	0.6198A	0.106 6A	0.0886A	0.030A	0.1914A	0.366A	4.25A
Input AC power	345W	108W	8.78W	136.364W	23.44 7W	19.5W	6.667W	42.11W	80.46W	935.67W
Output DC Voltage	48V	19V	12V	24V	12V	13v	5V	12V	24V	24V
output DC Current	6.25A	5A	0.6A	5A	1.7A	1.2A	1A	3A	2.92A	33A
output DC power	300W	95W	7.2W	120W	20W	15.6W	5W	36W	70w	800W
Power loss	**45W**	**13W**	**1.58W**	**16.364W**	**3.447 W**	**3.9W**	**1.667W**	**6.11W**	**10.46W**	**135.67W**
DC-DC converter efficiency	90%	90%	90%	90%	90%	90%	90%	90%	90%	90%
DC-AC(inverter) efficiency	85%	85%	85%	85%	85%	85%	85%	85%	85%	85%
AC motor efficiency	87%							85.50%	87%	
AC-DC Converter efficiency		88%	82%	88%	85.30 %	80%	75%			85.50%
Hour uses per day	10hrs.	6hrs.	8hrs.	4hrs.	9hrs.	10hrs.	2.5hrs.	4hrs.	2hrs.	6hrs.
Energy Consumption per day	3000Whr/d	570whr/ d	57.6wh r/d	480whr/d	180w hr/d	156whr/d	12.5whr/d	144whr/ d	140whr/d	2400whr/ d
Energy loss per day	**450whr/d**	**78whr/d**	**12.64w hr/d**	**65.456wh r/d**	**31wh r/d**	**39whr/d**	**1.466whr/ d**	**24.44wh r/d**	**20.92whr/d**	**814whr/d**

To calculate the above table 3.5 of AC distribution of home equipment performance and efficiency evaluation of converter, inverter and AC drive motor are take an example of an equipment refrigerator is as follow:

Therefore, the refrigerator requires 87% efficient input voltage of 220V, 50Hz single-phase AC motor for AC distribution system is supplied from solar PV system.

The losses are calculated as the subtraction of its output from its input power and energy quantity per day. $P_{loss} = P_{in} - P_{out} = 345W – 300W = 45W$

$E_{loss} = P_{loss} * T = 45W*10Hrs./d = 450Whr/d$. Where, T: is hour uses per day.

Table 3. 6: Summarized data collection of DC distribution of home equipment performance and efficiency evaluation of converter, inverter and DC drive motor.

Equipment type	Refrigerator	Laptop	LED Light	Television	Radio	Stabilizer	Cellphone	DC Fan	Washing Machine	Stove
Input DC Voltage	48V	48V	48V	48V	48V	48V	48V	48V	48V	48V
Input DC Current	6.443A	2.083A	0.15A	2.632A	0.463A	0.365A	0.113A	0.787A	1.585A	17A
Input DC power	309.28W	100W	7.2W	126.32W	22.22 W	17.53W	5.4348W	37.78W	76.087 W	816.33 W
Output DC Voltage	48V	19V	48V	24V	12V	13v	5V	12V	24V	24V
output DC Current	6.25A	5A	0.15A	5A	1.7A	1.2A	1A	3A	2.92A	33A
output DC power	300W	95W	7.2W	120W	20W	15.6W	5W	36W	70w	800W
Power loss	**9.28W**	**5W**	**0W**	**6.32W**	**2.22W**	**1.93W**	**0.4348W**	**1.78W**	**6.087W**	**16.33W**
DC-DC Boost converter efficiency	90%	90%	90%	90%	90%	90%	90%	90%	90%	90%
DC-DC Buck converter efficiency		95%	100%	95%	90%	89%	92%			98%
BLDC motor efficiency	97%							93.50%	92%	
Hour uses per day	10hrs.	6hrs.	8hrs.	4hrs.	9hrs.	10hrs.	2.5hrs.	4hrs.	2hrs.	6hrs.
Energy Consumption per day	3000Whr/d	570whr/d	57.6whr/d	480whr/d	180whr/d	156whr/d	12.5whr/d	144whr/d	140whr/d	2400whr/d
Energy loss per day	**92.8whr/d**	**30whr/d**	**0whr/d**	**25.25whr/d**	**19.98whr/d**	**19.3whr/d**	**1.087whr/d**	**7.12whr/d**	**12.174whr/d**	**97.98whr/d**

To calculate the above table 3.6 of DC distribution of home equipment performance and efficiency evaluation of converter, inverter and DC drive motor are take an example of an equipment refrigerator is as follow below:

Therefore, the refrigerator requires 97% efficient input voltage of 48V Brushless DC motor for DC distribution system is supplied from a solar PV system.

The losses are calculated as the subtraction of its output from its input power and energy quantity per day. $P_{loss} = P_{in} - P_{out} = 345W – 300W = 45W$

$E_{loss} = P_{loss} * T = 45W*10Hrs./d = 450Whr/d$. Where, T: is hour uses per day.

Table 3. 7: Comparison of AC and DC distribution by using Energy and Power evaluation of consumption, losses, and saving of residential appliances.

Equipment type	**Energy Consumption per day**	**AC distribution System**		**DC distribution System**		**Power saving by DC System**	**Energy-saving by DC System**
		Power loss	Energy loss per day	Power loss	Energy loss per day		
Refrigerator	3000Whr/d	45W	450whr/d	9.28W	92.8whr/d	35.72W	357.2whr/d
Laptop	570whr/d	13W	78whr/d	5W	30whr/d	8W	48whr/d
LED Light	57.6whr/d	1.58W	12.64whr/d	0W	0whr/d	1.58W	12.64whr/d
Television	480whr/d	16.364 W	65.456whr/d	6.32W	25.25whr/d	10.044W	40.2whr/d
Radio	180whr/d	3.447W	31whr/d	2.22W	19.98whr/d	1.227W	11.02whr/d
Stabilizer	156whr/d	3.9W	39whr/d	1.93W	19.3whr/d	1.97W	19.7whr/d
Cellphone	12.5whr/d	1.667W	1.466whr/d	0.4348 W	1.087whr/d	1.2322W	0.379whr/d
DC Fan	144whr/d	6.11W	24.44whr/d	1.78W	7.12whr/d	4.33W	17.32whr/d
Washing Machine	140whr/d	10.46W	20.92whr/d	6.087 W	12.174whr/d	4.373W	8.746whr/d
Stove	2400whr/d	135.67 W	814whr/d	16.33 W	97.98whr/d	119.34W	716.02whr/d
Total	**7140.1whr/d**	**237.198 w**	**1536.922whr/d**	**49.382 w**	**305.691whr/d**	**187.82W**	**1231.225whr/d**

To calculate the consumption, losses, and saving of residential appliances shown in table 3.7 is take an example of an equipment refrigerator where the consumption and losses are already calculated in table 3.5 and 3.6. Then to calculate the power and energy saving of DC distribution system over the AC system is as follow below:

$$\text{Saving (P, E)} = \text{AC dist. System (P, E)} – \text{DC dist. System (P, E)} \quad (3.48)$$

Where P = power and E= energy

$$\text{Saving (P)} = P_{loss\ ac} - P_{loss\ dc} \qquad (3.49)$$

P_{saving} = 45W- 9.28W = **35.72W**

E_{saving} = P_{saving} *T = 35.72W * 10hr/d = **357.2Whr/d**

Total P_{saving} = 187.82W and Total E_{saving} = 1231.225Whr/d

$$\text{Total } P_{loss} = \text{Total } P_{loss\ ac} = \text{Total } P_{loss\ dc} + \text{Total } P_{saving} \qquad (3.50)$$

Percentage of Total P_{saving} = $\frac{\text{Total Psaving}}{\text{Total Ploss}} * 100\% = \frac{187.82}{237.198} * 100\%$ = 0.7918= **79.18%**

Where, Total P_{loss}= 237.198W

Percentage of Total E_{saving} = $\frac{\text{Total Esaving}}{\text{Total Eloss}} * 100\% = \frac{1231.225}{1536.922} * 100\%$ = **80.11%**

Where, Total E_{loss} = 1536.922W

$$\text{Total Input consumption Energy} = \text{output consumption Energy} + \text{Total } E_{loss} \qquad (3.51)$$

Input $E_{cons.}$ = 7140.1 +1536.922= **8677Whr/d**

Percentage of Total E_{saving} = $\frac{\text{Total Esaving}}{\text{Total input Econs.}} * 100\% = \frac{1231.225}{8677} * 100\%$ = **14.2%**

Percentage of Total E_{saving} = $\frac{\text{Total Esaving}}{\text{Total output Econs.}} * 100\% = \frac{1231.225}{7140.1} * 100\%$ = **17.24%**

Therefore, using DC distribution system rather than AC system is saving power 79.18% and energy 80.11% of Total losses. Due to DC system energy is saving 14.2% of Total input consumption energy and 17.24% of output consumption energy.

Table 3. 8: Comparison of AC and DC distribution of home equipment Energy and Power consumption in terms of system efficiency

		AC distribution System				DC distribution System			`		
Equipment type	PV module system efficiency	DC-DC converter efficiency	DC-AC (inverter) efficiency	AC motor efficiency	AC-DC Converter efficiency	DC-DC Boost converter efficiency	BLDC motor efficiency	DC-DC Buck converter efficiency	AC distribution Efficiency Loss	DC distribution Efficiency Loss	Efficiency Saving by DC system
Refrigerator	19.50%	90%	85%	87%		90%	97%		12.67%	6.50%	6.17%
Laptop	19.50%	90%	85%		88%	90%		95%	13.33%	7.50%	5.83%
LED Light	19.50%	90%	85%		82%	90%		100%	14.33%	5%	9.33%
Television	19.50%	90%	85%		88%	90%		95%	12.33%	7.50%	4.83%
Radio	19.50%	90%	85%		85.50%	90%		90%	13.17%	10%	3.17%
Stabilizer	19.50%	90%	85%		80%	90%		89%	15%	10.50%	4.50%
Cellphone	19.50%	90%	85%		75%	90%		92%	16.67%	9%	7.67%
DC Fan	19.50%	90%	85%	85.50%		90%	94%		13%	8%	5%
Washing Machine	19.50%	90%	85%	87%		90%	92%		13%	9%	4%
Stove	19.50%	90%	85%		85.50%	90%		98%	13.17%	6%	7.17%
Average efficiency	19.50%	90%	85%	86.50%	83.40%	90%	94%	94.14%	13.65%	8.10%	5.55%
Total system for motor drive	0.195*0.9*0.85*0.865 = 0.129= 12.9%					0.195*0.9*0.9433 = 0.1655 = 16.55%			87.10%	83.45%	3.65%
Total system for other appliance	0.195*0.9*0.85*0.834 = 0.1244 = 12.44%					0.195*0.9*0.9414 = 0.1652 = 16.52%			87.56%	83.48%	4.08%

To calculate the AC and DC distribution of home equipment Energy and Power consumption in terms of system efficiency is shown in table 3.8 is take an example of an equipment refrigerator and for further evaluation calculate the total system. Then to calculate the system efficiency of the DC distribution system over the AC system is as follow below:

For AC motor drive efficiency: all taken from average efficiency.

AC dist. System eff. = DC-DC Conv. Eff. * inv. Eff. * AC motor eff. (3.52)

AC dist. System eff. = 0.9*0.85*0.865=0.661725= **66.1725%**

For without AC motor drive efficiency: all taken from average efficiency.

AC dist. System eff. = DC-DC conv. Eff. * inv. Eff. * AC-DC Effi. (3.53)

AC dist. System eff. = 0.9*0.85*0.834 = 0.638 = **63.8%**

Overall AC System Effi. = PV module Effi. * AC dist. System eff. (3.54)

19.5% * 66.1725% = **12.90%** for AC drive where, PV mod. Effi. = 19.5%

19.5% * 63.8% = **12.44%** for without AC drive

For DC motor drive efficiency: all taken from average efficiency.

DC dist. System eff. = DC-DC boost Conv. Eff. * BLDC motor eff. (3.55)

DC dist. System eff. = 0.9*0.9433=0.84897= **84.897%**

For without DC motor drive efficiency: all taken from average efficiency.

DC dist. System eff. = DC-DC boost conv. Eff. * DC-DC buck conv. Eff. (3.56)

DC dist. System eff. = 0.9*0.9414=0.84726= **84.72%**

Overall DC System Effi. = PV module Effi. * DC dist. System eff. (3.57)

19.5% * 84.897% = **16.55%** for DC drive where, PV mod. Effi. = 19.5%

19.5% * 84.72% = **16.52%** for without DC drive

Efficiency Saving = DC dist. System eff. - AC dist. System eff. (3.58)

84.897% - 66.1725% = **18.72%** for drive

84.72% - 63.8% = **20.92%** for without drive

Overall Saving System Effi. = DC dist. System eff. - AC dist. System eff. (3.59)

16.55% - 12.90% = **3.65%** for drive

16.52% - 12.44% = **4.08%** for without drive

Therefore, using a DC distribution system rather than AC system is saving efficiency for drive 18.72% and for without drives 20.92% of distribution System. Due to DC system the

Overall system efficiency is saving for drive 3.65% and for without drives 4.08% of Solar PV System.

3.15 Economic Assessment of the Modeling DC Refrigerator and AC Refrigerator Running on Inverter all Powered by Solar PV

For the comparative economic analysis, the AC refrigerator and DC refrigerator were both powered by solar PV to ascertain their economic implications in running them on solar energy. The cost of the two modes of solar refrigeration considered in this study has been evaluated based on the following equations:

Total Cost of DC Refrigeration System (Without Inverter) = Cost New AC Refrigerator + Cost of BLDC motor and Accessories + Cost of Conversion + Cost of Solar PV System (3.60)

Total Cost of AC Refrigeration System (with Inverter) = Cost New AC + Refrigerator Cost of Inverter + Cost of Solar PV System (3.61)

These equations have been evaluated based on the measured daily energy consumption of each refrigerator and presented. The cost of the solar PV system depends on the sizes of solar PV system components required by each refrigerator.

The calculation is performed concerning the PV system for residential applications. The economic analysis has been evaluated using simple payback time (SPP), saving to investment ratio (SIR), Internal Rate of Return (IRR) and Net present esteem (NPW).

Net Present Worth (NPW): Net Present Value (NPW) is the difference between the present value of cash inflows (saving) and the present value of cash outflows (investment).Net present worth greater than zero demonstrates that the anticipated profit produced by a venture surpasses the expected expenses. For the most part, a venture with a positive NPW is considered to be profitable and one with a negative NPW indicates the project might not to be financial profitable.

$$NPW = \sum PW_{AS} - \sum PW_{LCI} \tag{3.62}$$

Where:

PW_{AS} = present worth of annual saving

PW_{LCI} = present worth of life cycle investment

Present worth (PW) can be defined as the future cash worth at the present time, and it is calculated by the following formula:

$$PW = \frac{\text{FW}}{(1+i)n} \tag{3.63}$$

Where FW is the future value, i is the interest rate, and n is the analysis period.

PW_{AS} includes the worth of annual saving (electricity exported + avoided fuel cost + GHG reduction income + feed-in tariff) of the project. PW_{LCI} considers the value of life cycle investment (purchase cost + M&O cost + imported electricity cost) of the system.

Saving-To-Investment Ratio (SIR): The savings-to-investment ratio (SIR) is the ratio between the net present worth net savings to the present worth net costs of a project. In general, if SIR is greater than 1, the intended project or investment is considered to be profitable.

$$SIR = \frac{\sum \text{PWAS}}{\sum PWLCI} \tag{3.64}$$

Internal Rate of Return (IRR): Internal rate of return (IRR) is just simply the interest rate at which the net present value of all the cash flows from a project equal zero. The investment is indicated to be feasible if the IRR is greater than the discount rate.

Simple Payback Period (SPP): The simple payback period (SPP) is the ratio between initial investment (IC) and annual saving (AS). It provides a rough estimation how long it will take a project to recover the initial investment. This method ignores inflation rate, so caution should be taken when considering SPP to determine whether to undertake a project or not. The shorter SPP period is desirable since longer payback periods are typically not desirable for financer investors.

$$SPP = \frac{\text{IC}}{AS} \tag{3.65}$$

The estimating price includes PV module, battery, convertor (Brushless DC motor for DC system), inverter (single phase AC motor for AC system), energy (electricity) cot and Balance of System (BOS) costs are calculated. But it is not calculate the mechanical part of Refrigerator because this fixed cost is equally affected on both DC and AC distribution system. The main concern of this cost analysis is regarding to the objectives in chapter one to show the feasibility of DC /AC distribution system economic benefit. In the next chapter four is the modeling and simulation concern only load of home appliance equipment of to be specifically Refrigerator. The other load equipment’s are not model and simulate but it is analytically calculated the performances and efficiency in the above of in this chapter.

CHEPTER FOUR

RESULT AND DISCUSION

In this study, the methodology of developing a stand-alone solar powered DC refrigerator and the approach of sizing a solar PV system for powering the refrigerator has been developed.
The design considerations formulated have been used to convert 300W AC refrigerator to serve as a stand-alone solar powered DC refrigerator. A solar PV system for powering the refrigerator is designed and simulated at the 2015Ra Matlab/SIMULINK and HOMER Software for economic analysis. Simulation has been conducted on the system and performance comparison with an identical conventional AC refrigerator has been made. This chapter presents and discusses the results obtained from this study. The Chapter is grouped under four major sections by making reference to the specific objectives documented in Chapter 1. These are:

- Simulating and modeling of the solar-powered DC refrigerator using Matlab/SIMULINK.
- Simulating and modeling of the solar-powered AC refrigerator using Matlab/SIMULINK.
- Economic analysis of the modeled solar-powered AC/DC refrigerator using HOMER Software.
- The performance and efficiency of the solar-powered DC refrigerator compared to a conventional AC refrigerator

These are discussed in the following sections:

4.1 Simulating and modeling of PV powered DC Refrigerator using Matlab/SIMULINK

DC distribution system in DC Refrigerator is a combination of PV module, Boost converter, MPPT, Battery, charge controller and BLDC motor from DC source to load the flow power is direct current system which is simulated and model to below.

4.1.1 Simulation Result and Discussion of Boosting converter

A Boost converter circuit converts a DC voltage to another DC voltage by controlled chopping or switching of the source voltage. The request for a certain load voltage is translated into a corresponding requirement for the transistor duty cycle. The duty cycle modulation is typically several orders of magnitude slower than the switching frequency. The net effect is the attainment of an average voltage with relatively small ripples.

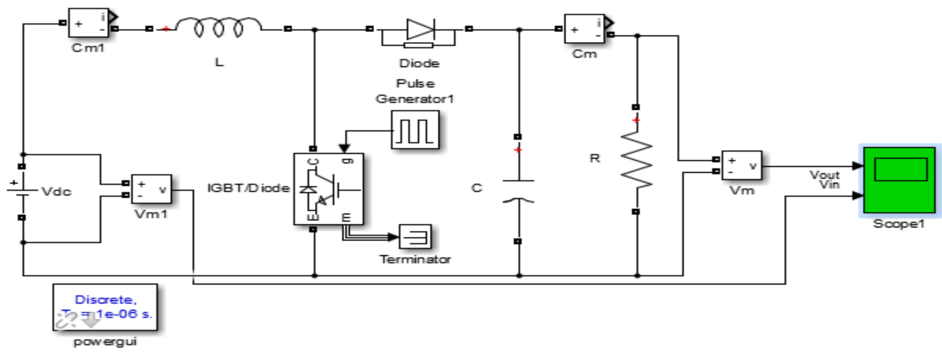

Figure 4. 1: Modeling of Boost DC/DC Converter

The circuit in the model is characterized by high-frequency switching. The model uses a sample time of 1μs. The model takes the duty cycle value as its only input and produces three outputs - the inductor current, the load current, and the load voltage.

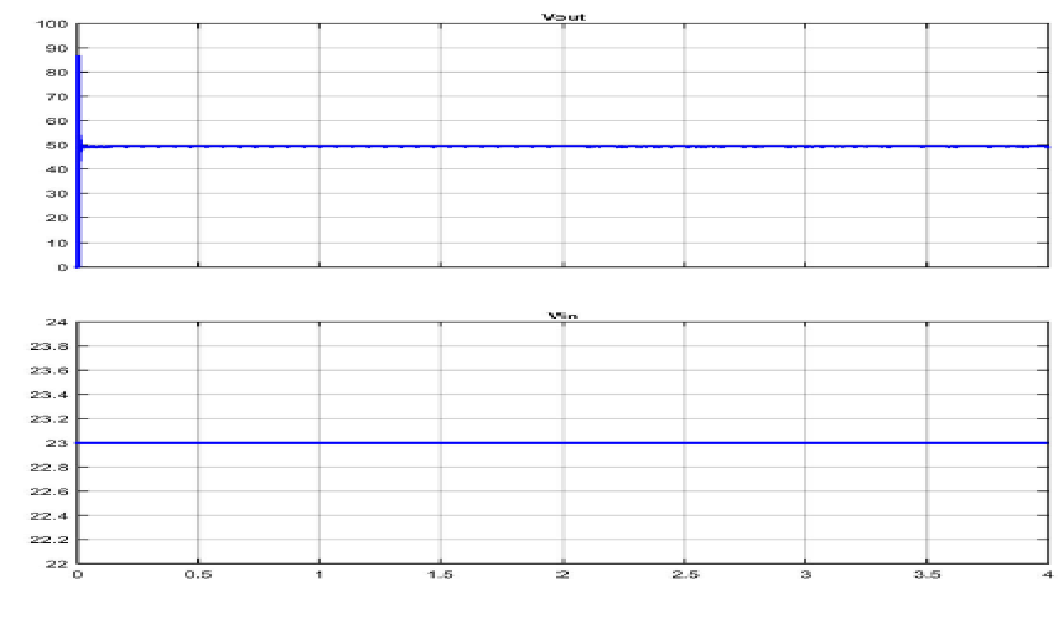

Figure 4. 2: simulating Result of 24V to 48 V Boost converters

The simulation of boost convertor is shown in fig. 4.2 and its result is 48V boost from the input of 23V PV module source to achieve the desired system voltage that operate for the assessed load.

4.1.2 Modeling and Simulating Result of MPPT

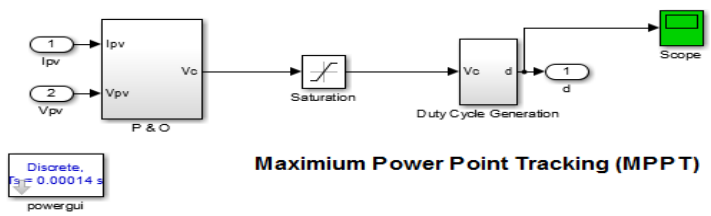

Figure 4. 3: Modeling of MPPT

Maximum Power Point Tracking (MPPT) is implemented in the boost converter by means of a Simulink model using the 'Incremental Conductance + Integral Regulator' technique. In this average model the controller is based on the 'Perturb and Observe' technique.

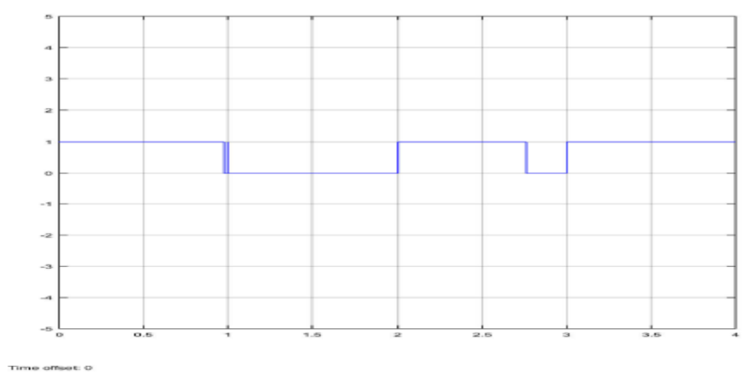

Figure 4. 4: Simulation of MPPT

The simulation starts with operating site location conditions (12.72 deg. C, 717W/m^2).

At t=1sec MPPT is enabled. The regulate MPPT or starts regulating PV voltage by varying the duty cycle in order to extract maximum power. Maximum power (300W) is obtained when duty cycle is D=0.454.

At t=2sec, PV array mean voltage =30 V as expected from PV module specifications (Nser*Vmp=1.6*30= 48 V).

From t=2sec to t=2.5sec, solar irradiance is ramped down from 1000 W/m^2 to 250 W/m^2. MPPT continues tracking maximum power.

4.1.3 Modeling and Simulating Result of Lithium-ion Battery

The Battery block implements a generic dynamic model parameterized to represent the most popular types of rechargeable batteries. The equivalent circuit of the battery is shown below:

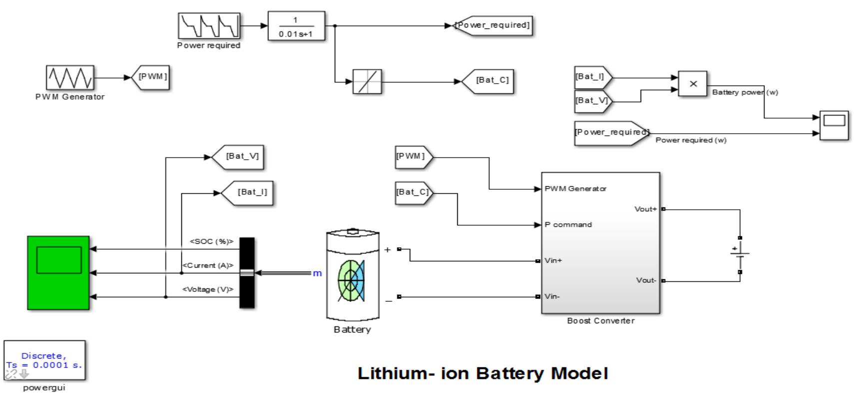

Figure 4. 5: Modeling of Lithium-ion battery

The nominal voltage (*Vnom*) of the battery (volts) is 29.3v. The nominal voltage represents the end of the linear zone of the discharge characteristics. The rated capacity of the battery in ampere-hour is 71.24Ah. The rated capacity is the minimum effective capacity of the battery.

The initial State-Of-Charge (SOC) of the battery. 100% indicates a fully charged battery and 0% indicates an empty battery. This parameter is used as an initial condition for the simulation and does not affect the discharge curve (when the option Plot Discharge Characteristics is used) shown in fig 3.15. Load the corresponding parameters in the entries of the dialog box, depending on the selected Lithium-ion Battery type, the Nominal Voltage, and the Rated Capacity.

The maximum theoretical capacity of when a discontinuity occurs in the battery voltage. This value is generally equal to 105% of the rated capacity. Note that the fully charged voltage is not the no-load voltage.

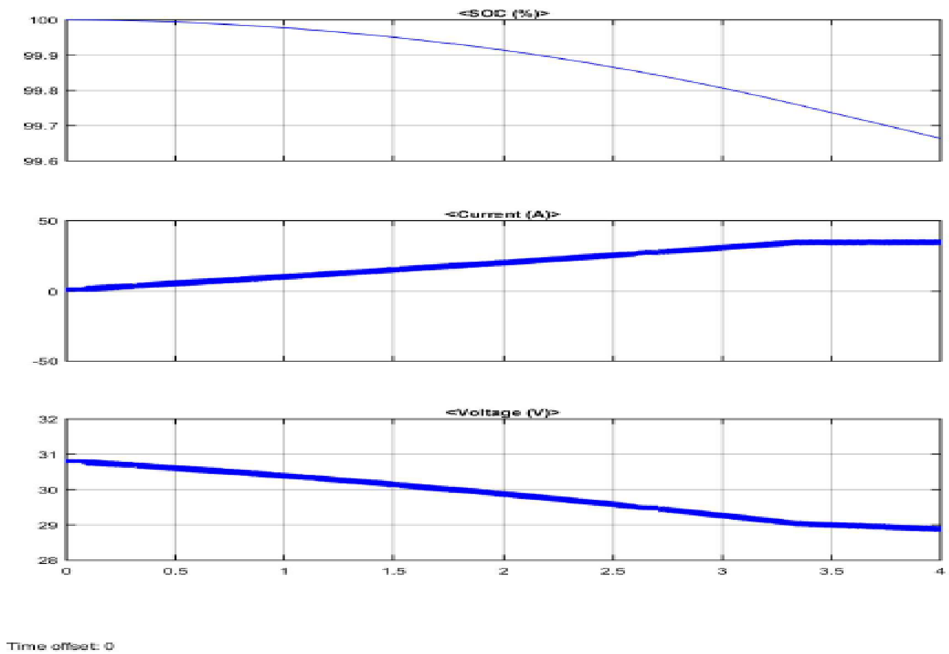

Figure 4. 6: Simulation Result of Lithium-ion battery

The battery is discharged by the constant DC load of 6.357 A. When the SOC drops under 0.2, a mechanical torque of −10 Nm is applied so the machine acts as a generator and provides a current of 12.714 amps. Hence, 6.357 amps go to the load and 6.357 amps go to recharge the battery. When the SOC goes over 0.8, the mechanical torque is removed and the machine operates freely. And then the cycle restarts.

4.1.4 Modeling and Simulating Result of Supercapacitor

Supercapacitors are gaining more attention as electrical energy storage elements for renewable energy sources which tend to have a high charge-discharge cycle frequency, and high cycle efficiency and good depth of discharge (DOD) properties.

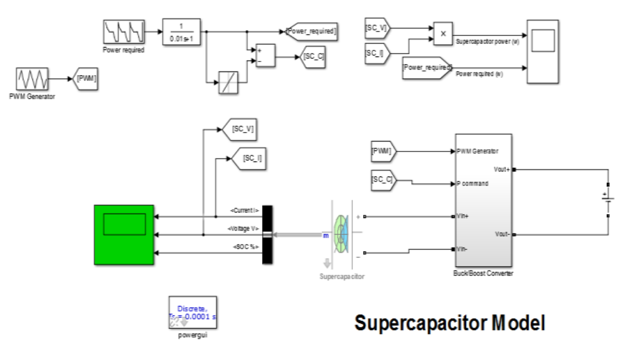

Figure 4. 7: modeling of supercapacitor

The Rated capacitance of Specify the nominal capacitance is 99.5F in the supercapacitor, Specify the internal resistance of the supercapacitor is 8.9mΩ, Specify the rated voltage of the supercapacitor is 48V, in volts. Specify the number of series capacitors to be represented. Specify the number of parallel capacitors to be represented. Specify the initial voltage of the supercapacitor is zero, in volts. Specify the operating temperature of the supercapacitor. The nominal temperature is 25° C. The supercapacitors are widely exploited to mitigate the load current fluctuation in the battery. It has a superior efficiency, which is defined as the ratio of the energy output to energy input, which reaches almost 100%, and so it is suitable for energy storage situation with frequent charge-discharge cycles.

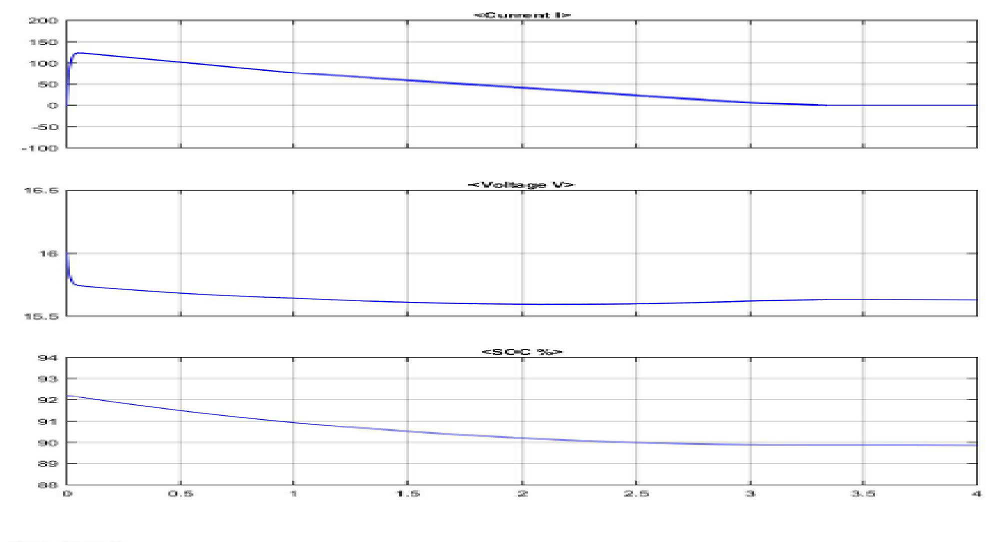

Figure 4. 8: Simulating Result of supercapacitor

The simulation of supercapacitor of rate capacity effect in the energy storage system decreases the discharging efficiency as the load current increases. The supercapacitor, have extremely low internal resistance.

4.1.5 Modeling of Lithium-ion Battery parallel with supercapacitor

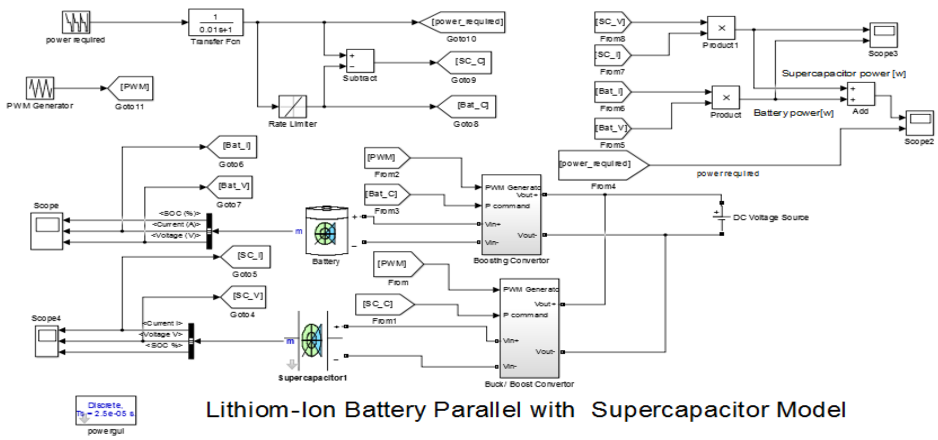

Figure 4. 9: Modeling of Lithium-ion Battery parallel with Supercapacitor

The circuit illustrates a simple hybridization of a supercapacitor with a battery. The supercapacitor is connected to a Buck/Boost converter and the battery is connected to a Boost converter. Power of the battery is limited by a rate limiter block; therefore the transient power is supplied to the DC bus by the supercapacitor. A battery-supercapacitor hybrid may mitigate the rate capacity effect for high pulse discharge current. This hybrid system is that employs a constant-current regulator isolating the batter from supercapacitor to improve the end-to-end efficiency from the battery to the load while accounting for the rate capacity effect for Li-ion batteries and conversion efficiency data for regulator.

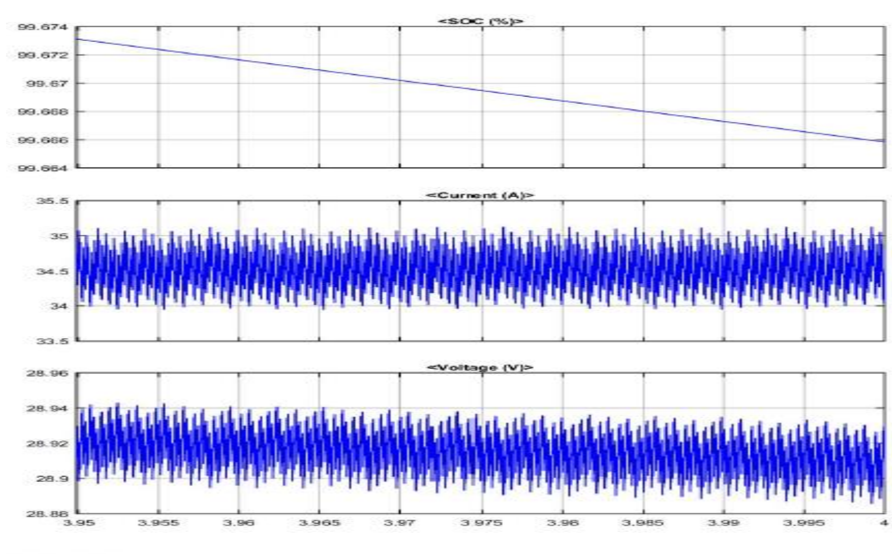

Figure 4. 10: Simulating Result of Lithium-ion Battery parallel with Supercapacitor

The simulation of battery-supercapacitor parallel connection hybrid shown in fig. 4.9 is an intuitive way of reducing the effect of load fluctuation on the supplied voltage level. The supercapacitor connected in parallel act as a low pass filter that prunes out rapid voltage changes. This paper deals with a system in which DC motor is started by using a parallel combination of supercapacitor and battery, for enhancing the battery life. Supercapacitor delivers energy during ride through periods, which typically are during starting or during overloads. While delivering the energy, their current demands heavily increase. For the cases of heavy drainage of energy, for a longer time, the reduction in terminal voltage of supercapacitor reduces the power fed by the supercapacitor.

4.1.6 Modeling and Simulation Result of Lithium-ion Battery Bank

The characteristics of Li-ion battery bank High energy density: more energy with less weight, High charge currents (shortens the charge period), High discharge currents, Long battery life (up to seven times the battery life of a conventional battery), High efficiency between charging and discharging (very little energy loss due to heat development) and Higher continuous power available.

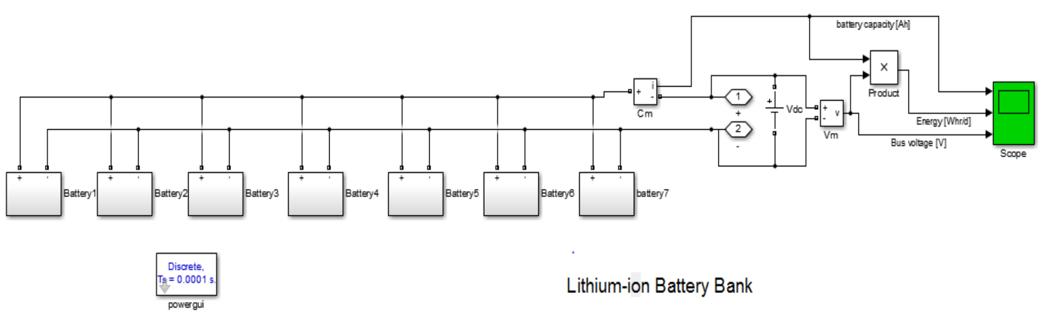

Figure 4. 11: modeling of lithium-ion Battery Bank

The modeling of battery bank is very important to handle the desired battery capacity. The number of batteries needed for a solar power system mainly depends on the days of autonomy desired. Days of autonomy are the number of days a battery bank will supply a given load without being recharged by a PV array or another source. In this thesis as shown in fig. 4.11 there are seven batteries connected parallel and 71.24Ahrs battery capacity per single storage, then the seven batteries capacity has 445Ahrs in the bank. The voltage of battery bank is the same as to the system bus voltage, 48V in number. The modeling of the battery bank delivers the output on the scope of energy, bus voltage and battery capacity. These the three quantities are simulate and the results are approximately matched with the mathematical design calculation.

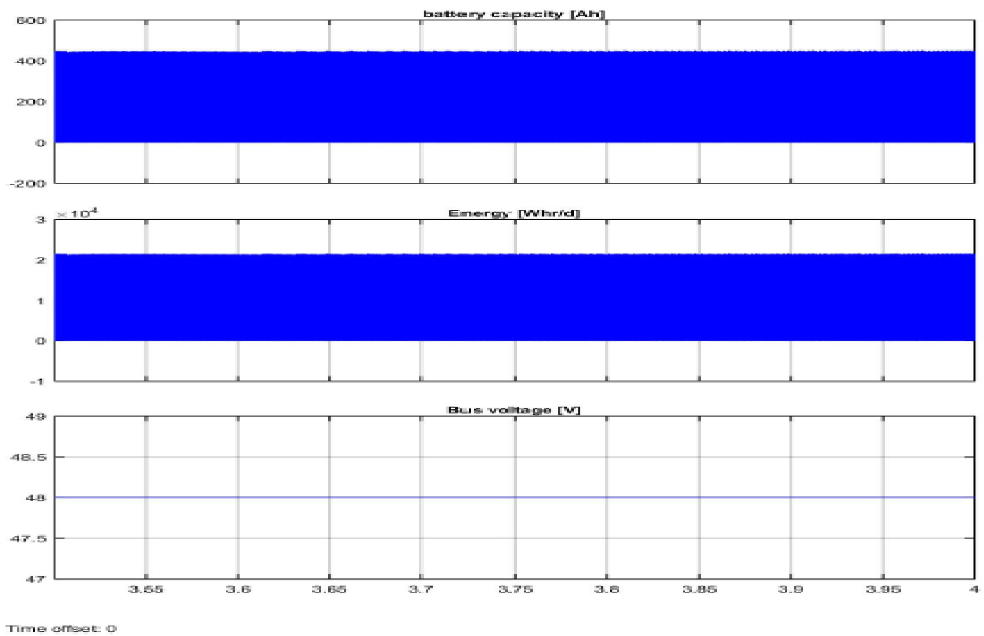

Figure 4. 12: Simulating Result of Lithium-ion Battery Bank

The simulation of the battery bank is symmetric with the calculating value in chapter three and the curves are described sufficiently shown in fig. 4.12. Obviously the battery bank capacity measures 445Ahrs, energy = 2.136*10^4 Whr. And the bus voltage is 48V. The battery bank is giving a source to the load at night time and cloudy season up to three days automation.

4.1.7 Modeling and Simulation Result of the Charge controller

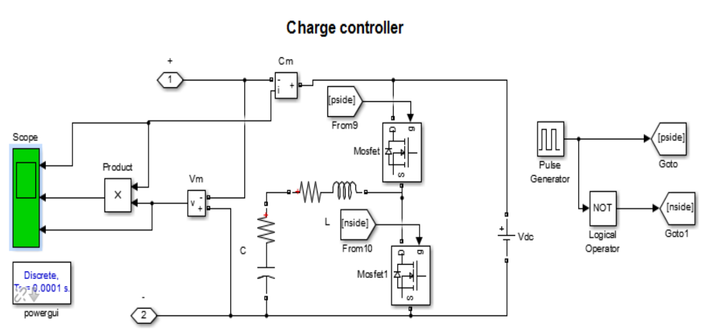

Figure 4. 13: Modeling of the Charge controller

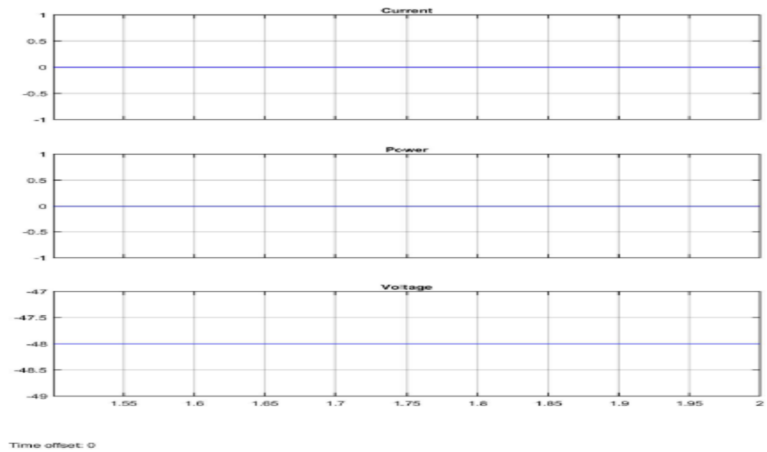

Figure 4. 14: Simulation of a charge controller

The simulation charge controller is shown in fig.4.14 that is controlled the charging/ discharging and regulating the system voltage and current for the rechargeable battery. The minimum function of a PV charge controller is to disconnect the array when the battery is fully charged and keep the battery fully charged without damage. In the normal operating conditions of the simulating power and current value is zero. But the battery voltage is -48V to be controlled.

4.1.8 Modeling and Simulation Result of battery series with Charge controller

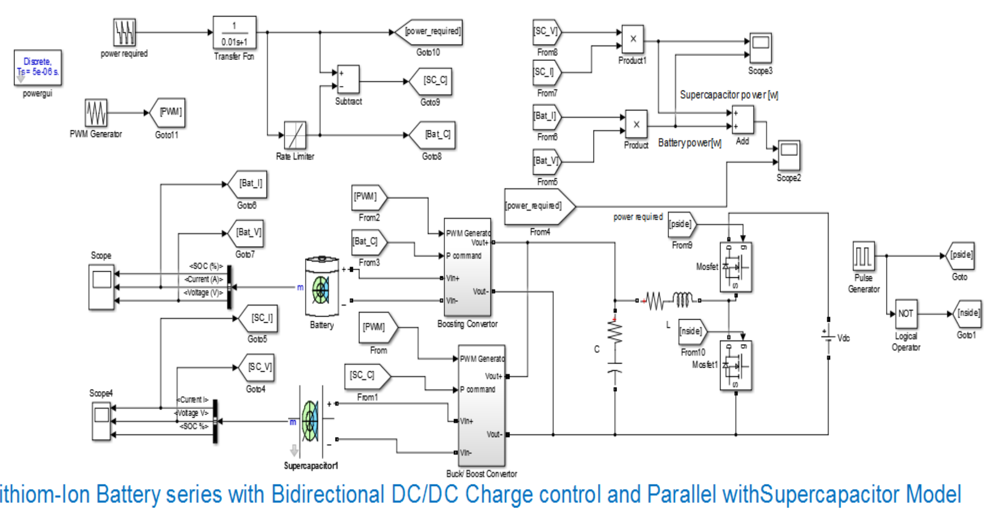

Figure 4. 15: Modeling of Battery series with charge controller

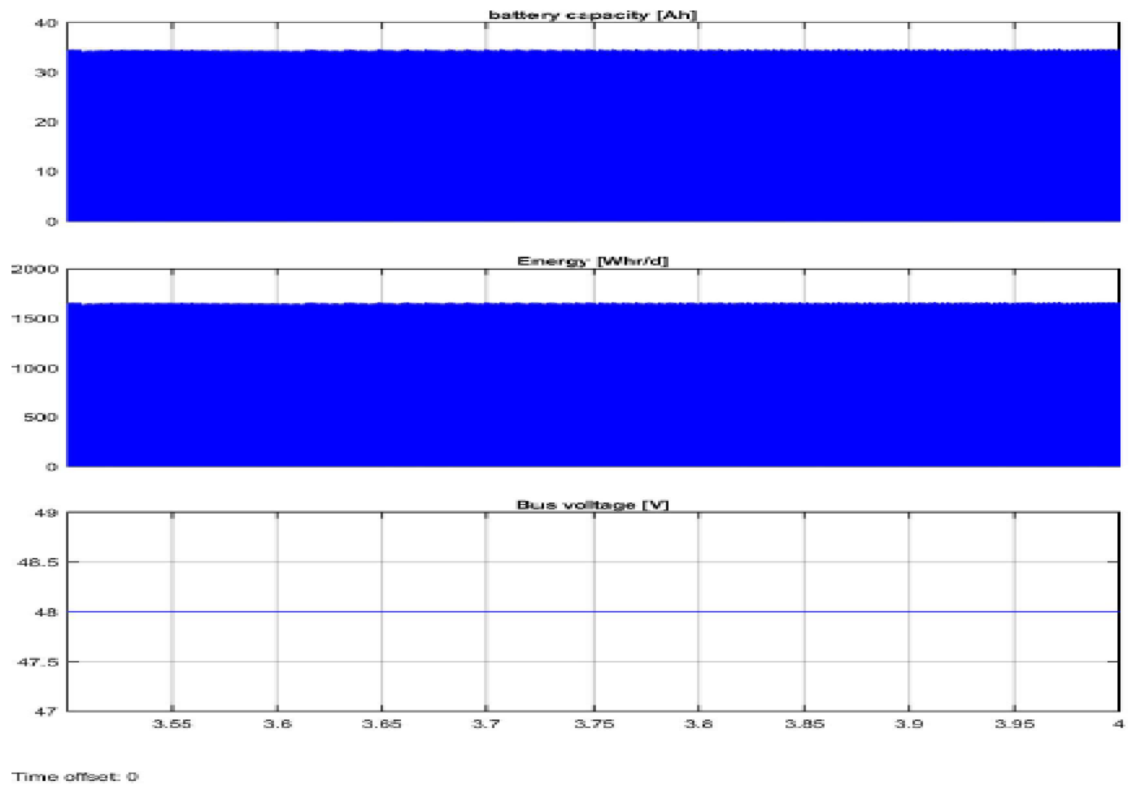

Figure 4. 16: Simulating Result of Battery series with charge controller

4.1.9 Modeling and Simulation Result of battery Bank series with Charge controller

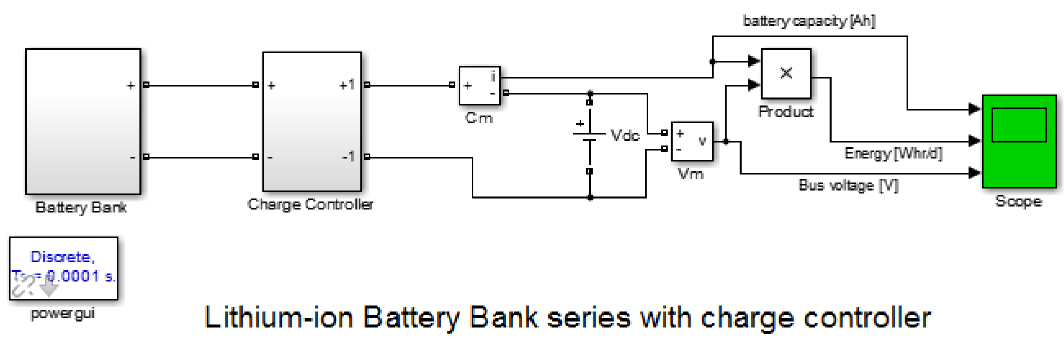

Figure 4. 17: modeling of battery Bank series with Charge controller

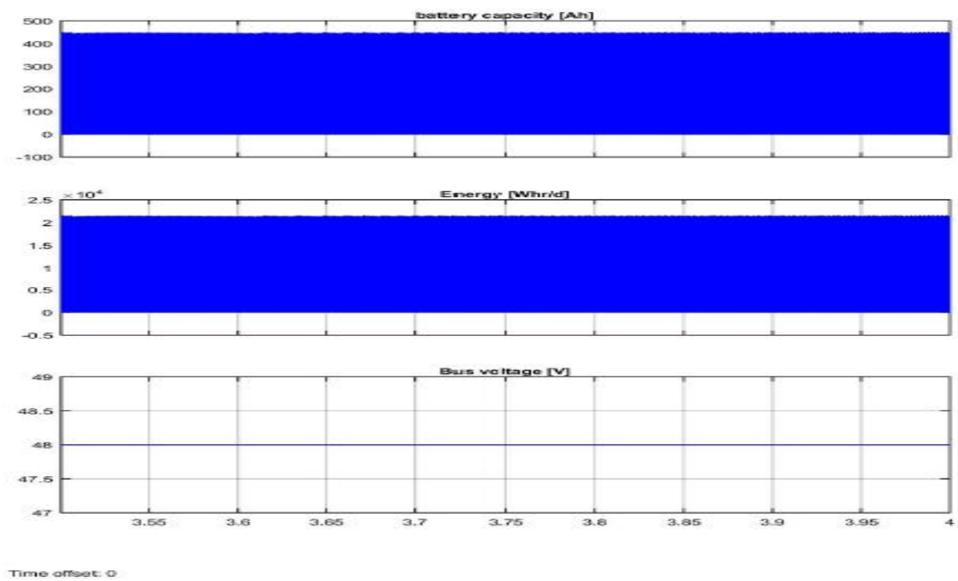

Figure 4. 18: Simulating Result of battery Bank series with Charge controller

4.1.10 Modeling and Simulation Result of Brushless DC motor

This circuit is the models of a brushless DC motor drive with a braking chopper for a motor. The permanent magnet synchronous motor (with trapezoidal back-EMF) is fed by a PWM voltage source converter, which is built using a Universal Bridge Block. The speed control loop uses a PI regulator to produce the torque reference for the current control block. The current control block computes the three reference motor line currents, in phase with the back electromotive forces, corresponding to the torque reference and then feeds the motor with these currents using current regulator.

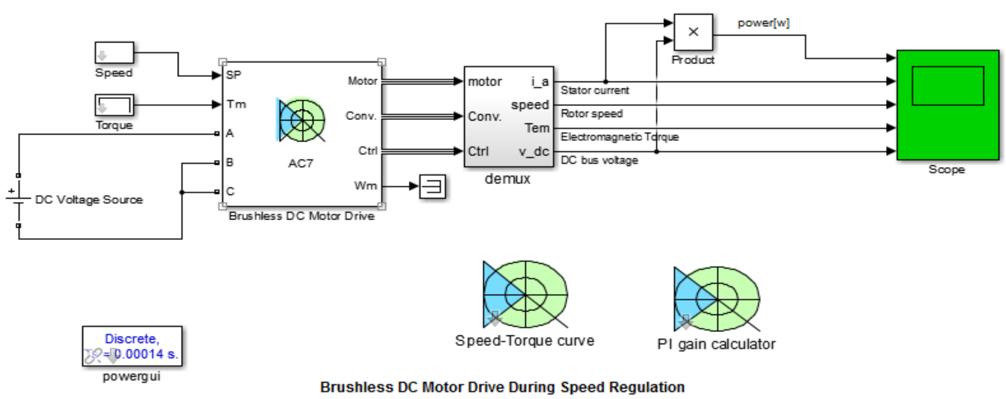

Figure 4. 19: Modeling of Brushless DC motor

It is important to give the precise value of torque to the model in order to design BLDC Motor drive system because it is related to back-Emf and torque [10].For energizing the stator winding in correct sequence the knowledge of rotor position is necessary since in order to rotate the rotor-stator winding has to be energized sequentially and also commutation has to be done electronically.

The speed control has been done on the variable dc-link voltage control technique and finally the results are verified.

Motor current, speed, and torque signals are available at the output of the block.

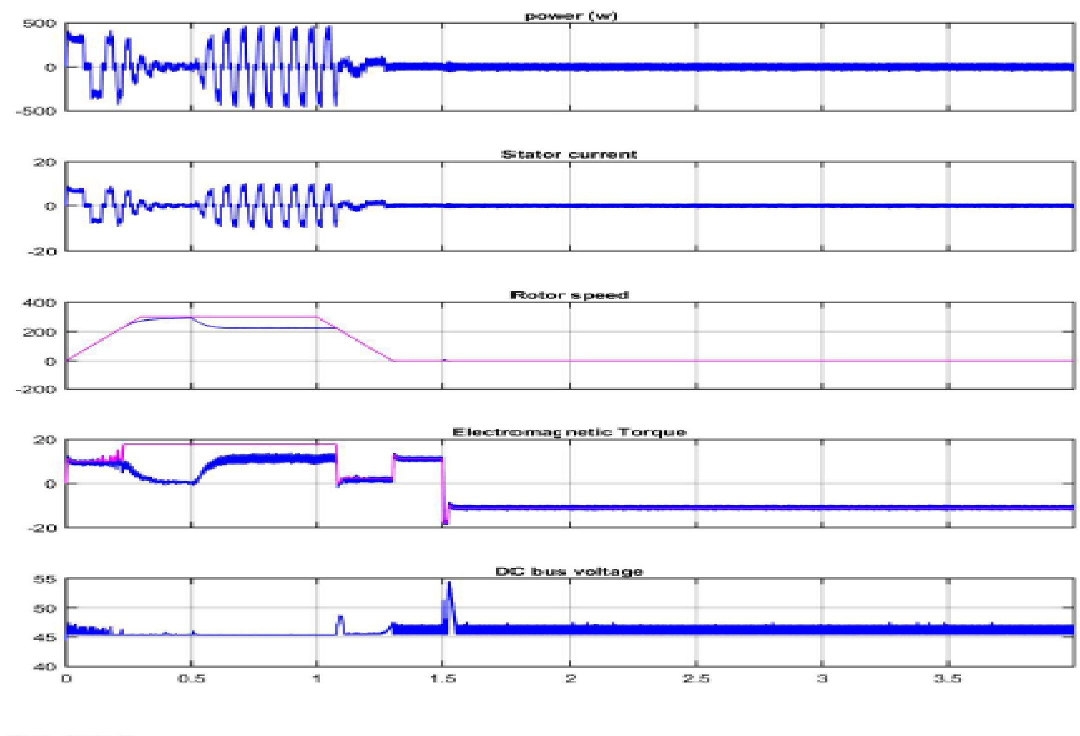

Figure 4. 20: Simulating Result of Brushless motor

Start the simulation. You can observe the motor stator current, the rotor speed, electromagnetic load torque disturbance is applied at 0.01 sec, and the speed regulation is obtained at the set speed and the DC bus voltage on the scope. The speed setpoint and the torque setpoint are also shown. At time t = 0 s, the speed setpoint is 300 rpm. Observe that the speed follows precisely the acceleration ramp. At t = 0.5 s, the full load torque is applied to the motor. You can observe a small disturbance in the motor speed, which stabilizes very quickly.

At t = 1 s, the speed setpoint is changed to 0 rpm. The speed decreases down to 0 rpm following precisely the deceleration ramp. At t = 1.5 s., the mechanical load passes from 11 Nm to -11 Nm. The motor speed stabilizes very quickly after a small overshoot.

Finally, note how well the DC bus voltage is regulated during the whole simulation period.

- The power system has been discretized with a 0.14µs time step. The speed controller uses a 9.6µs sample and the current controller uses a 1.4µs sample time in order to simulate a microcontroller control device.

4.1.11 Modeling and Simulating Result of PV powered dc motor drive

The converter is fed by a 48 V DC bus obtained by boosting 30V solar PV system voltage source in standard irradiance (1000 w/m^2) and temperature of 25℃. In order to limit the DC bus voltage during dynamic braking mode, a braking chopper has been added between the diode rectifier and the DC7 block. The IGBT switching frequency is 20 kHz.

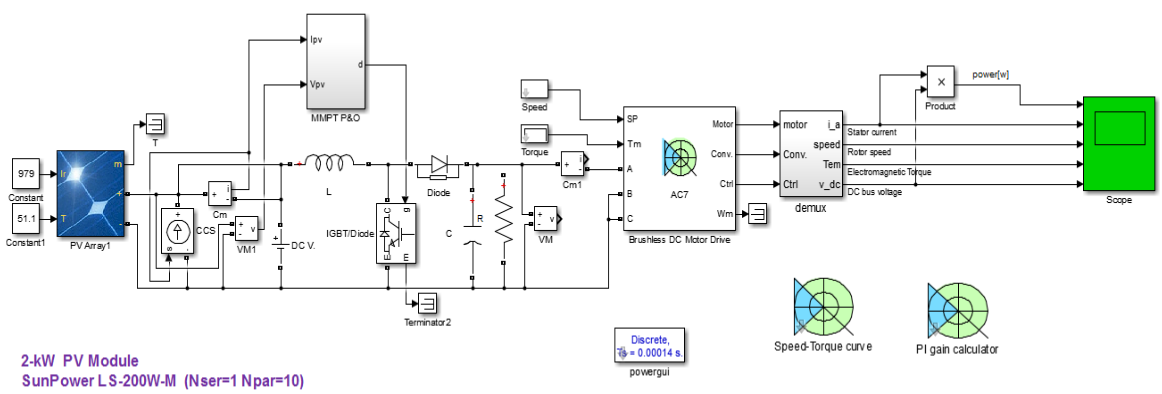

Figure 4. 21: Modeling of PV powered dc motor drive

The motor is coupled to a linear load, which means that the mechanical torque of the load is proportional to the speed. The speed reference is set at 300 rpm at t = 0.3 s. Observe that the motor speed follows the reference ramp accurately (+200 rpm/s) and reaches steady-state around t = 0.5 s. The armature current follows the current reference very well, with fast response time and small ripples. Notice that the current ripple frequency is 20 kHz. At t = 1 s, speed reference drops to zero rpm. The current reference decreases to reduce the electromagnetic torque and causes the motor to decelerate with the help of the load torque. At t

= 1.2 s, the current reverses in order to produce a braking electromagnetic torque (dynamic braking mode). This causes the DC bus voltage to increase. At t = 1.3s, the motor reaches 0 rpm and the load torque reverses and becomes negative. The negative current now produces an accelerating electromagnetic torque to allow the motor to follow the zero speed ramp (0 rpm/s). At t = 4 s, the speed reaches 0 rpm and stabilizes around its reference. The following figure shows the DC bus voltage, armature current, and speed waveforms.

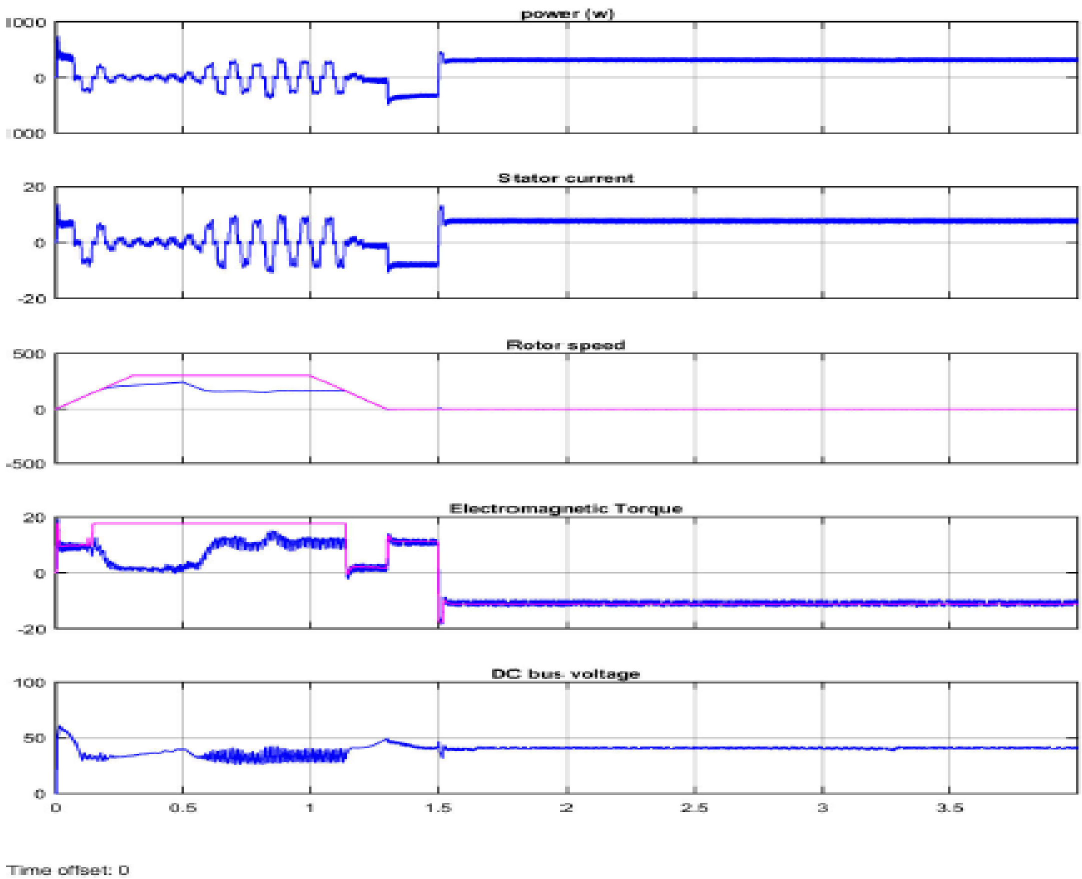

Figure 4. 22: simulating Result of PV powered dc motor drive

From the above simulation result the load power, DC bus voltage, and stator current curves are approximately approach to the mathematical design calculation and it is compatible with the desired load refrigerator, to give precise value of torque to the model in order to design BLDC Motor drive system because it is related to back-Emf and torque, by controlling the speed to its reference.

4.1.12 Modeling and Simulating Result of PV with Battery Bank powered dc motor drive

The selected site of the PV system of including the battery bank is powered to the DC motor drive of load circuit model was designed as shown in fig. 4.23. the selected site solar PV radiation depends on its annual average temperature of 12.72℃ and the worst operating calculation of design irradiance value of 717 W/m^2 is fed the solar PV as shown in fig. 4.23. if the PV panel is off at night or cloudy, then the battery bank is the only source to supply the desired load.

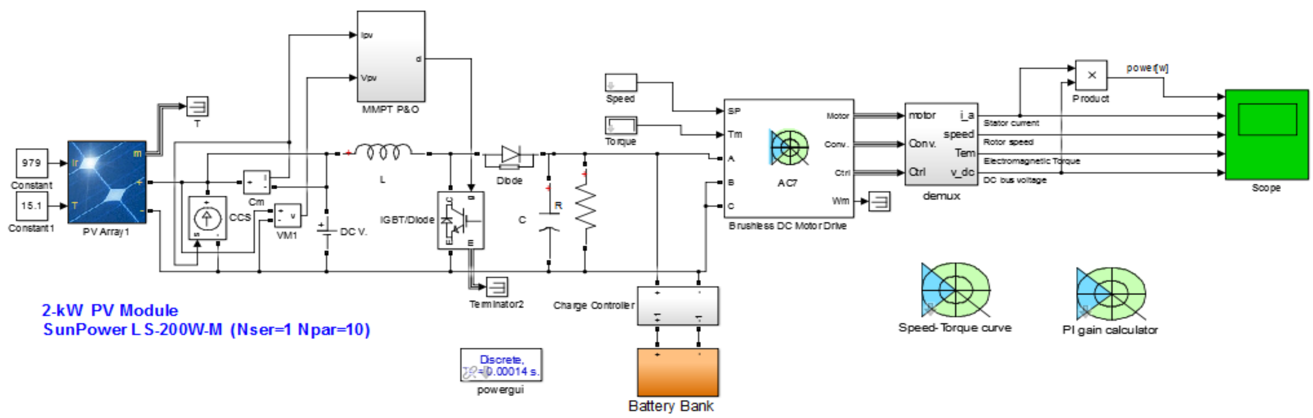

Figure 4. 23: modeling of PV with Battery Bank powered dc motor drive

In daily time the source is PV panel and the balance of system feds the load and charges the battery bank side by side. Therefore, the rechargeable battery bank is recycled, i.e. charge at daily time then discharge at night time and again.

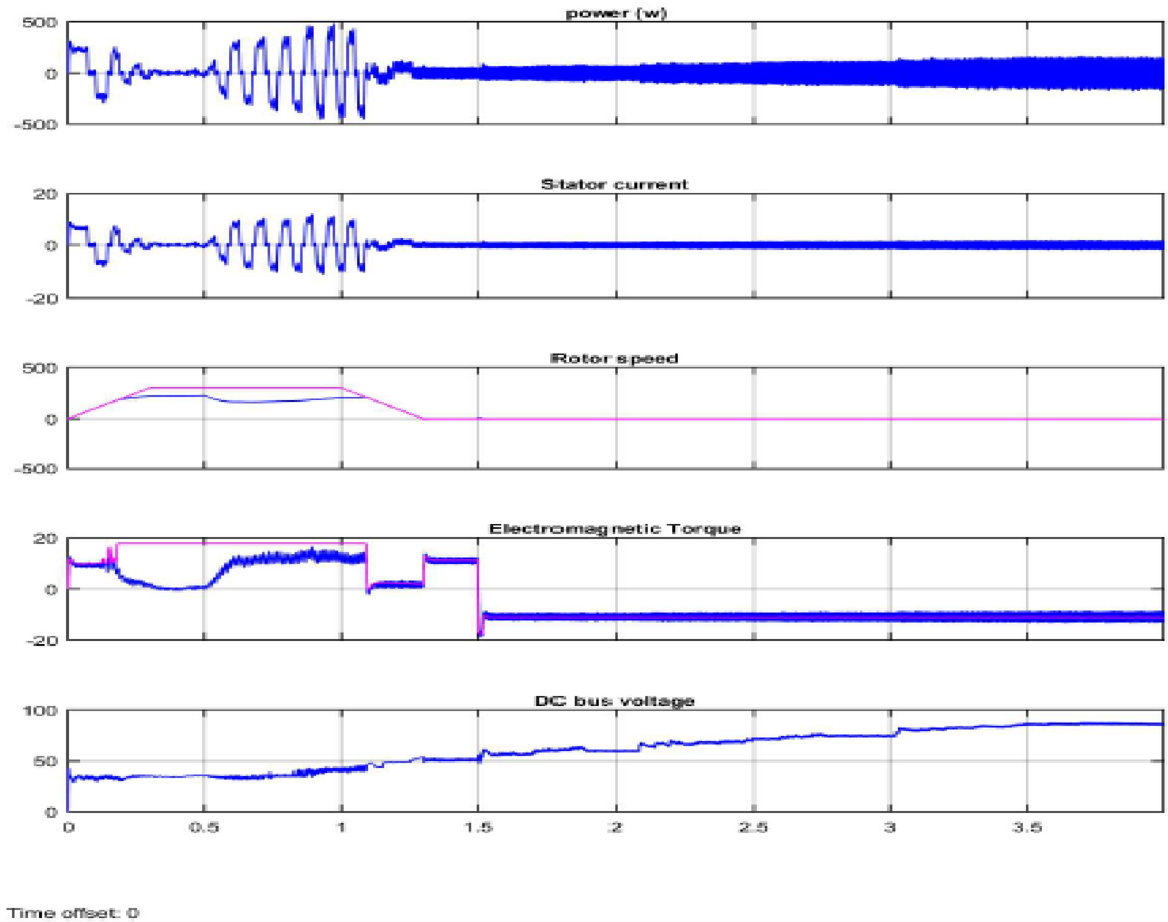

Figure 4. 24: modeling of PV with Battery Bank powered dc motor drive

From the above simulation result the load power, DC bus voltage, and stator current curves are to the mathematical design calculation and it is compatible with the desired load refrigerator, to give precise value of torque to the model in order to design BLDC Motor drive system because it is related to back-Emf and torque, by controlling the speed to its reference. A daily time, when the battery bank charge controller is "on state", then the curve characteristics of load power, stator current, and load torques are denser and bus DC voltage reaches gradually in doubled by speed control character.

4.2 Simulating and modeling of the solar-powered DC refrigerator using Matlab/ SIMULINK

4.2.1 Modeling and Simulation Result of DC/AC Inverter

The inverter get DC power from solar panels and this converter inverts DC to AC. This design and modulation is based on the level of inverter power. A 3765 W of 48V DC inverter input voltage and 220V AC sine wave inverter output voltage is desirable for the PV System.

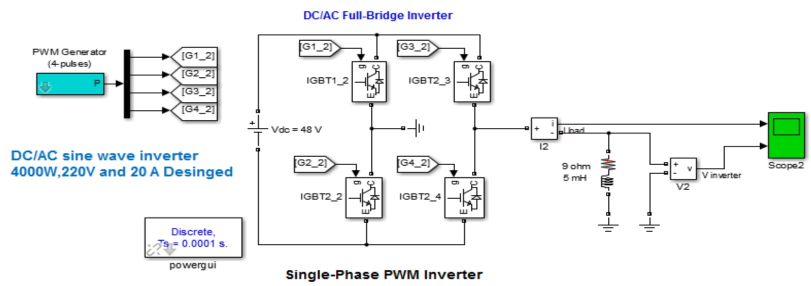

Figure 4. 25: modeling of single-phase PWM inverter

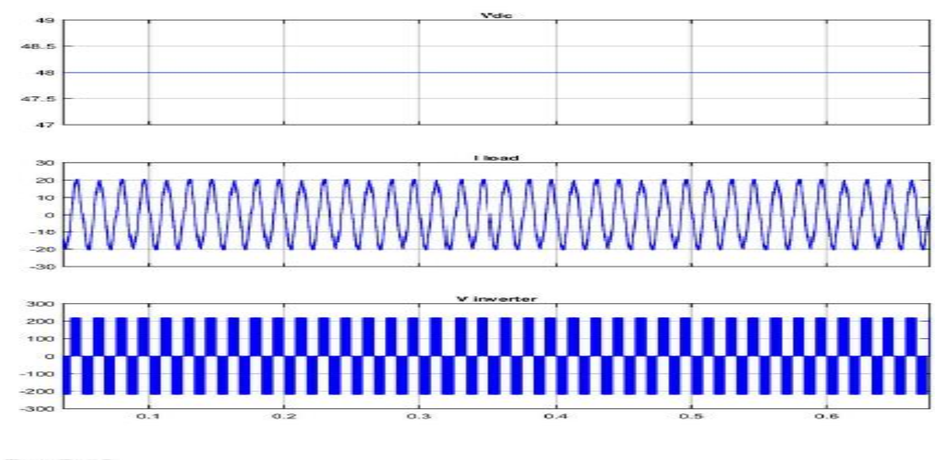

Figure 4. 26: modeling of single-phase PWM inverter

The simulation of the inverter starts from 0.1sce, you can observe the current sine wave and the single-phase inverter output of AC voltage, and their values are 18.18A and 220Vac.

4.2.2 Modeling and Simulating Result of PV powered AC motor drive

a two-quadrant single-phase rectifier drive for a 300w DC motor. The 300w DC motor is separately excited with a constant 48 V DC field voltage source. The armature voltage is provided by a single-phase rectifier controlled by two PI regulators. The rectifier is fed by a 220V AC 50 Hz voltage source followed by a linear transformer to boost the voltage up to a sufficient value.

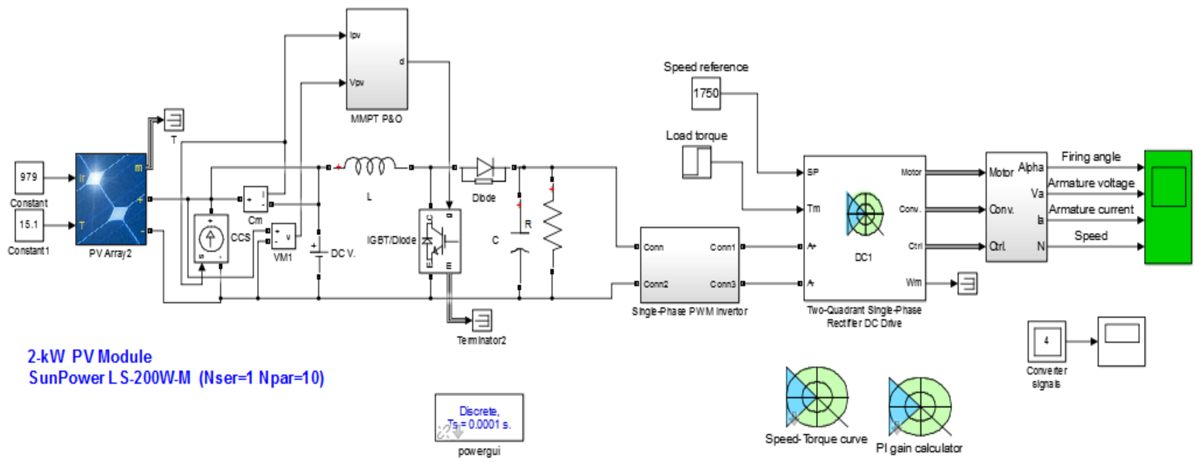

Figure 4. 27: modeling of the existing AC distribution system

The regulators control the firing angle of the rectifier thyristors. The first regulator is a speed regulator, followed by a current regulator. The speed regulator outputs the armature current reference (in p.u.) used by the current controller in order to obtain the electromagnetic torque needed to reach the desired speed. The speed reference change rate follows acceleration and deceleration ramps in order to avoid sudden reference changes that could cause armature over-current and destabilize the system. The current regulatory controls the armature current by computing the appropriate thyristor firing angle. This generates the rectifier output voltage needed to obtain the desired armature current. A 150 mH smoothing inductance is placed in series with the armature circuit to reduce armature current oscillations.

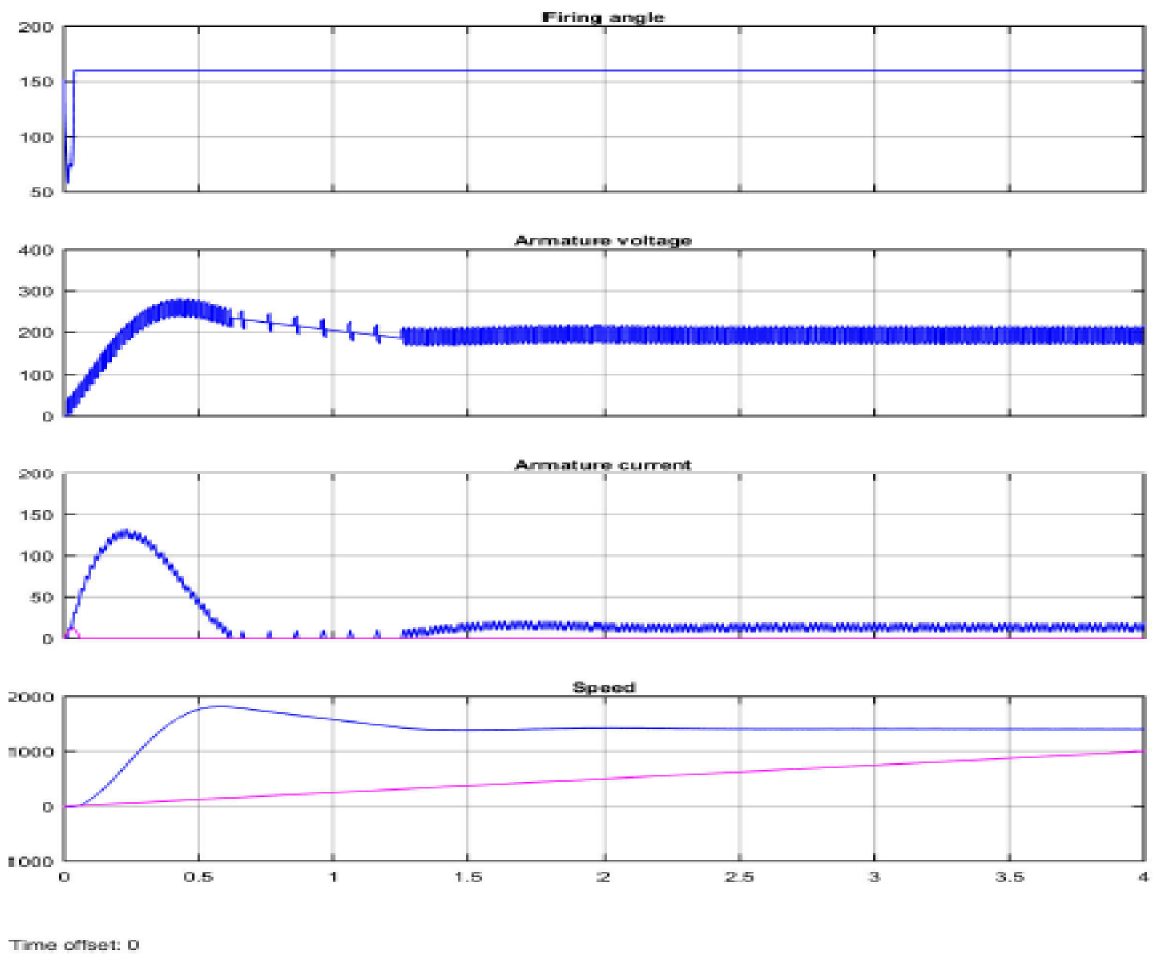

Figure 4. 28: simulation result of the existing AC distribution system

Start the simulation. You can observe the motor armature voltage and current, the rectifier firing angle and the motor speed on the scope. The current and speed references are also shown.

The speed reference is set at 1750 rpm at t = 0 s. The initial load torque is 15 N.m.

Observe that the motor speed follows the reference ramp accurately (+250 rpm/s) and reaches steady-state around t = 8.5 s. The armature current follows the current reference very well, and the firing angle stays below 90 degrees, the converter being in rectifier mode (first quadrant operating mode). The lower limit of the firing angle has been set to 20 degrees.

At t = 8.75 s, the load torque passes from 15 N.m to 20 N.m. the motor speed recovers fast and is back at 1750 rpm at t = 10 s. The current reference rises to about 17.5 A to generate a higher electromagnetic torque to maintain the needed speed. As observed before, the armature current follows its reference perfectly.

- The power system has been discretized with a 25 us time step. The control system (regulators) uses a 100 us time step in order to simulate a microcontroller control device.
- In order to reduce the number of points stored in the scope memory, a decimation factor of 20 is used.
- A simplified version of the model using an average-value rectifier can be used by selecting 'Average' in the 'Model detail level' menu of the graphical user-interface. The time step can then be increased up to the control system sample time value. This can be done by typing 'Ts = 100e-6'.

4.2.3 Modeling and Simulating Result of PV with Battery powered AC motor drive

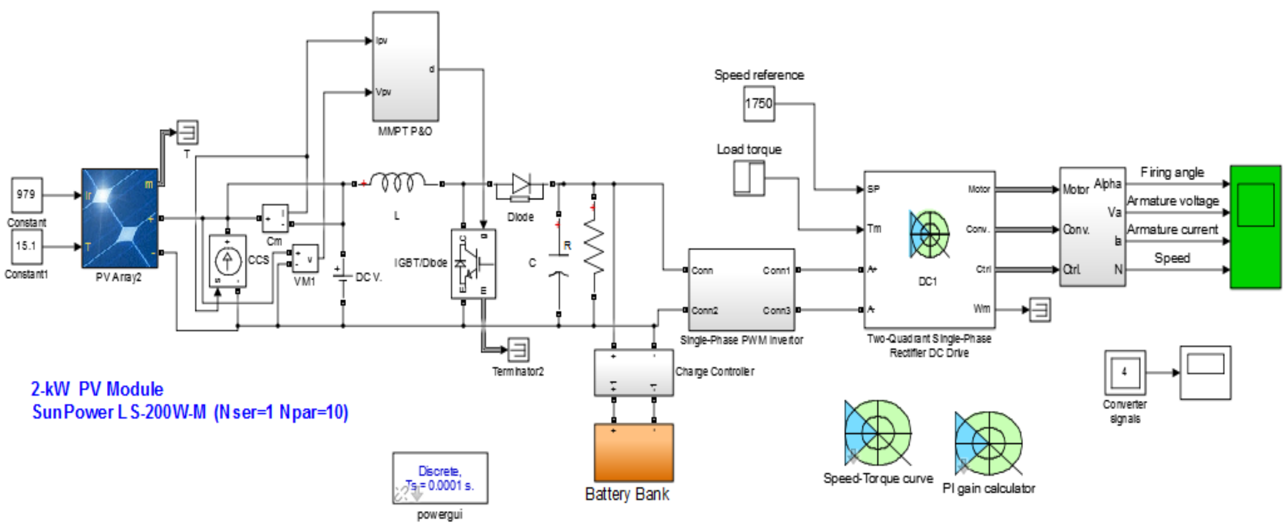

Figure 4. 29: modeling of PV with Battery Bank powered dc motor drive

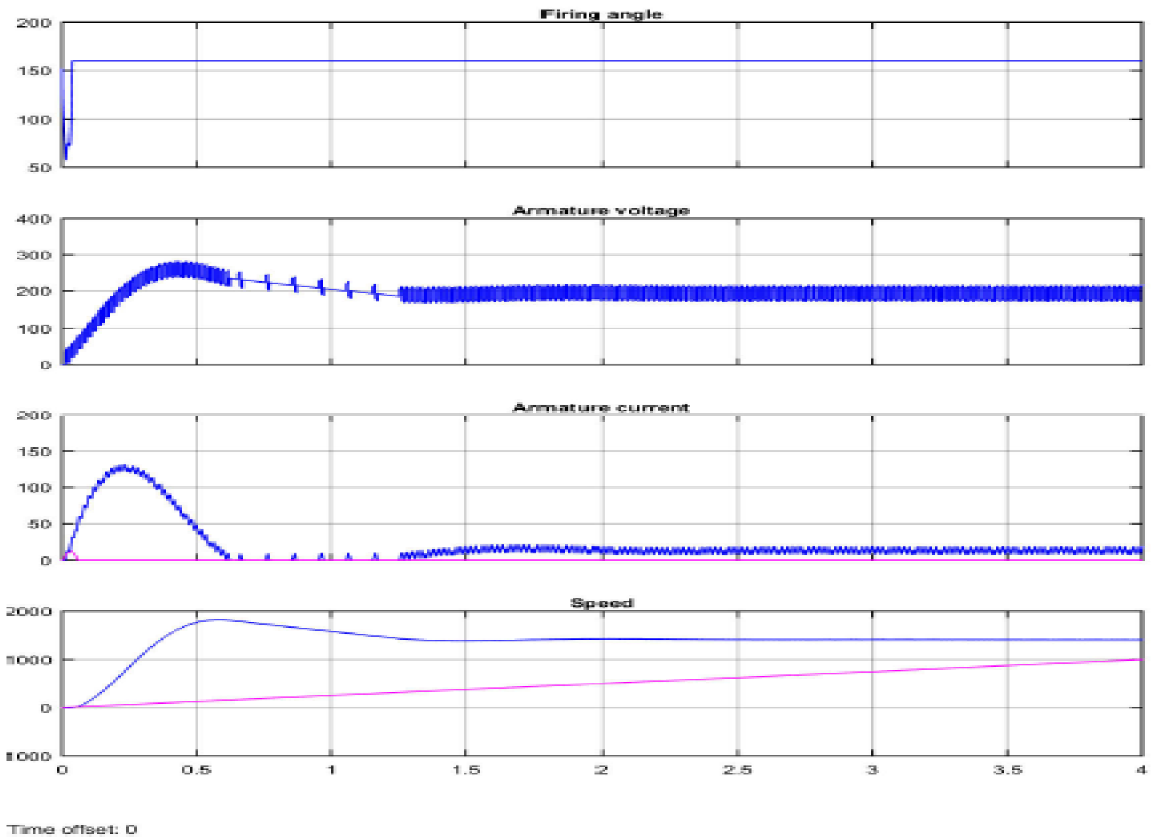

Figure 4. 30: Simulating Result of PV with Battery Bank powered dc motor drive

4.3 Economic comparison analysis of DC distribution system and AC existing system

4.3.1 Modeling of DC system cost analysis using HOMER Software

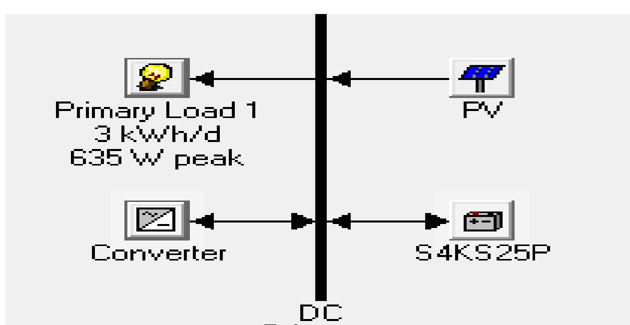

PV (kW)	S4KS25P	Conv. (kW)	Initial Capital	Operating Cost ($/yr)	Total NPC	COE ($/kWh)	Ren. Frac.	Capacity Shortage
	7	1	$ 368	15	$ 555	0.382	0.00	0.99
10	7	1	$ 4,868	65	$ 5,695	0.407	1.00	0.00

Figure 4. 31: modeling of PV module DC refrigerator cost analysis

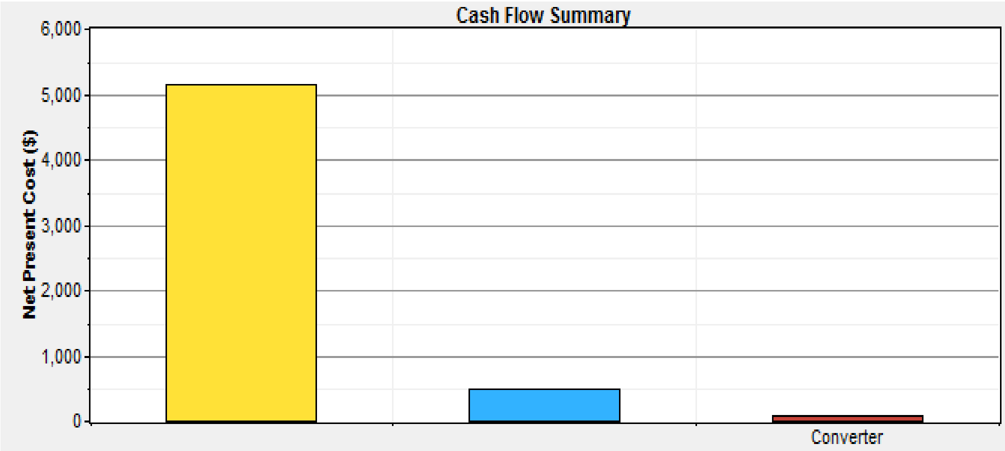

Component	Capital ($)	Replacement ($)	O&M ($)	Fuel ($)	Salvage ($)	Total ($)
PV	4,500	0	639	0	0	5,139
Copy of Copy of Copy of	300	74	128	0	-21	481
Converter	68	8	0	0	-2	75
System	4,868	83	767	0	-23	5,695

Figure 4. 32: Simulating Result of solar PV of DC system cost analysis

Cost summary

Total net present cost	$ 5,695
Levelized cost of energy	$ 0.407/kWh
Operating cost	$ 64.7/yr

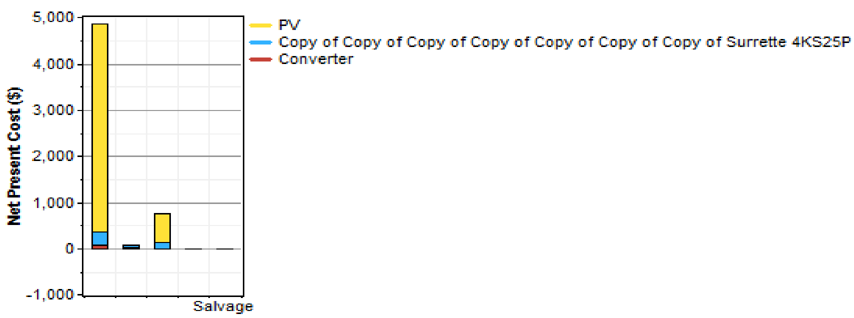

Figure 4. 33: Simulating net present cost versus salvage in PV module of the DC system

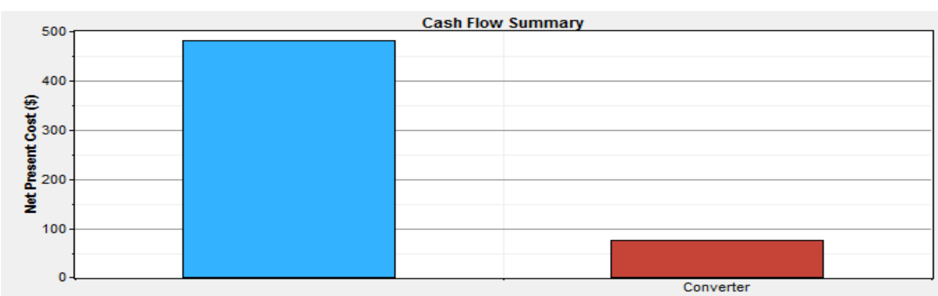

Component	Capital ($)	Replacement ($)	O&M ($)	Fuel ($)	Salvage ($)	Total ($)
Copy of Copy of Copy of	300	74	128	0	-21	481
Converter	68	8	0	0	-2	75
System	368	83	128	0	-23	555

Figure 4. 34: Simulating Result of DC system from Battery to load cost analysis

Cost summary

Total net present cost	$ 555
Levelized cost of energy	$ 0.382/kWh
Operating cost	$ 14.7/yr

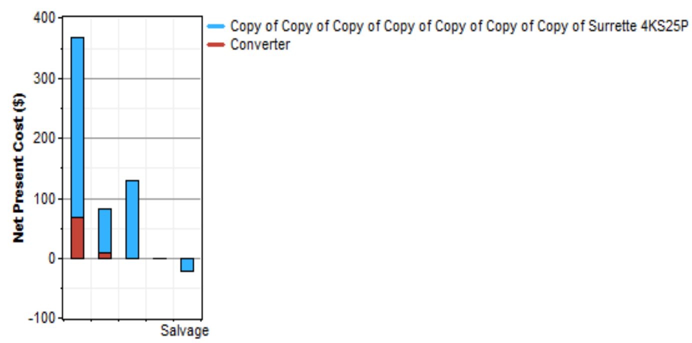

Figure 4. 35: Simulating Result net present cost versus salvage from battery to load DC system

4.3.2 Modeling of AC system cost analysis using HOMER Software

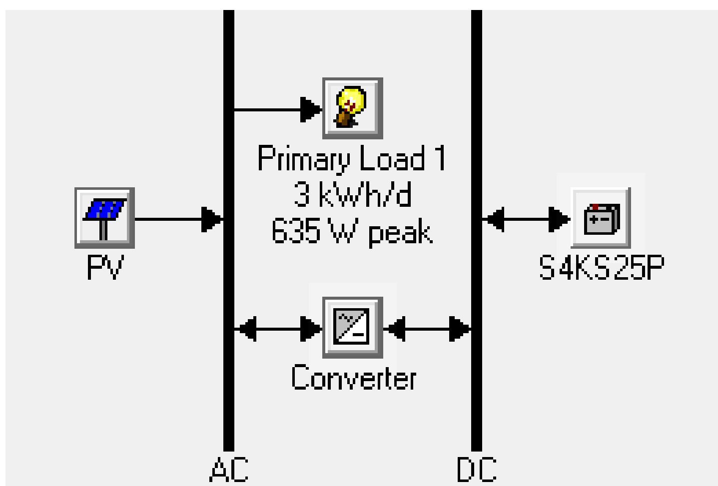

			PV (kW)	S4KS25P	Conv. (kW)	Initial Capital	Operating Cost ($/yr)	Total NPC	COE ($/kWh)	Ren. Frac.	Capacity Shortage
				7	1	$ 798	32	$ 1,211	0.926	0.00	1.00
			10	7	1	$ 5,298	82	$ 6,350	0.454	1.00	1.00

Figure 4. 36: modeling of PV module AC refrigerator cost analysis

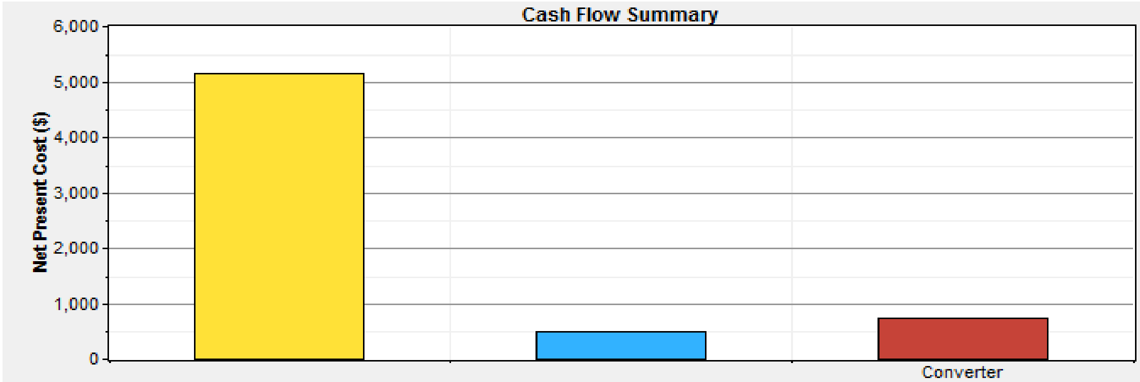

Component	Capital ($)	Replacement ($)	O&M ($)	Fuel ($)	Salvage ($)	Total ($)
PV	4,500	0	639	0	0	5,139
Copy of Copy of Copy of	300	74	128	0	-21	481
Converter	498	208	64	0	-39	730
System	5,298	282	831	0	-60	6,350

Figure 4. 37: Simulating Result of solar PV of DC system cost analysis

Cost summary

Total net present cost	$ 6,350
Levelized cost of energy	$ 0.454/kWh
Operating cost	$ 82.4/yr

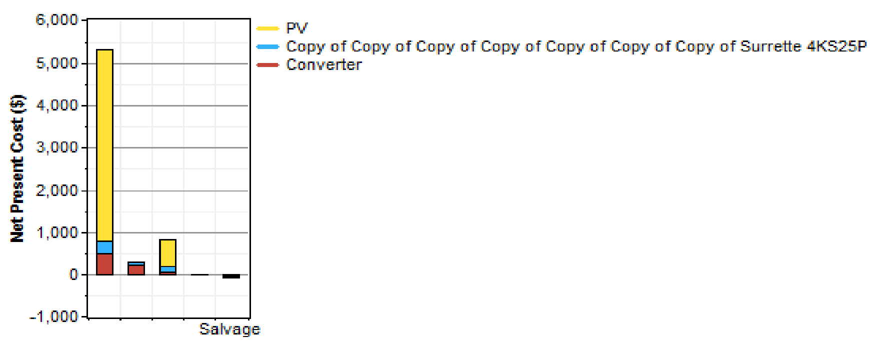

Figure 4. 38: Simulating net present cost versus salvage in PV module of the AC system

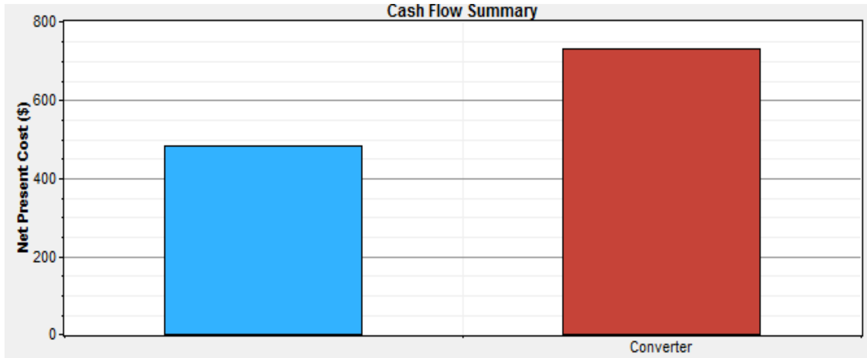

Component	Capital ($)	Replacement ($)	O&M ($)	Fuel ($)	Salvage ($)	Total ($)
Copy of Copy of Copy of	300	74	128	0	-21	481
Converter	498	208	64	0	-39	730
System	798	282	192	0	-60	1,211

Figure 4. 39: Simulating Result of AC system from Battery to load cost analysis

Cost summary

Total net present cost	$ 1,211
Levelized cost of energy	$ 0.926/kWh
Operating cost	$ 32.4/yr

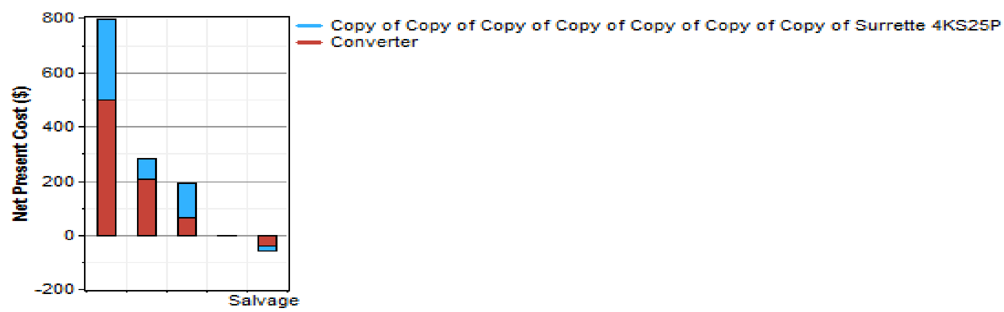

Figure 4. 40: Simulating Result net present cost versus salvage from the battery to load AC system

To calculate the cost-saving of an equipment refrigerator from the above HOMER software simulating result cost analysis of DC distribution system over the AC system is as follow below:

DC distribution of PV module DC refrigerator cost analysis = $5695

From battery to DC refrigerator cost analysis = $555

AC distribution of PV module AC refrigerator cost analysis = $6350

From battery to DC refrigerator cost analysis = $1211

Cost-saving = AC distribution system – DC distribution system = $6350 - $5695 = **$655**

Cost-saving from battery = battery of AC distribution system – battery of DC distribution system

= $1211 - $555 = **$656**

Percentage of cost-saving (%) = $\frac{\text{Total saving}}{\text{Total AC system NPC}}$*100% = $\frac{\$655}{\$6350}$*100%=**10.32%**

Percentage of cost-saving (%) of battery only = $\frac{\text{Total saving by battery}}{\text{Total AC system NPC}}$*100% = $\frac{\$656}{\$6350}$ =**10.33%**

Therefore, using the DC distribution system rather than AC system is saving costs for drive 10.32% of AC system Net Present Cost.

4.4 The solar-powered DC refrigerator compared to a conventional AC refrigerator

The overall feasibility of DC distribution system compared with the existing AC distribution system in terms of efficiency, energy, and power-saving, energy consumption and cost benefits of using DC instead of AC is calculating, modeling for refrigerator and simulating as the following table 4.1 as shown below.

Table 4. 1: simulating Result existing AC system compared with the new DC distribution system

Measurement in terms of	**for drive**	**for without drives**	**of Total losses**	**of Total input consumption**	**of output consumption**	**Refrigerator**
Efficiency saving	**18.72%**	**20.92%**				
Cost-saving						**10.32%**
Power saving by DC System			**79.18%**			
Energy-saving by DC System			**80.11%**	**14.20%**	**17.24%**	
Overall system efficiency Saving	**3.65%**	**4.08%**				

CHAPTER FIVE

CONCLUSIONS AND RECOMMENDATIONS

5.1 Conclusion

The development of renewable energy technology creates an opportunity for electrifying home appliances in the off-grid area by using DC power sources. The renewable energy can be supplied to the equipment direct by using a DC-DC converter depending on the source and equipment voltage. The DC-DC converter can help to adjust the voltage values to the rating of the equipment at higher efficiency. The study shows that the AC-DC converter has less efficiency compared with the DC-DC converter.

To bring the desired design of the DC distribution system primarily data have been collected and analyzed at the place of the site located in Kombolcha at Latitude of 11.08° North, Longitude of 39.72° East and Elevation of 1857 m above sea level. The solar radiation is developed based on the meteorological sunshine hour data to generated electricity by PV modules. Sizing of the photovoltaic system is based on the worst operating condition that annual solar data is available and August month is minimum solar irradiation. The declination (δ) angle, Hour angle ω, zenith (θz) angle, the angle of incidence of surfaces sloped due north or due south (θ) can be calculated 13.5°, 18.75°, 18.56°, and 49° respectively. The calculated total solar radiation on inclined surface is that taken from data collection is 717W/m^2 and an annual average temperature is 12.72℃. The minimum monthly solar irradiation (designing for worst conditions) is used in determining the peak sunshine hours is 8.4h/day (this PSH is in August). From the load assessments, the peak load is 1600W and the amount of energy needed for operate load is 7600Wh/day. But the selected an equipment Refrigerator has 300W load and the annual energy of refrigerator is 1095kwh/y. A 200W PV Module is selected for the site and 10 units of each are parallel connected to deliver 2000 watt load with 48Vdc system voltage of home appliances.

The cost-benefit of the DC system was saved as 10.32% of the AC system total Net Present Cost for refrigerator only. In this study, 80.11% of annual energy loss could be saved using the DC system, 18.72% of drive equipment and 20.92% of non-drive home appliance efficiency saved. The overall system including solar PV module efficiency was saved 3.65% and 4.08% of with drive and without drives respectively.

5.2 Recommendation

The result of simulation from the study the power loss, energy loss of DC system is less than the AC system and the reduction of cost of energy consumption made the DC power cost-effective and efficient to be used widely in off-grid areas to supply the various home appliances. The availability of renewable energy resources can encourage the manufacturer to produce equipment to be operated from DC source.

Another option to the manufacturer is to develop dual-input (DC and AC) products that can operate off either power source. This would allow consumers to purchase long-lived appliances today to ensure DC compatibility in the future, even if the distribution infrastructure will not be in place for months or years.

In addition, the lack of awareness of alternative DC products is another factor that limits the size of the DC-ready product market. A marketing campaign to educate consumers about the potential benefits of DC-ready products would help overcome this barrier.

Finally, the lack of DC power infrastructure in homes to provide suitable input power. Other than low-power USB hubs and battery chargers, most homes have no DC infrastructure. The solution to this problem has been the sale of complete solar kits that include the power source, distribution and storage "hub," and the DC-ready end-use products.

5.3 Future Work

This thesis study the feasibility of DC supply for home appliance equipment has been seen. In the study power and energy loss comparison of converter and inverters, efficiency, cost-benefit and environmental impact of AC and DC systems have been seen for steady-state operation of the equipment. Future studies will be doing on the voltage drop in (THD), power quality, transient operation, protection of the DC system, and better standards low voltage DC operation.

References

[1]. Getachew B, Palm B (2010) “Feasibility study for standalone solar–wind-based hybrid energy system for application in Ethiopia”. Appl Energy 87: 487-495.

[2]. Wolde-Ghiorgis W (2002) “Renewable energy for rural development in Ethiopia: the case for new energy policies and institutional reform”. Energy Policy 30: 1095-1105.

[3]. Vossos, Evangelos, "Optimizing energy savings from "Direct-DC" in U.S. residential buildings" (2011). Master's Theses. Paper 4078.

[4]. Mohammad Amin and Yasir Arafat, “Feasibility Study of Low Voltage DC Distribution System for House.’’ Electric Power Engineering, Chalmers University of Technology, Sweden (A4.014).

[5]. Nobuyoshi Mutoh, Masahiro Ohno, and Takayoshi Inoue, “A Method for MPPT Control While searching for Parameters Corresponding to Weather Conditions for PV Generation Systems”, IEEE Transactions on Industrial Electronics, vol. 53, no. 4, 2006.

[6]. Sung Sae Lee, Gun Woo Moon, “High-Efficiency Boost Half-Bridge Converter With Fast Boost Current Transferring ZVS Operation”, IEEE Transactions on Power Electronics, vol. 23, no. 4, 2008, pp. 1822-1829.

[7]. Seung-Wu Rhee, Gun Woo lee, “Coupled Inductor Incorporated Boost Half-Bridge Converter with Wide ZVS Operation Range”, IEEE Transactions on Industrial Electronics, vol. 56, no. 7, 2009, pp. 2505-2512.

[8]. Dan Chiras. Solar Electricity Basics: A Green energy Guide. New Society Publishers, 2010.

[9]. Seung-Wu Rhee, Gun Woo lee, “Coupled Inductor IncorporatedBoost Half-Bridge Converter with Wide ZVS Operation Range”, IEEE Transactions on Industrial Electronics, vol. 56, no. 7, 2009, pp. 2505-2512.

[10]. T. Lowand M. A. Jabbar, “Permanent-magnet motors for brushless operation,” IEEE Trans. Ind. Applicat., vol. 26, pp. 124–129, Jan./Feb. 1990.

[11]. “Demand DC: Adoption Paths for DC Power Distribution in Homes” Stephen Pantano, CLASP Peter Ostendorp, PhD, Xergy Consulting Katherine Dayem, PhD, Xergy Consulting.

[12]. Andrej Cotar, et al. photovoltaic systems, commissioning party: IRENA- Istrian regional energy agency; January 2012.

[13]. Munuswamy, S., Nakamura, K., Katta, A. (2011) ‘Comparing the cost of electricity sourced from a fuel cell-based renewable energy system and the national grid to electrify a rural health centre in India: A case study’, Renewable Energy 36, pp. 2978 – 2983.

[14]. Golma Boyena, 2011 Design of a photovoltaic wind hybrid power generation system for Ethiopian remote area. Master thesis.

[15]. F. Valenciaga and P. F. Puleston, "Supervisor control for a stand-alone hybrid generation system using wind and photovoltaic energy", IEEE Trans. Energy Conversion, vol. 20, no. 2, June 2005, pp. 398 -405.

[16]. Joara Cronemberger, Estefanía Caamaño-Martín, “Assessing the solar irradiation potential for solar photovoltaic applications in buildings at low latitudes – Making the case for Brazil”, Energy and Buildings, Vol. 55, pp. 264–272, 2012. [9]

[17]. To cite this article: Peng Zhang et al 2017 IOP Conf. Ser.: Mater. Sci. Eng. 199 012134 "An Overview of Different Approaches for Battery Lifetime Prediction”

[18]. G.K. Singh, “Solar power generation by PV (photovoltaic) technology: A review” Energy, vol. 58, No. 1, pp. 1-13, 2013.

[19]. Isis Portolan dos Santos, Ricardo Rüther, “Limitations in solar module azimuth and tilt angles in building integrated photovoltaic at low latitude tropical sites in Brazil”, Renewable Energy, Vol. 63, pp. 116–124, 2014.

[20]. Caisheng Wang. Modeling and Control of Hybrid Wind/Photovoltaic/Fuel cell Distributed Generation Systems, PhD thesis, Montana State University, Bozeman, 2006

[21]. Roger A Messenger & Jerry Ventre. Photovoltaic Systems Engineering. CRC, 2003.

[22]. Mukund R Patel. Wind and Solar Power Systems: Design, Analysis, and Operation, CRC, 2005.

[23]. C. Del Pero together with M. Buffoli and M. Butera developed the idea of the system

[24]. Kadir Bakirci, "General models for optimum tilt angles of solar panels: Turkey case study", Renewable and Sustainable Energy Reviews, Vol. 16, no. 8, pp. 6149–6159, 2012. [8]

[25]. Akella, A.K., Sharma, M.P., Saini, R.P. (2007) 'Optimum utilization of renewable energy sources in a remote area', Renew Sustain Energy Rev 11, pp. 894-908.

[26]. Assessment of Resource Potential and Modeling Of Standalone Pv/Wind Hybrid System For Rural Electrification, 2014.

[27]. Kun Wei, Zhengli Lou, Zhongchao Zhang, "Research on the Commutation Current Prediction Control in Brushless DC Motor".

[28]. Aldo V., 2005, "Fundamentals of Renewable Energy processes", Elsevier Inc., 2005.

[29]. Assessment of Resource Potential and Modeling Of Standalone Pv/Wind Hybrid System For Rural Electrification, 2014.

[30]. Nema, P., Nema, R.K., Rangnekar, S. (2010) „PV-solar / wind hybrid energy system for GSM/CDMA type mobile telephony base station", International Journal of Energy and Environment 1(2), pp.359-366 (available from: www.IJEE.IEEFoundation.org).

[31]. Wagner, H. and Mathur, J., (2009) Introduction to Wind Energy Systems: Basics, Technology and Operation. Berlin Heidelberg: Springer-Verlag.

[32]. R. Bharanikumar "Modeling and Simulation of Wind Turbine Driven Permanent Magnet Generator with New MPPT Algorithm" Asian Power Electronics Journal, Vol. 4 No.2, 2010.

[33]. Patel, M.R., (2006) Wind and Solar Power Systems: Design, Analysis, and Operation. 2nd Ed. Boca Raton: Taylor & Francis Group.

[34]. Gipe, P. (2004). Wind Power: Renewable Energy for Home, Farm, and Business.

[35]. ShivrajSDudhe, Archana G Thosar "Mathematical Modeling and Simulation Of Three phase Bldc Motor Using MATLAB/SIMULINK"Nov., 2014. ISSN: 22311963

[36]. WHO Performance, Quality, and Safety. Updated regularly and available online at http://apps.who.int/ immunization_standards/vaccine_quality/pqs_catalogue/

[37]. Ramchandra P, Boucar D. “Green Energy and Technology” Springer, London Dordrecht Heidelberg New York, 2011.

[38]. Berihun G.(2013) modeling and simulating of a micro hydro wind hybrid power generation system for rural area of Ethiopia. Master thesis in Addis Ababa University.

[39]. Abiyot Mekonnen “Feasibility Study of Renewable Energy Resources for Electrification of Small Islands. A Case Study on Tana Lake Islands”, MSC thesis, AAU, 2013.

[40]. Yohannes Tesfaye, “Application of micro-hydro PV/battery off- grid hybrid energy system for Ethiopian rural area” Master thesis at Addis Ababa Institute of Technology.

[41]. Getnet Tadesse, “Feasibility Study of Small Hydro/PV/Wind Hybrid System for Off-Grid Rural Electrification in Ethiopia” master of thesis at Addis Ababa Institute of Technology.

[42]. Dhanabal.R et al. Comparison of Efficiencies of Solar Tracker Systems with Static Panel, Single-Axis Tracking System and Dual-Axis, International Journal of Engineering and Technology (IJET), ISSN: 0975-4024, 2013

[43]. HOMER, the Micro-Power Optimization Model; ver.2.68Beta, NREL; 2009.

[44]. John A. Duffie (Deceased) and William A. Beckman “Solar Engineering of Thermal Processes” Book Fourth Edition, 2013.

[45]. Alibaba,[online]. Available: https://www.alibaba.com/productdetail/Efficiency -level VI acdcadapter_60789104476.html?spm=a2700.7724857.normalList.42.33ec2115KXaZoi [Accessed on July 24, 2019].

[46]. RS,[online]. Available: https://uk.rs-online.com/web/p/embedded-switchmode-power-supplies-smps/1227873/ [Accessed on January 15, 2019].

[47]. Alibaba, [online]. Available: https://www.alibaba.com/product-detail/Meanwe ll-SD-50C-12-50w-48V_60655694876.html [Accessed on March 18, 2019].

[48]. RS,[online]. Available: https://uk.rs-online.com/web/p/embedded-switchmode-power-supplies-smps/1227674/ [Accessed on May 12, 2019].

APPENDIX

APPENDIX-A1

Table 2: Typical 200W PV Module Characteristics

Typical 200W pv Module Characteristics-LS-200W-M	
pv module life	25-30 Years
No. of cells and connections	60 in series
open circuit voltage (Voc)	37.05 V
Maximum power voltage (Vpm)	30 V
short circuit current (Isc)	7.33 A
Maximum power current (Ipm)	6.67 A
Max power (Pm)	200 W
Module Efficiency	18.5%-19.5%
Weight	15Kg
Dimension (L*W*H) in mm	1320*992*35
FF (%)	70-76%
Tolerance Wattage (e.g. +/-5%)	±3%, or 0-3%
Front Glass Thickness(mm)	3.2
Temperature Coefficients of Isc (%)	0.04
Temperature Coefficients of Voc (%)	-0.38
Temperature Coefficients of Pm (%)	-0.47
Temperature Coefficients of Im (%)	0.04
Temperature Coefficients of Vm (%)	-0.38
Temperature Range	-40°C to +85°C
Warranty	90% of 10 years, 80% of 25 years.
Standard Test Conditions	AM1.5 1000W/ 25 +/-2°C

The parameters required for simulation are initialized by the following script file

```
Iscn= 7.33;     %Nominal short-circuit current [A]
Vocn= 37.05;   %Nominal array open-circuit voltage [V]
Imp = 6.67;     %Array current @ maximum power point [A]
Vmp = 30v;     %Array voltage @ maximum power point [V]
Pmax-e = Vmp*Imp;   %Array maximum output peak power [W]
Kv =-0.38;     %Voltage/temrature coefficient [V/K]
Ki = 0.04;      %Current/temperature coefficient [A/K]
Ns = 60;           %Number of series cells
%%Constants
K = 1.3806503e-23; %Boltzmann [J/K]
q = 1.60217646e-19; %Electron charge [C]
a = 1.3;   %Diode constant
%%Nominal values
Gn = 1000;   %Nominal irradiance [W/m^2] @ 25oC
Tn = 25+273.15;   %Nominal operating temperature [K]
%%Adjusting algorithm
%The model is adjusted at the nominal condition
T = 25+273.15;
G = 800;
Vtn = k*Tn/q;      %Thermal junction voltage (nominal)
Vt = k*T/q;         %Thermal junction voltage (current temperature)
Ion = Iscn/(exp(Vocn/a/Ns/Vtn)-1);      %Nominal diode saturation current
Io = Ion;
%Reference values of Rs and Rp
Rs-max = (Vocn-Vmp)/Imp;
Rp-min = Vmp/(Iscn-Imp)- Rs-max;
%Initial guesses of Rp and Rs
Rp = Rp-min;
Rs = 0;
tol = 0.001;    %power mismatch tolerance
```

```
P = (0);
error = inf;    %Dummy value
%iterative process for Rs and Rp until Pmax, model = Pmax, exponential
While (error>tol)
%temperature and irradiance effect on the current
dT= T-Tn;
Ipvn = (Rs+Rp)/Rp*Iscn;     %Nominal light-generated current
Ipv = (Ipvn+Ki*dT)*G/Gn;    %Actual light-generated current
Isc = (Iscn+ Ki*dT)* G/Gn;     %Actual short circuit current
%Increments Rs
Rs =Rs+ 0.01;
%Parallel Resistance
Rp = Vmp*(Vmp+ Imp*Rs)(Vmp*Io*exp((Vmp+Imp*Rs)/Vt/Ns/a) +Vmp*Io – Pmax-e)
%solving the I-V equation for several (V, I) pairs
Clear V
Clear I
V = 0: 0.1:50:     %Voltage vector
I = zeros (I, size (v,2)); %Current vector
For j=1: size (v, 2)   % calculates for all voltage values
%solves g = 1-f(1,v) = 0 with Newntonn-Raphson
g(j)=Ipv- Io*(exp((V(j) + I(j) *Rs)/Vt/Ns/a) – 1) - (V(j) +I(j) * Rs)/Rp)- I(j);
while (abs(g(j)) >0.001)
g(j)=Ipv- Io*(exp((V(j) + I(j) *Rs)/Vt/Ns/a) – 1) - (V(j) +I(j) * Rs)/Rp)- I(j);
glin(j)=-Io*Rs/Vt/Ns/a*exp((V(j)+ I(j)*Rs)/Vt/Ns/a) – Rs/Rp-1;
I_(j)-I(j)-g(j)/glin(j);
I(j)=I_(j);
end
end% for j=1: size(V,2)
% calculates power using the I-V equation
```

```
P= (Ipv- Io*(exp((V + I *Rs)/Vt/Ns/a) – 1) - (V +I * Rs)/Rp)*V;

Pmax_m= max(p);

Error = (Pmax_m – Pmax_e);

End % while (error>tol);

%% outputs

fprintf('model info;\n');

fprintf('Rp_min= %f', Rp_min);

fprintf('\n Rp=% f', Rp);

fprintf('\n Rs_max = % f', Rs_max);

 fprintf('\n Rs=% f', Rs);

fprintf('\n a=% f,' a);

fprintf('\n T=% f', T-273.15);

fprintf('\n G=% f', G);

fprintf('\n P_max = % f (model)', P_max);

fprintf('\n P_max = % f (expermental)', P_max);

fprintf('\n tol=% f', tol);

fprintf('\n P_error=% f', error);

fprintf('\n Ipv=% f', Ipv);

fprintf('\n Isc=% f', Isc);

fprintf('\n Ion=% f', Ion);
```

APPENDIX-A2

Voltage loss per 100m of wire run (volts per 200m of wire)			
	wire cross section (mm^2)		
Flow (Amps)	**1.5**	**2.5**	**4**
0.1	0.21	0.14	0.08
0.2	0.43	0.27	0.17
0.3	0.64	0.41	0.25
0.4	0.86	0.54	0.34
0.5	1.07	0.68	0.42
0.6	1.29	0.81	0.51
0.7	1.5	0.95	0.59
0.8	1.72	1.08	0.68
0.9	1.93	1.22	0.76
1	2.15	1.35	0.85
2	4.29	2.7	1.69
3	6.44	4.05	2.4
4	8.58	5.41	3.38
5	10.73	6.76	4.23
6	12.87	8.11	5.08
7	15.02	9.46	5.92
8	17.16	10.81	6.77
9	19.31	12.16	7.62
10	21.45	13.51	8.46

APPENDIX-A3